Chapter 8

Stress and deformation analysis—finite element method

8.1 Introduction

8.2 Framework and principles

Linear elastic material, plastic behavior consideration, nonlinear behavior consideration

8.3 Effective stress analysis and total stress analysis

8.4 Commonly used soil models and related parameters: MC model, DC model, MCC model, HS model, small strain model

8.5 Determination of soil parameters

8.6 Determination of initial stresses:

Direct input method, gravity generation method

8.7 Structural material models and related parameters

8.8 Mesh generation

Shape of the element, density of mesh, boundary condition

8.9 Plane strain analysis and 3D analysis

8.10 Finite element stability analysis

8.11 Finite element analysis procedure

8.1 Introduction

The finite element method is capable of simulating **actual geometry of an excavation, the conditions of soil layers, stress-strain behavior of soil, the level and pressures of groundwater, the excavation depth, construction sequence**. It is more accurate than those derived from simplified methods or the beam on elastic foundation method

Successful modeling the real stress-strain behavior of soil is a crucial point to obtain a reasonable performance of an excavation for the finite element method

Finite difference method is similar to finite element method but with different theories and solution procedures. Advanced soil models used to simulate the stress-strain behavior of soil can also be implemented in the finite difference method.

8.2.1 Linear elastic behavior

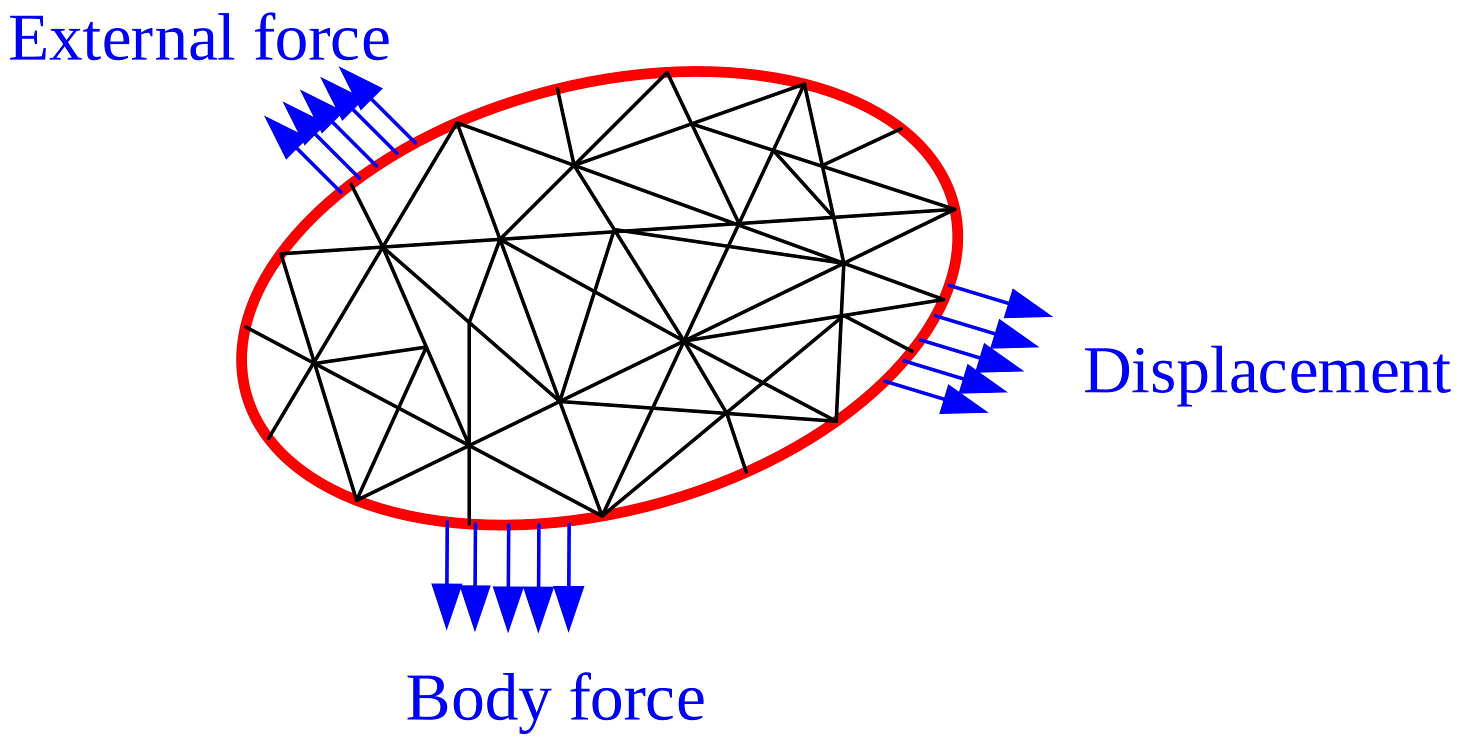

FIGURE 8.1 Finite element mesh and boundary conditions

The constitutive law for **elastic isotropic material** can be expressed

$$\{\sigma\}=[D]\{\varepsilon\} \qquad (8.1)$$

[σ]= stress matrix, In three dimensional space, the stress matrix contains six components such as σ_x, σ_y, σ_z, τ_{xy}, τ_{yx}, τ_{zx}. In plane strain or stress condition, it contains only 3 components.

{ε}= strain matrix. In three dimensional space, the stress matrix contains six components such as ε_x, ε_y, ε_z, γ_{xy}, γ_{yx}, γ_{zx}. In plane strain or stress condition, it contains only 3 components.

[*D*]=stress-strain or constitutive matrix. The main entries are Young's modulus **(*E*)** and Poisson's ratio **(μ)**, which are also called the deformation parameters.

The relation between the displacement $\{u\}$ at any point within the element and the displacement $\{q\}$ at the nodal points of the element

$$\{u\}=[N]\{q\} \qquad (8.2)$$

$[N]$= displacement shape function

According to the theory of elasticity, the strain and displacement at a point within the element

$$\{\varepsilon\}=[L]\{u\}=[L][N]\{q\}=[B]\{q\} \qquad (8.3)$$

$[L]$= linear partial differential operator,
such as $\partial/\partial x, \partial/\partial y$

$[B]$=$[L][N]$= relational matrix between the strain and the nodal displacement

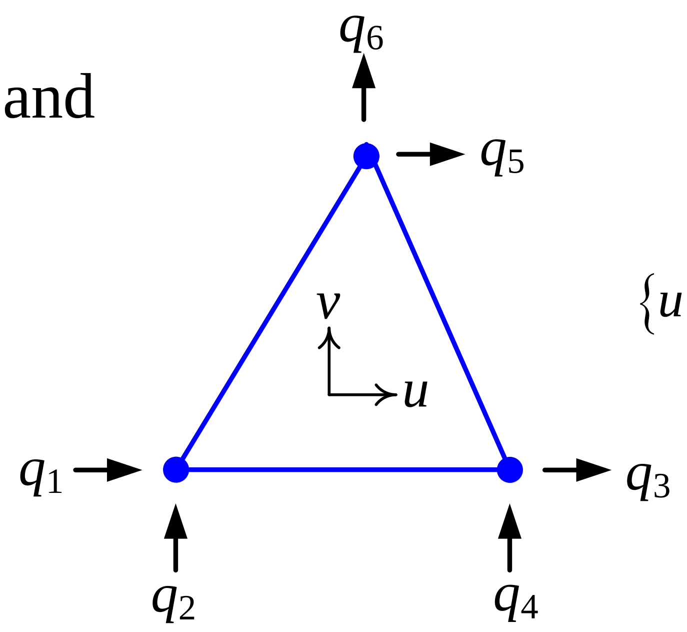

$$\{u\}=\begin{Bmatrix} u \\ v \end{Bmatrix} \qquad \{q\}=\begin{Bmatrix} q_1 \\ \cdot \\ \cdot \\ \cdot \\ q_6 \end{Bmatrix}$$

FIGURE 8.2 Three-node element

According to the principle of virtual work, we can derive the work done by the internal force and the external force in an element

$$\int_{vol} \{\delta\varepsilon\}^T [\sigma]\, \mathrm{d(vol)} = \int_{vol} \{\delta u\}^T \{G\} \mathrm{d(vol)} + \int_{area} \{\delta u\}^T [T]\, \mathrm{d(area)} \quad (8.4)$$

$$\int_{vol} [B]^T [\sigma]\, \mathrm{d(vol)} = \int_{vol} [N]^T \{G\}\, \mathrm{d(vol)} + \int_{area} [N]^T [T]\, \mathrm{d(area)} \quad (8.5)$$

$[\delta\varepsilon]$=strain increment $\{\delta u\}$=displacement increment at any point with the element

$[\sigma]$ =the state of stress at the current stage

$[G]$=body force $[T]$=traction, which is the surface force acting on the element

The stiffness matrix of the element $[K_E]$

$$[K_E] = \int_{vol} [B]^T [D][B] dV \qquad (8.6)$$

The element stiffness matrix for all elements are then assembled into the global stiffness matrix [K] of the element

$$[K]\{q\} = \{F\} \qquad (8.7)$$

$[q]$= nodal displacement matrix

$[F]$=matrix of excavation-induced external force or equivalent load at nodal points

$$\{q\} = [K]^{-1}\{F\}$$

$$\mu = -\frac{\varepsilon_2}{\varepsilon_1} = -\frac{\varepsilon_3}{\varepsilon_1}$$

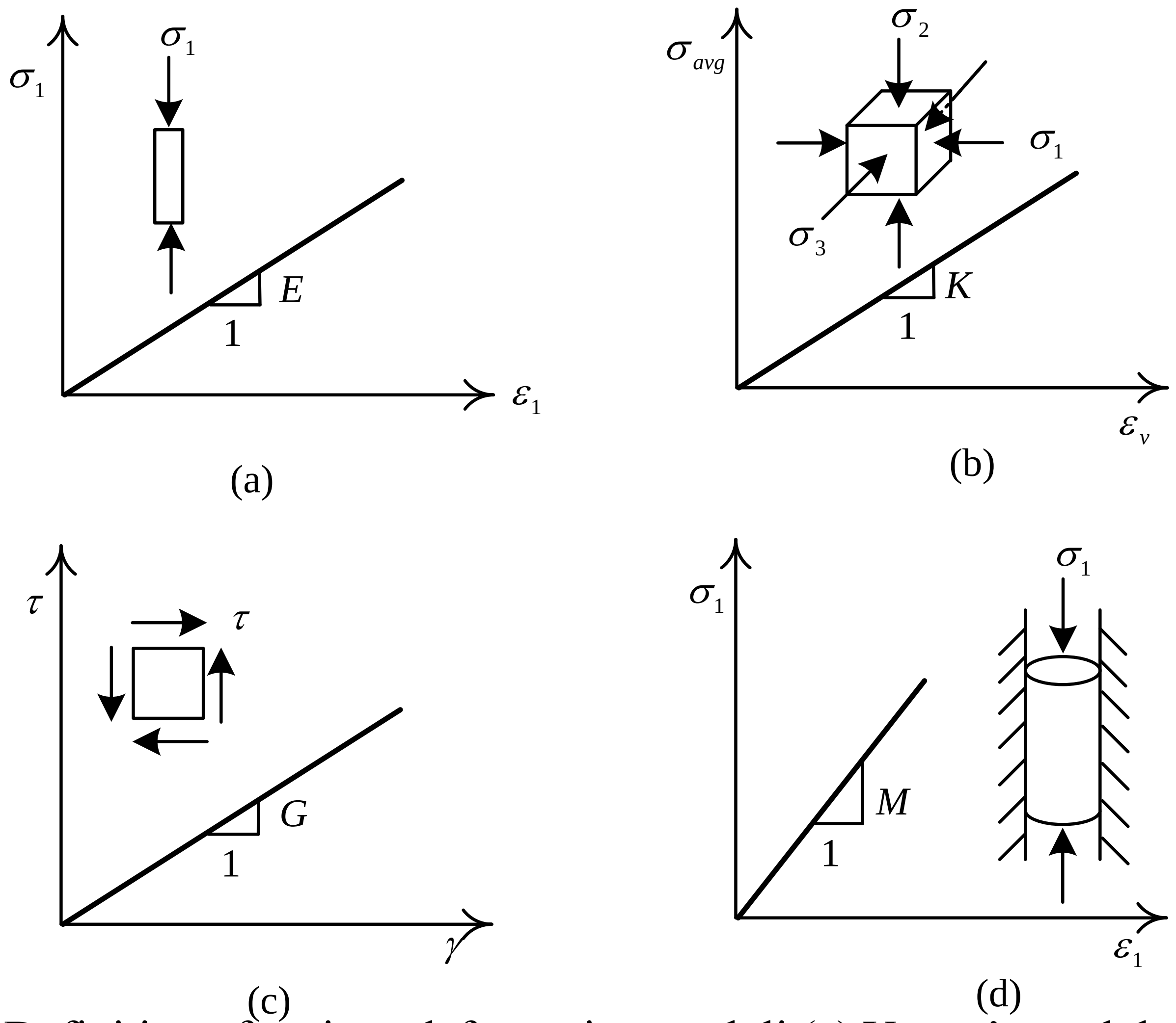

1-D compression test

Oedometer test

E_{oed}

FIGURE 2.22 Definition of various deformation moduli (a) Young's modulus (b) bulk modulus (c) shear modulus (d) constrained modulus

TABLE 2.13 Relations between elastic deformation parameters (after Chen and Saleeb, 1982)

	G	E	M	K	λ	μ
G, E	G	E	$\dfrac{G(4G-E)}{3G-E}$	$\dfrac{GE}{9G-3E}$	$\dfrac{G(E-2G)}{3G-E}$	$\dfrac{E-2G}{2G}$
G, M	G	$\dfrac{G(3M-4G)}{M-G}$	M	$M-\dfrac{4G}{3}$	$M-2G$	$\dfrac{M-2G}{2(M-G)}$
G, K	G	$\dfrac{9GK}{3K+G}$	$K+\dfrac{4G}{3}$	K	$K-\dfrac{2G}{3}$	$\dfrac{3K-2G}{2(3K+G)}$
G, λ	G	$\dfrac{G(3\lambda+2G)}{\lambda+G}$	$\lambda+2G$	$\lambda+\dfrac{2G}{3}$	λ	$\dfrac{\lambda}{2(\lambda+G)}$
G, μ	G	$2G(1+\mu)$	$\dfrac{2G(1-\mu)}{1-2\mu}$	$\dfrac{2G(1+\mu)}{3(1-2\mu)}$	$\dfrac{2G\mu}{1-2\mu}$	μ

	G	E	M	K	λ	μ
E, K	$\dfrac{3KE}{9K-E}$	E	$\dfrac{K(9K+3E)}{9K-E}$	K	$\dfrac{K(9K-3E)}{9K-E}$	$\dfrac{3K-E}{6K}$
E, μ	$\dfrac{E}{2(1+\mu)}$	E	$\dfrac{E(1-\mu)}{(1+\mu)(1-2\mu)}$	$\dfrac{E}{3(1-2\mu)}$	$\dfrac{\mu E}{(1+\mu)(1-2\mu)}$	μ
K, λ	$\dfrac{3(K-\lambda)}{2}$	$\dfrac{9K(K-\lambda)}{3K-\lambda}$	$3K-2\lambda$	K	λ	$\dfrac{\lambda}{3K-\lambda}$
K, M	$\dfrac{3(M-K)}{4}$	$\dfrac{9K(M-K)}{3K+M}$	M	K	$\dfrac{3K-M}{2}$	$\dfrac{3K(2M-1)+l}{3K(2M+1)-l}$
$K \ \mu$	$\dfrac{3K(1-2\mu)}{2(1+\mu)}$	$3K(1-2\mu)$	$\dfrac{3K(1-2\mu)}{1+\mu}$	K	$\dfrac{3K\mu}{1+\mu}$	μ

8.2.2 Plastic behavior consideration

$$\Delta\varepsilon = \Delta\varepsilon^e + \Delta\varepsilon^p \qquad \{\Delta\varepsilon\} = \{\Delta\varepsilon^e\} + \{\Delta\varepsilon^p\}$$

$$\{\Delta\sigma\} = [D^e]\{\Delta\varepsilon^e\} \qquad \{\Delta\varepsilon^e\} = [D^e]^{-1}\{\Delta\sigma\}$$

$$\{\Delta\varepsilon\} = \{\Delta\varepsilon^e\} + \{\Delta\varepsilon^p\} = [D^e]^{-1}\{\Delta\sigma\} + \{\Delta\varepsilon^p\}$$

$$[D^e]\{\Delta\varepsilon\} = \{\Delta\sigma\} + [D^e]\{\Delta\varepsilon^p\}$$

$$\{\Delta\sigma\} = [D^e]\{\Delta\varepsilon\} - [D^e]\{\Delta\varepsilon^p\}$$

According to the flow rule, we have

$$\{\Delta\sigma\} = \left([D^e] - [D^p]\right)\{\Delta\varepsilon\} = [D^{ep}]\{\Delta\varepsilon\} \tag{8.15}$$

$$[D^{ep}] = [D^e] - [D^p] \tag{8.16}$$

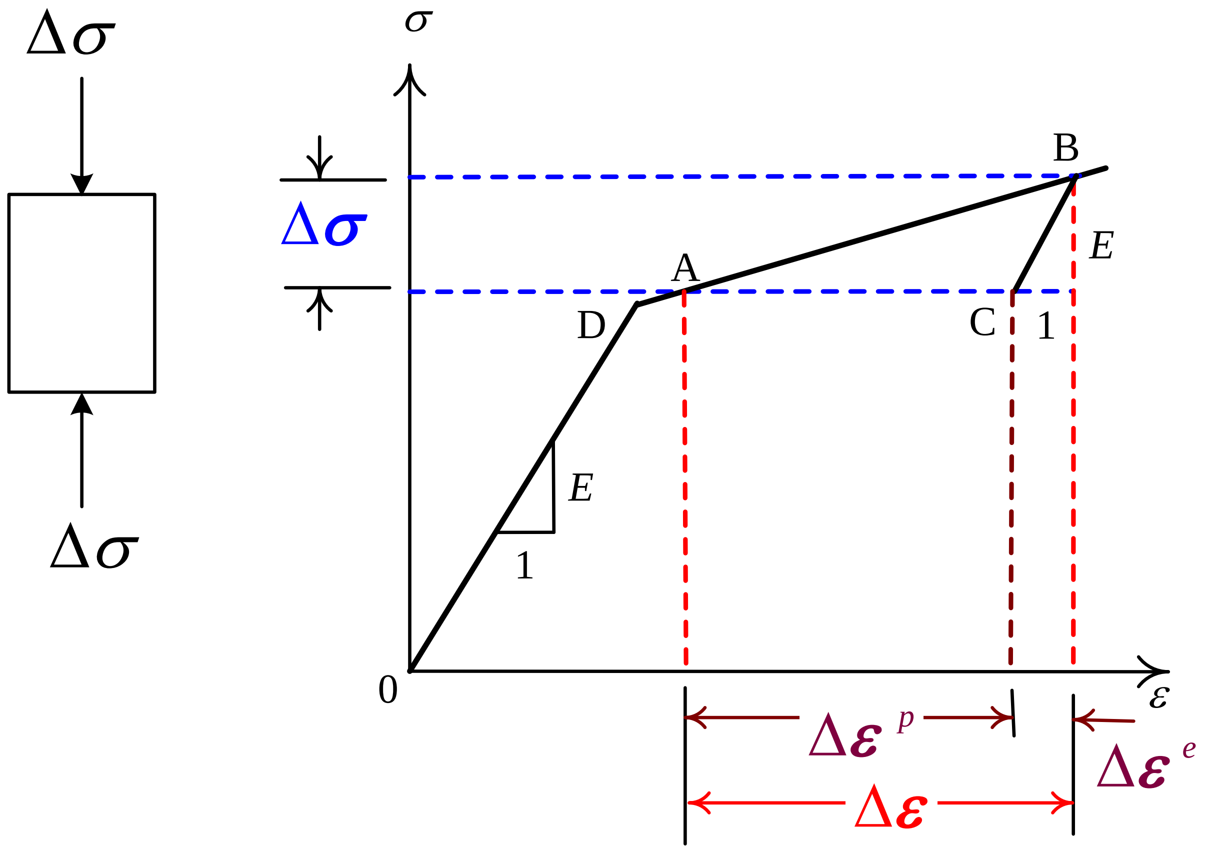

FIGURE 8.3 Total strain increment, elastic strain increment, and plastic strain increment

$[D^p]$ is the stress-strain or constitutive matrix for **plastic material**, which is a function of Y and Q

$[D^{ep}]$ is the stress-strain or constitutive matrix for **elastoplastic** material

Known the $[D^{ep}]$, the stiffness matrix for each element can be derived following Eq. 8.6, and global stiffness matrix can therefore assembled for all elements.

$$[K_E] = \int_{vol} [B]^T [D][B] dV \quad (8.6) \qquad \{\Delta\sigma\} = \left([D^e] - [D^p]\right)\{\Delta\varepsilon\} = [D^{ep}]\{\Delta\varepsilon\} \quad (8.15)$$

Associated flow rule: when $Y=Q$, $[D^{ep}]$ is symmetric matrix.

Non-associated flow rule: when $Y \neq Q$, $[D^{ep}]$ is not symmetric.

Required soil parameters: ***E, μ,*** and the **parameters for *Y* and *Q***

8.2.3 Nonlinear behavior consideration

1. $\{\Delta F_{ext}\}=\Delta\lambda_i\{F_{ext}\}$

2. $[K_E]$ and $[K]$ should consider Y and Q

3. $[K]\{q\}=\{F\}$, $\{q\}=[K]^{-1}\{F\}$ (8.7)

4. $\{\varepsilon\}=[B]\{q\}$

Iteration scheme
(e.g. Newton -Raphson Method)

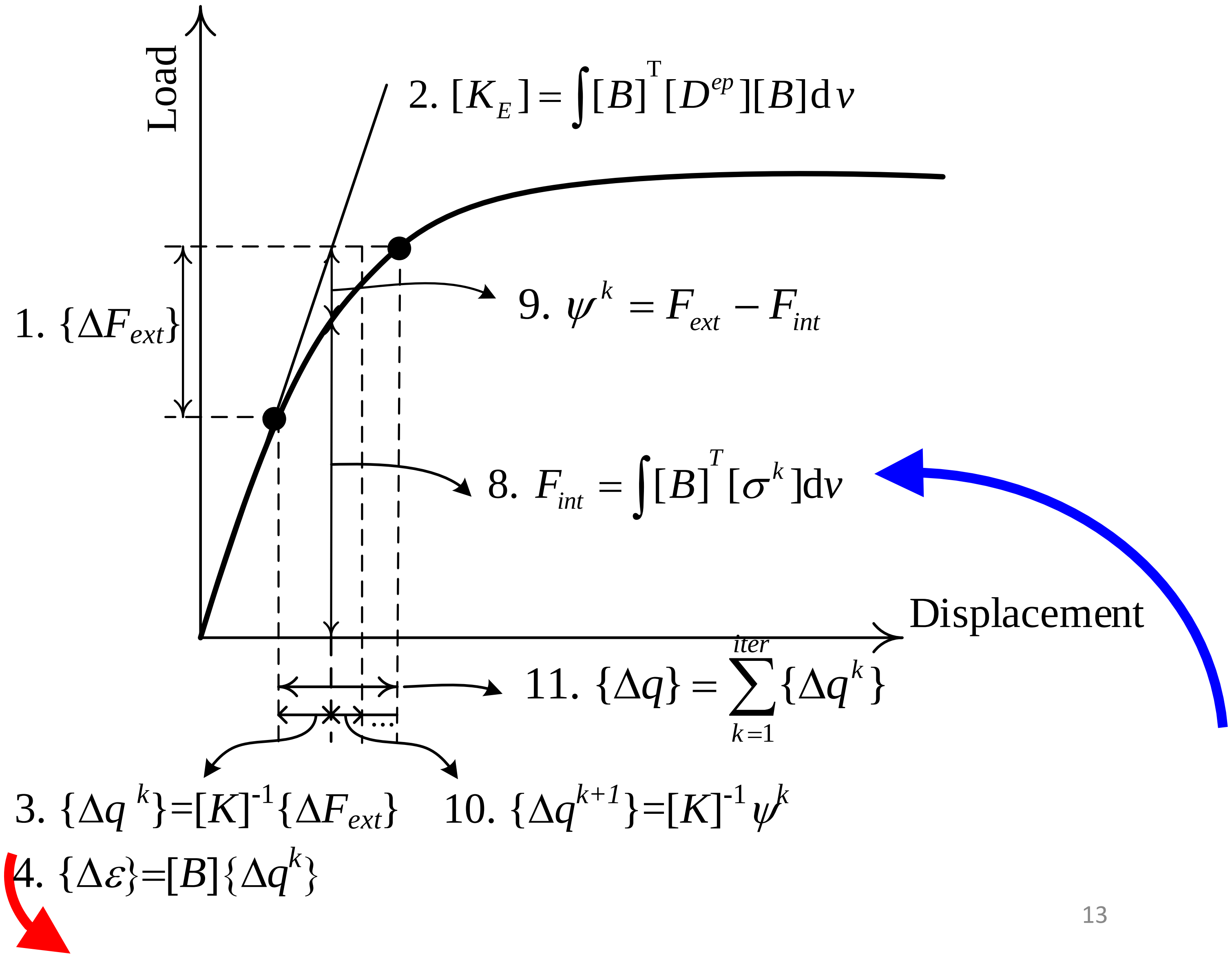

FIGURE 8.4 Procedure for nonlinear finite element computation

5. $[D^{ep}]=[D^{e}]-[D^{p}]$ (8.16)

6. $\{\varepsilon\}/m$, $\{\sigma\}=[D]\{\varepsilon\}/m$

7. Update the new stress state by $\{\sigma^{k}\}=\{\sigma^{k\text{-}1}\}+\{\Delta\sigma\}$ and hardening parameters of the yield function.

Stress integration scheme(e.g. Forward Euler method with subincrements)

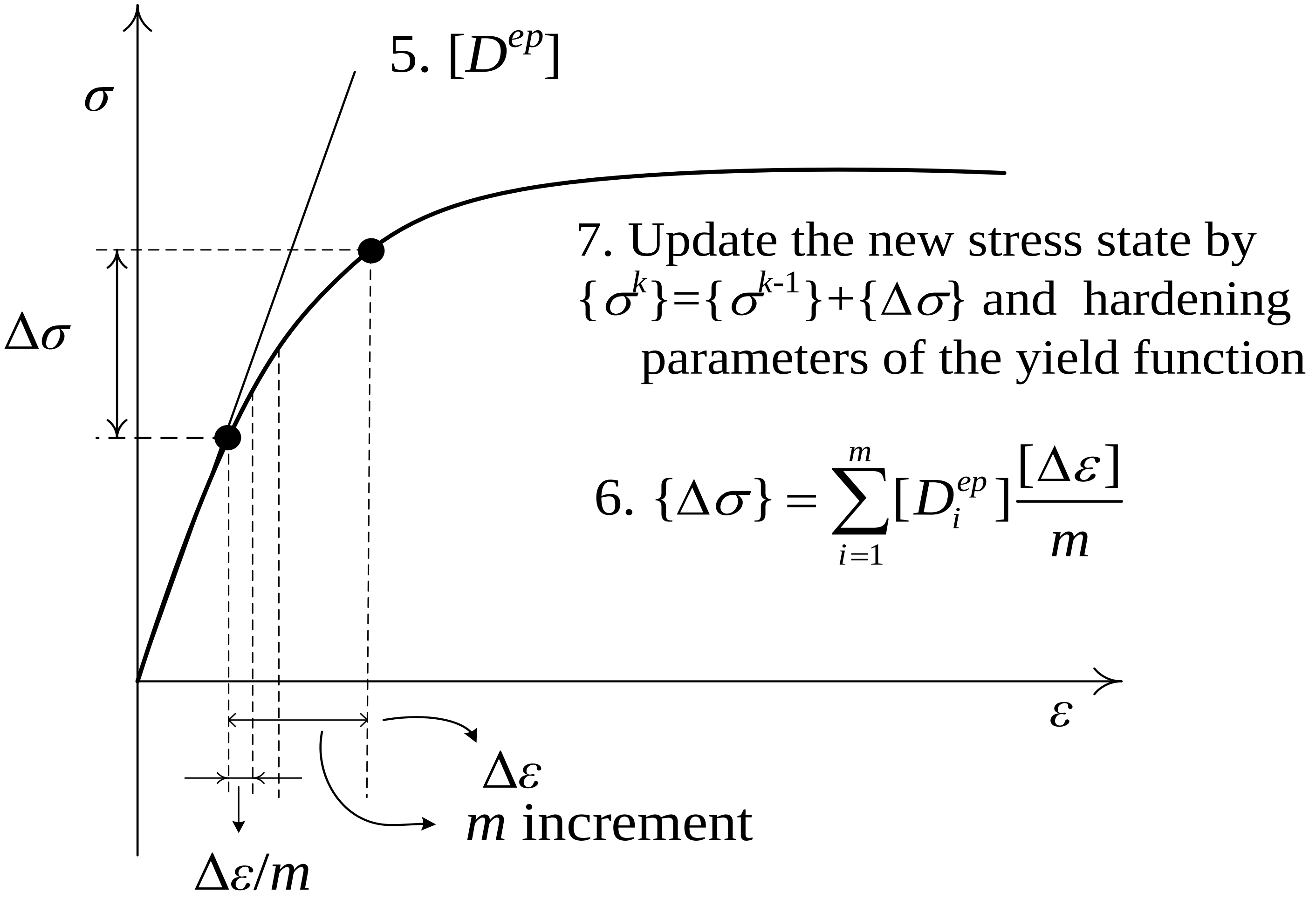

8. Obtain F_{int}

$$\int_{vol} [B]^T [\sigma]\, d(vol) = \int_{vol} [N]^T \{G\}\, d(vol) + \int_{area} [N]^T [T]\, d(area) \quad (8.5)$$

9. $$\frac{|F_{ext} - F_{int}|}{|F_{ext}|} < \text{tolerated error} \quad (8.18)$$

10. Use ψ as external force, repeat the procedure

11. Update the displacement increment $\{\Delta q\}$

Iteration scheme
(e.g. Newton -Raphson Method)

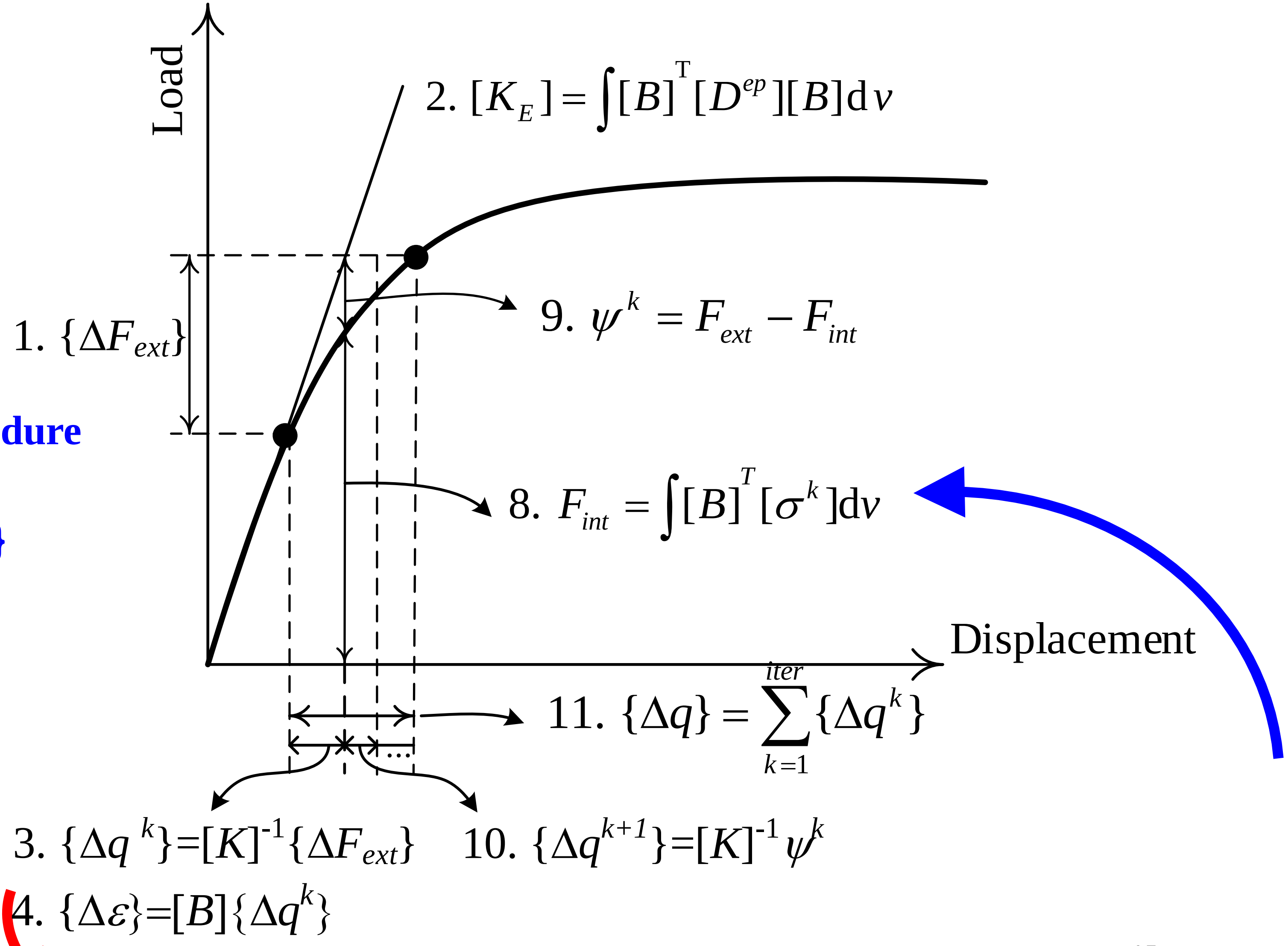

FIGURE 8.4 Procedure for nonlinear finite element computation

Detailed computation procedure

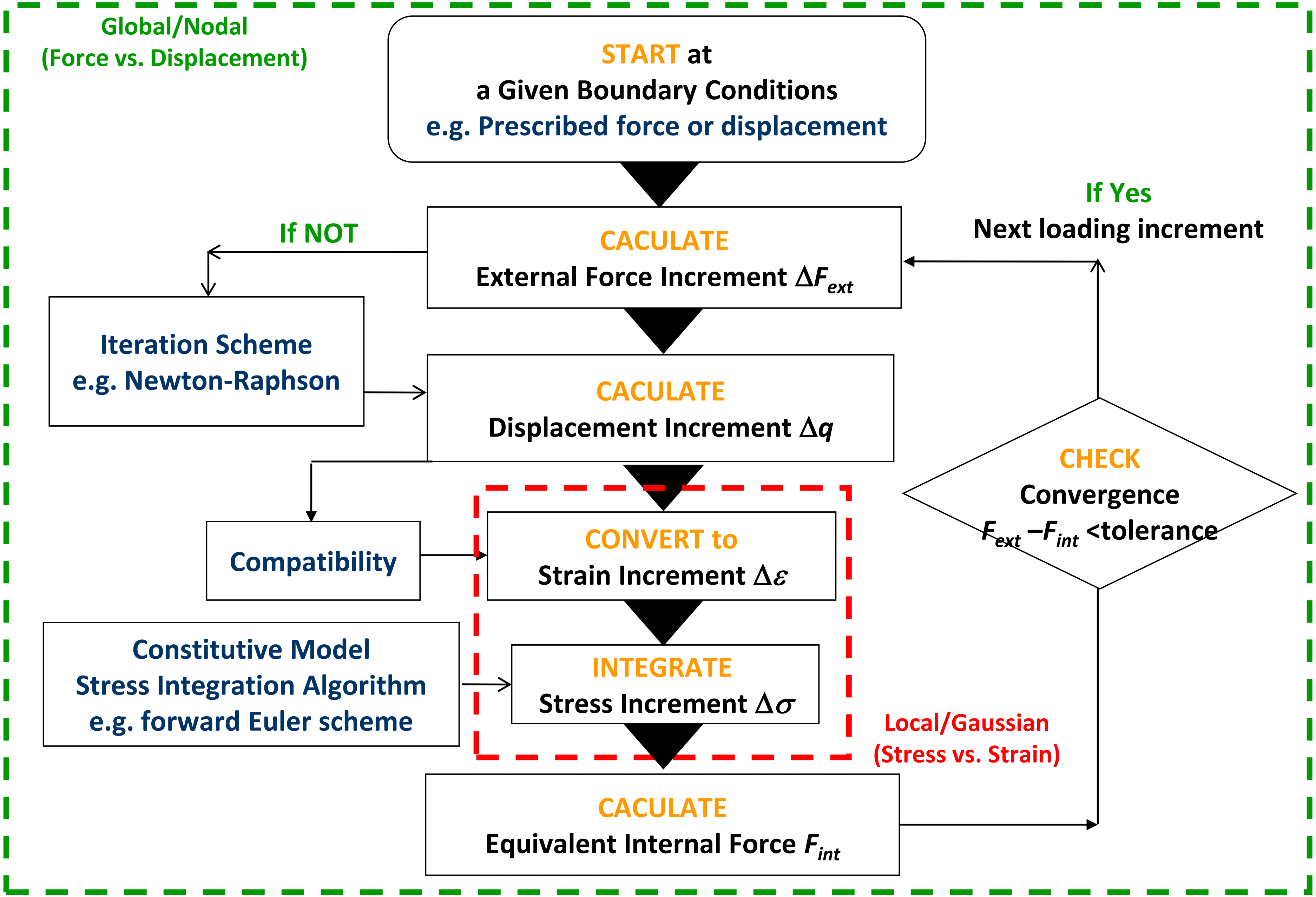

Courtesy of KH Yang

8.2.4 Types of elements

(1) Solid elements

T3 elements (CST elements):

the strain variation is constant

T6 elements (LST elements):

the strain variation is linear

T15 elements (CuST elements):

the strain variation is cubic or nonlinear

$$\{\boldsymbol{u}\}=[\boldsymbol{N}]\{\boldsymbol{q}\} \qquad (8.2)$$

$$\{\boldsymbol{\varepsilon}\}=[\boldsymbol{L}]\{\boldsymbol{u}\}=[\boldsymbol{L}][\boldsymbol{N}]\{\boldsymbol{q}\}=[\boldsymbol{B}]\{\boldsymbol{q}\} \qquad (8.3)$$

$$[L]= \partial/\partial x\,,\ \partial/\partial y$$

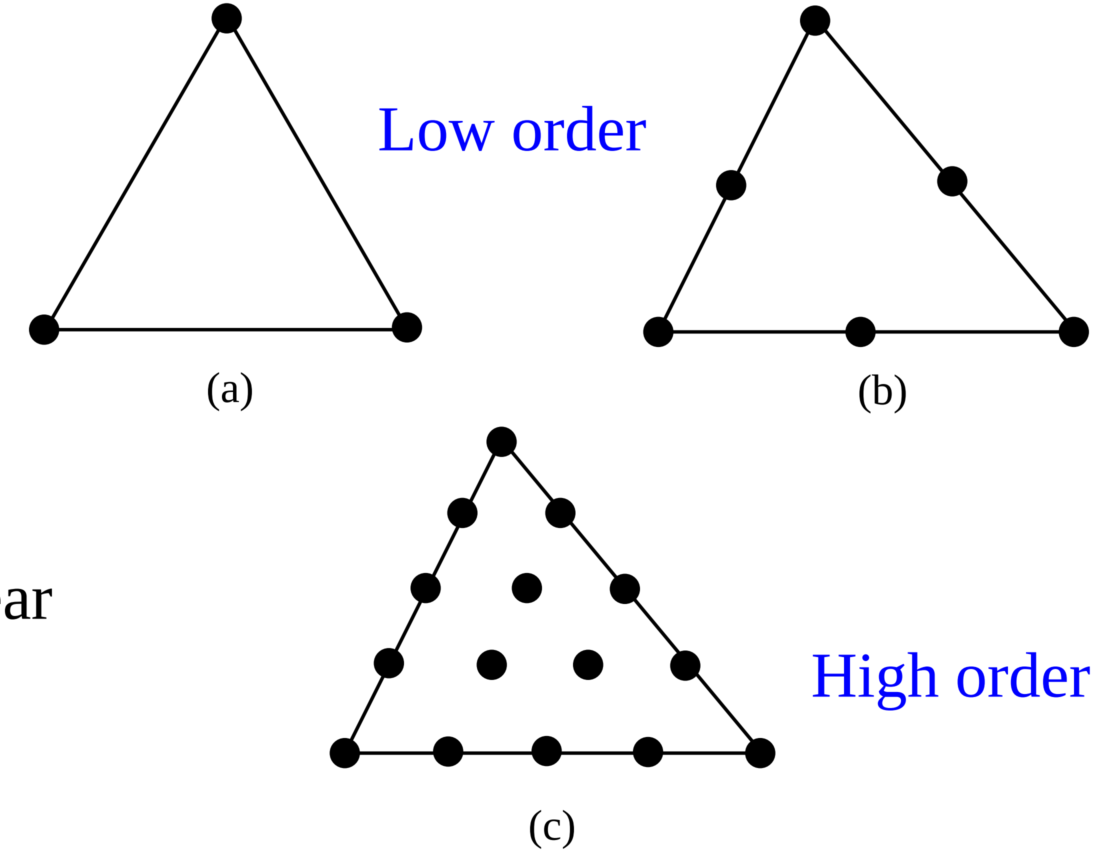

FIGURE 8.5 Triangular elements (a) CST element (b) LST element (c) CuST element

Quadrilateral elements:

Q4 elements:
strain change is linear (low order)

Q8 elements:
strain change is quadratic (nonlinear, high order)

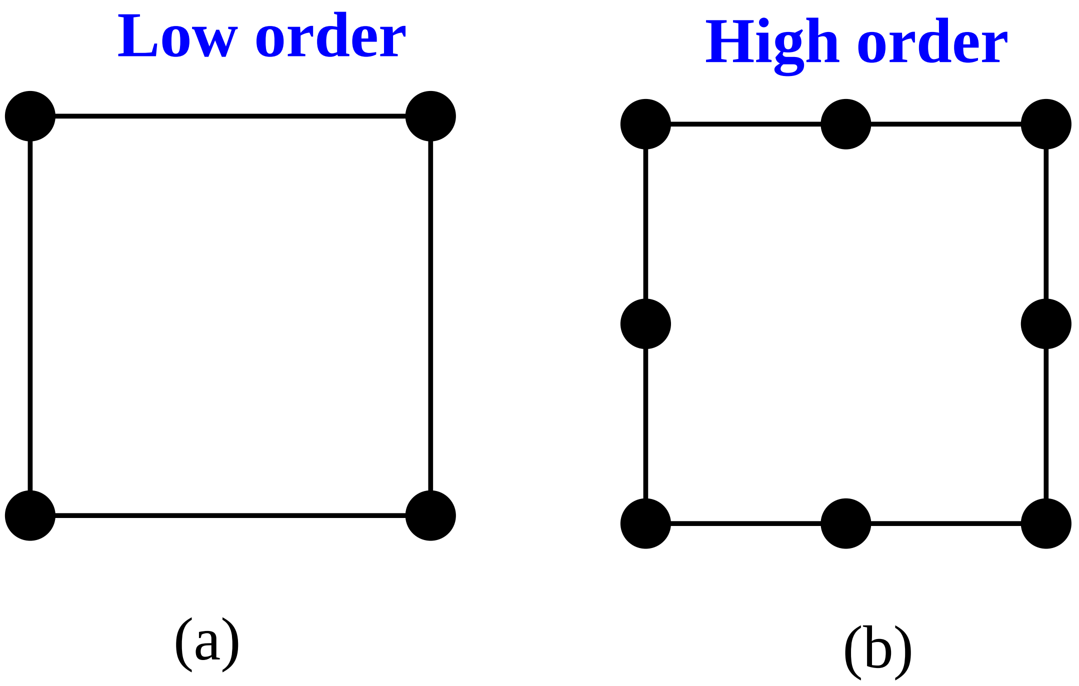

FIGURE 8.6 Quadrilateral elements
(a) Q4 element (b) Q8 element

Accuracy?

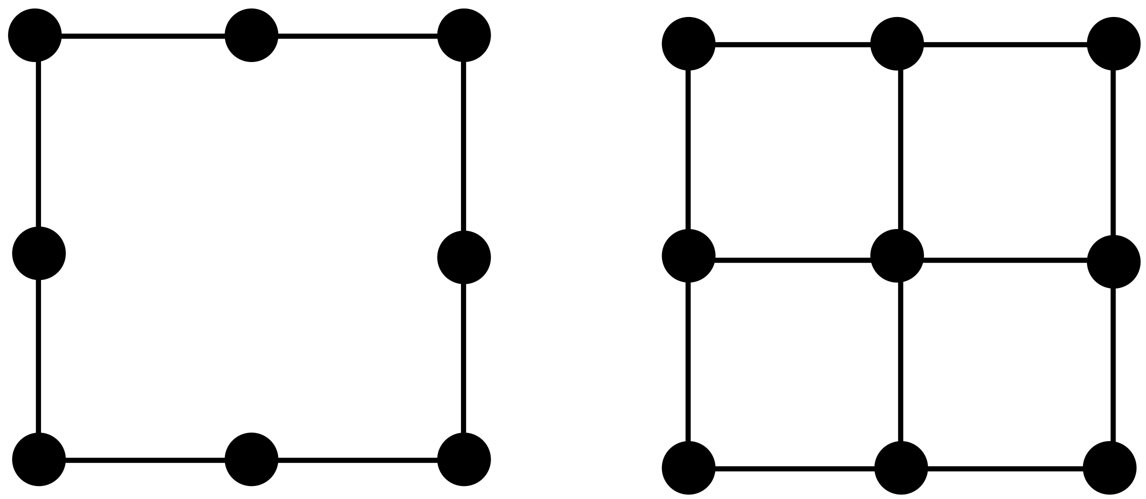

One Q8 element   Four Q4 element

FIGURE 8.7 Comparison of accuracy between a Q8 element and four Q4 elements

(2) Bar elements, truss elements,

Anchor elements

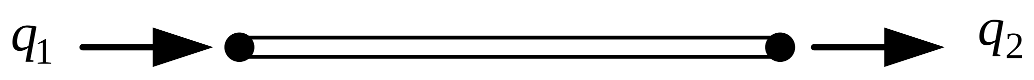

FIGURE 8.8 Two-node bar element

(3) Beam elements, plate elements

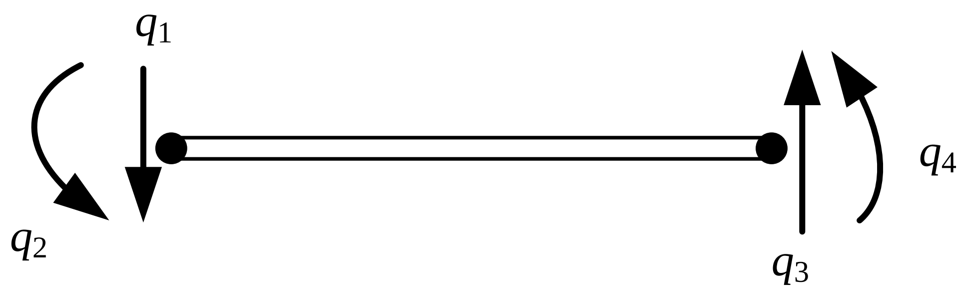

FIGURE 8.9 Two-node beam element

(4) Interface elements

- The interface element connects structures and soil
- With or without thickness
- Has a large normal stiffness but relatively small shear stiffness
- It can simulate the relative displacement between soil and structures.
- R_{inter} is often used to represent the behavior of interface element by reducing the shear strength of adjacent soils

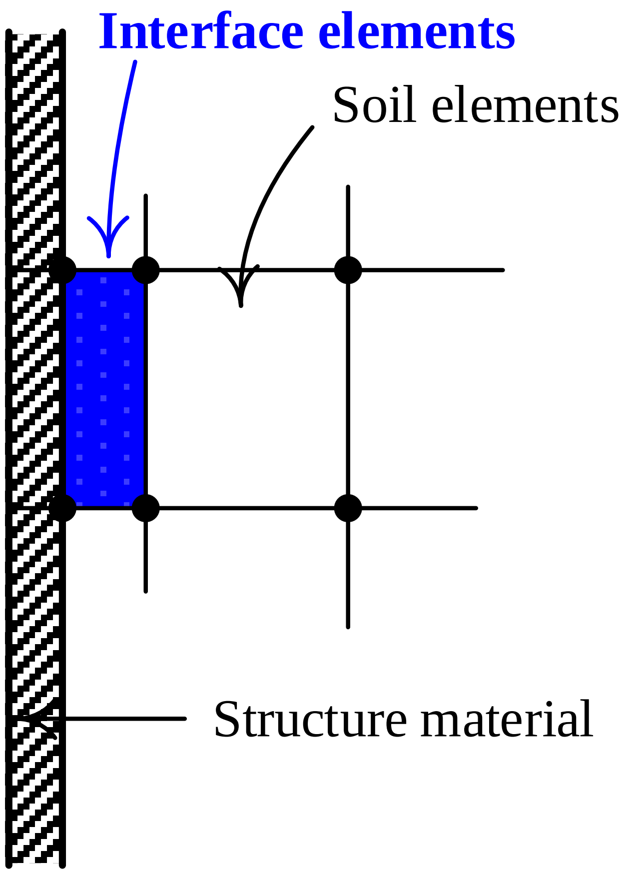

FIGURE 8.10 Interface element

R_{inter}=1.0 ? R_{inter}=0.0 ? R_{inter}=0.5 ?

No interface elements?

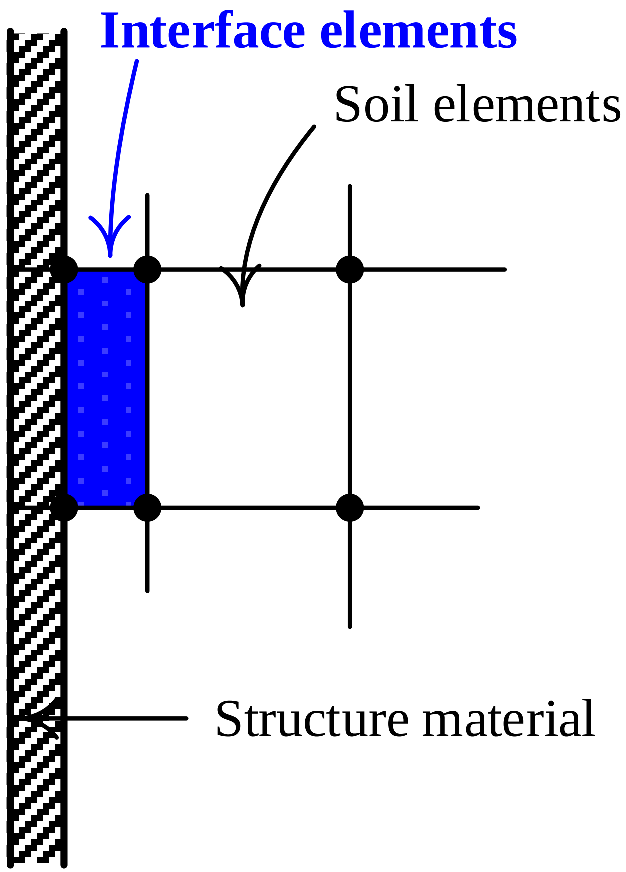

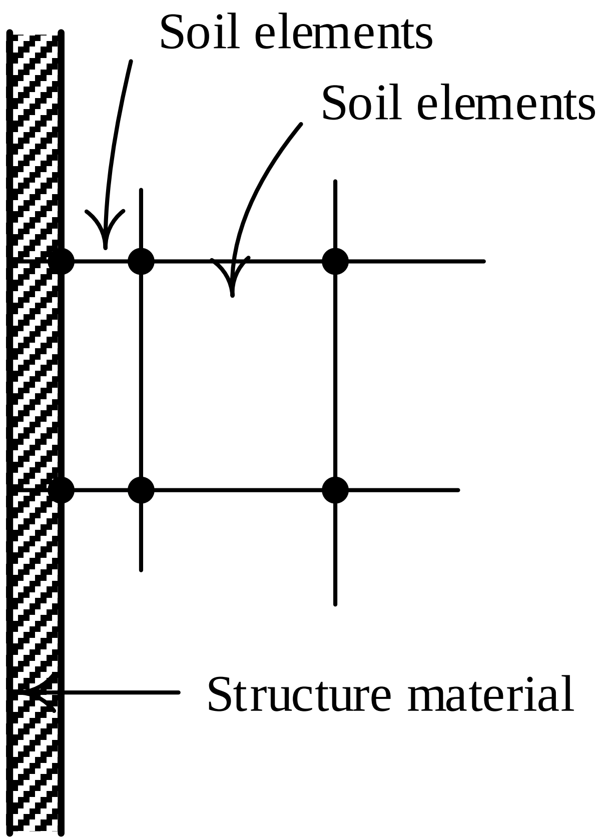

8.3 Effective stress analysis and total stress analysis

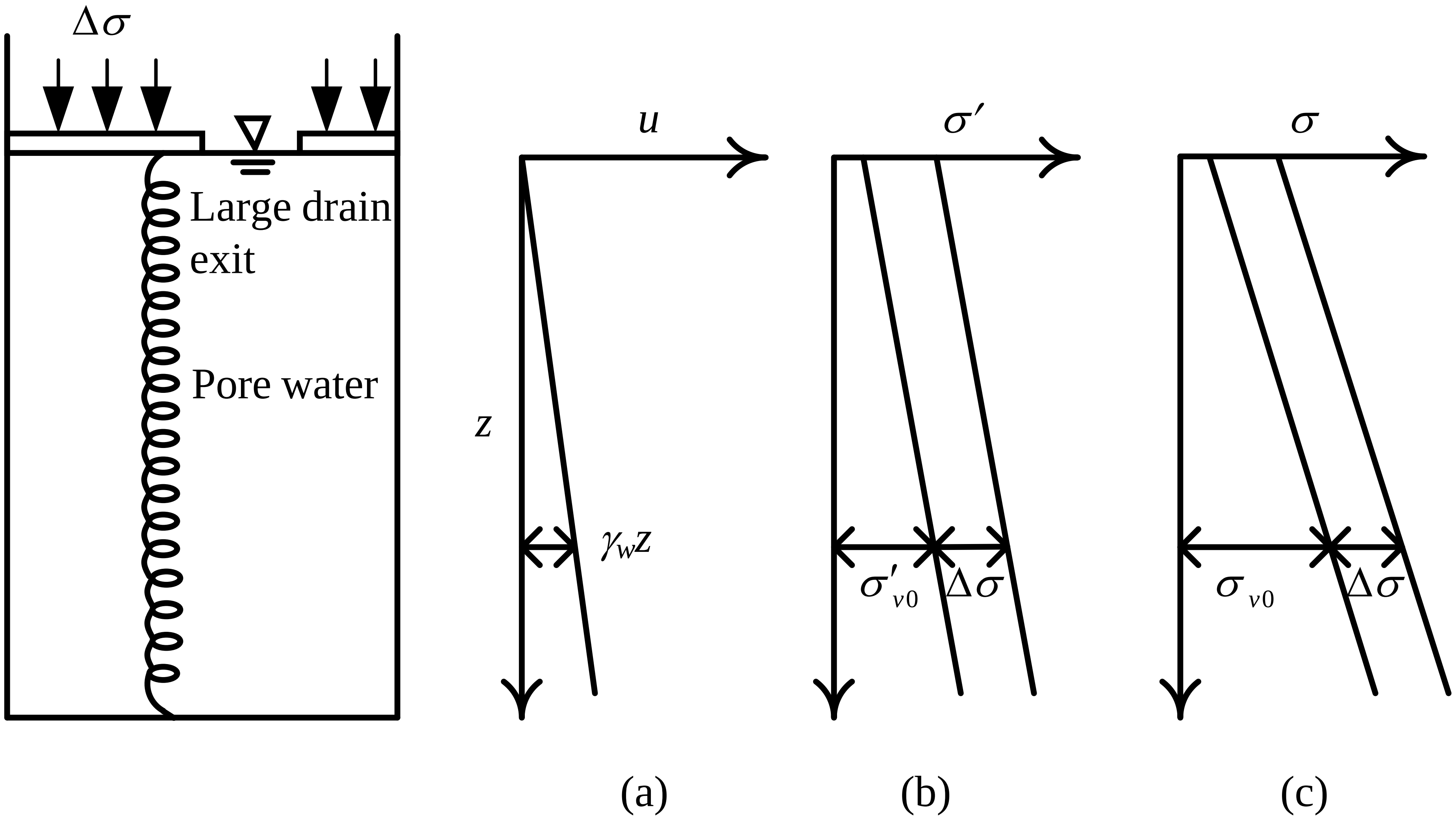

FIGURE 2.27 Drained behavior for saturated coarse granular

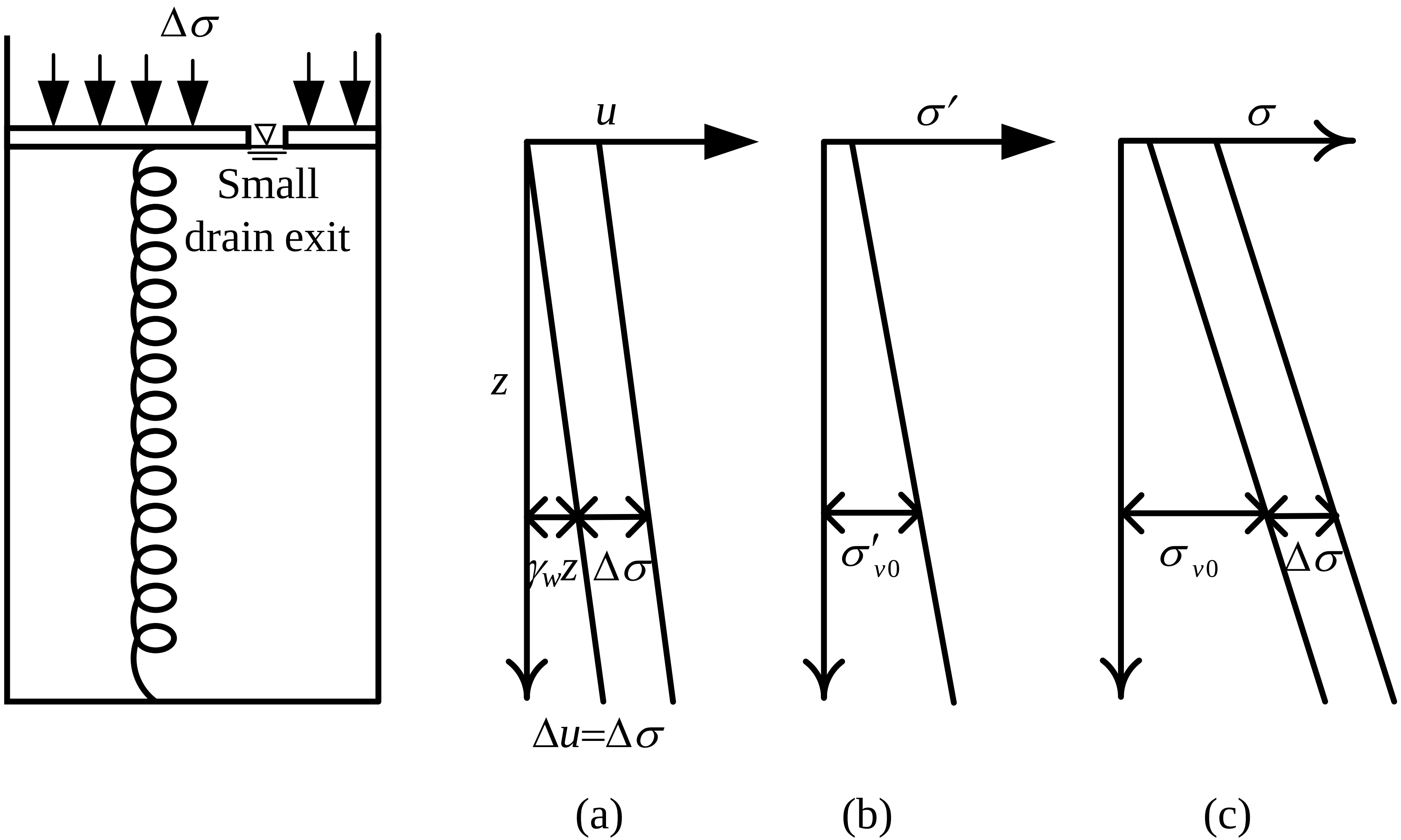

FIGURE 2.28 Undrained behavior

Effective stress analysis: soil and water are analyzed, respectively
Drained analysis: excess pore water pressure can be dissipated.

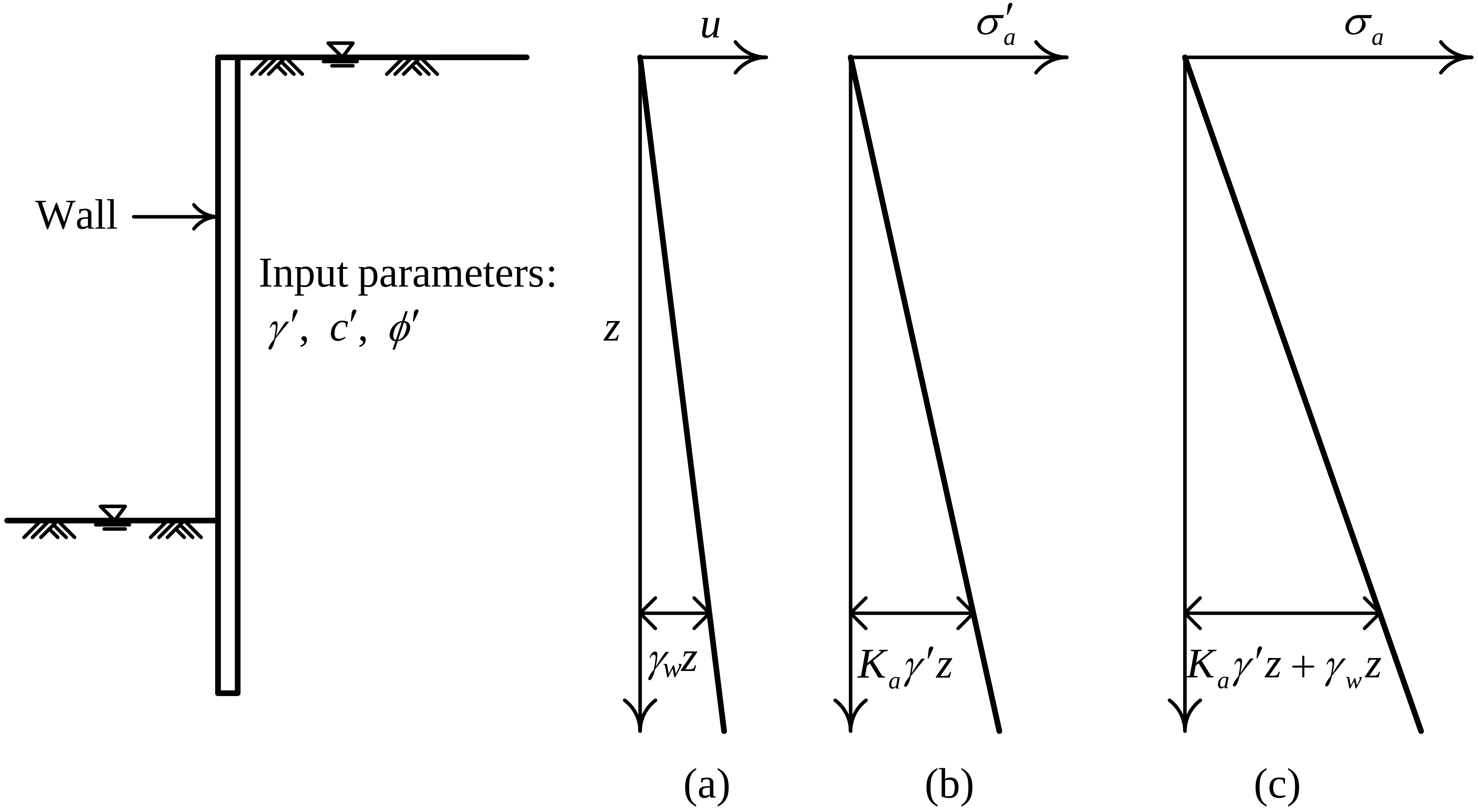

FIGURE 2.29 Active lateral earth pressure (drained analysis)

Effective stress analysis: water and soil were analyzed, respectively
Undrained analysis: excess pore water pressure is not dissipated.

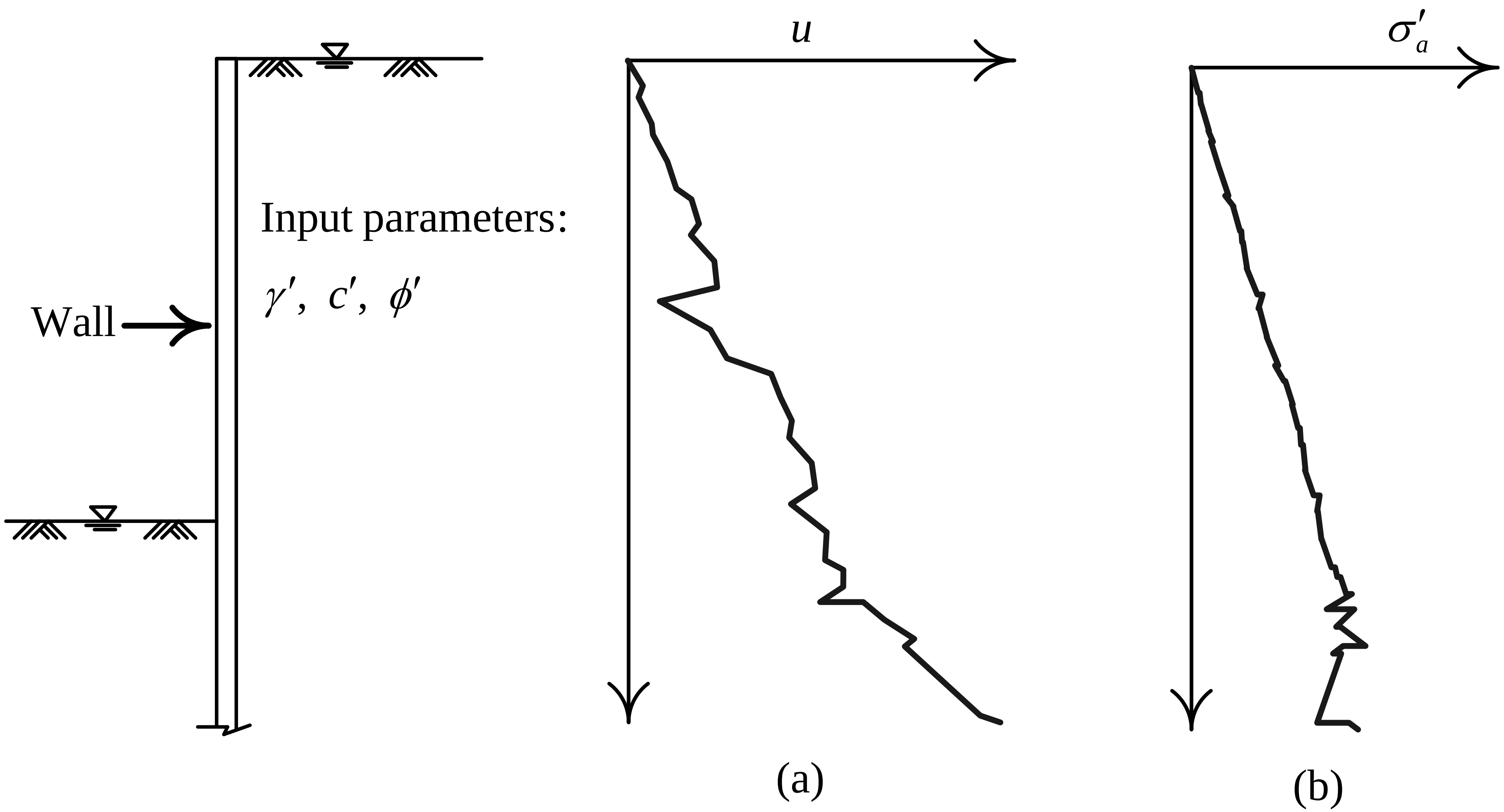

FIGURE 2.30 Active lateral earth pressure (effective stress undrained analysis)

Total stress undrained analysis: soil and water was analyzed as a single material

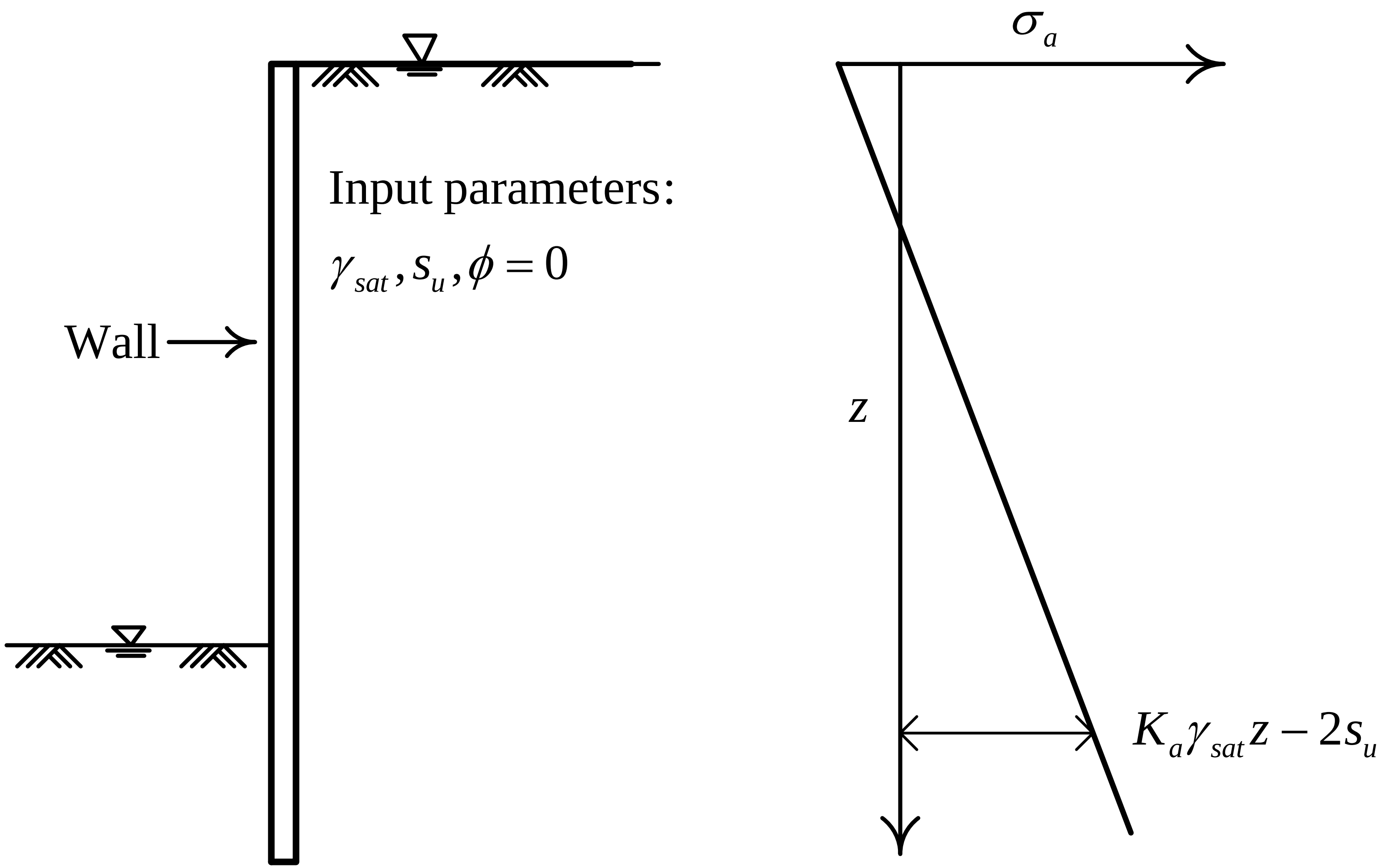

FIGURE 2.32 Active lateral earth pressure (total stress undrained analysis)

Summary

Drained analysis: No excess pore water pressure generation

Effective stress undrained analysis: soil and water are analyzed, respectively. Both the effective stress of the soil and water pressure can be computed simultaneously. The ground water level and water pressure **should be** set. Effective stress parameters such as c', ϕ', γ' ….

Total stress undrained analysis: soil and water are analyzed as a single material. No pore water and pore water pressure exist in the analysis. The ground water level and water pressure **should not** be set. Total stress parameters such as s_u, ϕ=0, γ, ….

Based on the principle of effective stress,

$$\{\Delta\sigma\} = \{\Delta\sigma'\} + \{\Delta u\} \qquad (8.19)$$

In the undrained condition, the soil and pore water will deform simultaneously, so the strain of the soil and pore water should be the same. The effective stress acting on the soil and the pore water pressure of the pore water can be obtained as :

$$\{\Delta\sigma'\} = [D']\{\Delta\varepsilon\} \qquad (8.20)$$

$$\{\Delta u\} = [D_w]\{\Delta\varepsilon\} \qquad (8.21)$$

$$\{\Delta\sigma\} = [D]\{\Delta\varepsilon\} = [D']\{\Delta\varepsilon\} + [D_w]\{\Delta\varepsilon\}$$

$$[D] = [D'] + [D_w] \qquad (8.22)$$

$[D']$ and $[D_w]$ represent the constitutive matrix for the soil and pore water, respectively.

Effective stress undrained analysis

FE computation procedure:

1. Estimate soil effective stress parameters（$c', \phi', E', \mu', \ldots$）
2. Compute water constitutive matrix $[D_w]$ and soil constitutive matrix $[D']$
3. Compute $[D]=[D']+[D_w]$
4. Establish the stiffness matrix $[K]$
5. Use FEM procedure $[K]\{q\}=\{F\}$ to obtain nodal displacement $\{q\}$
6. Compute $\{\varepsilon\}=[B]\{q\}$ to obtain strain $\{\varepsilon\}$
7. Use $\{\sigma'\}=[D']\{\varepsilon\}$ to obtain $\{\sigma'\}$
8. Use $\{\sigma_w\}=[D_w]\{\varepsilon\}$ obtain $\{\sigma_w\}$

Total stress undrained analysis

FE computation procedure:

1. Estimate soil total stress parameters（c, ϕ, E, μ, γ）
2. Compute the constitutive matrix [D]
3. Establish the stiffness matrix [K]
4. Use FEM procedure, $[K][q]=[F]$, to obtain nodal displacement [q]
5. Compute $\{\varepsilon\}=[B][q]$ to obtain strain$\{\varepsilon\}$
6. Use $[\sigma]=[D]\{\varepsilon\}$ to obtain [σ]

The coupled analysis:

Couple the continuity of equation or general consolidation equation with the constitutive and equilibrium equations.

In addition to the parameters **of soil models**, the coupled analysis also requires the **coefficient of permeability and loading time**.

The coupled method uses **displacement** and **porewater pressure** as unknowns and therefore results in both displacement and porewater pressure degrees of freedom at element nodes

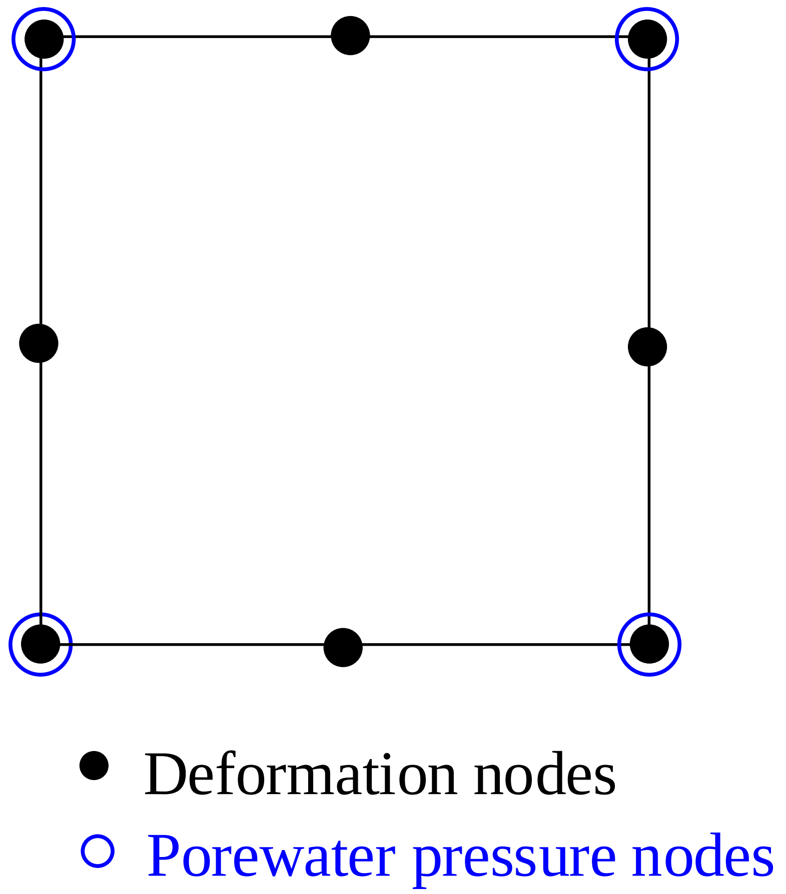

FIGURE 8.11 A element for the coupled analysis (eight deformation nodes and four porewater pressure nodes)

8.4 Commonly used soil models and related parameters

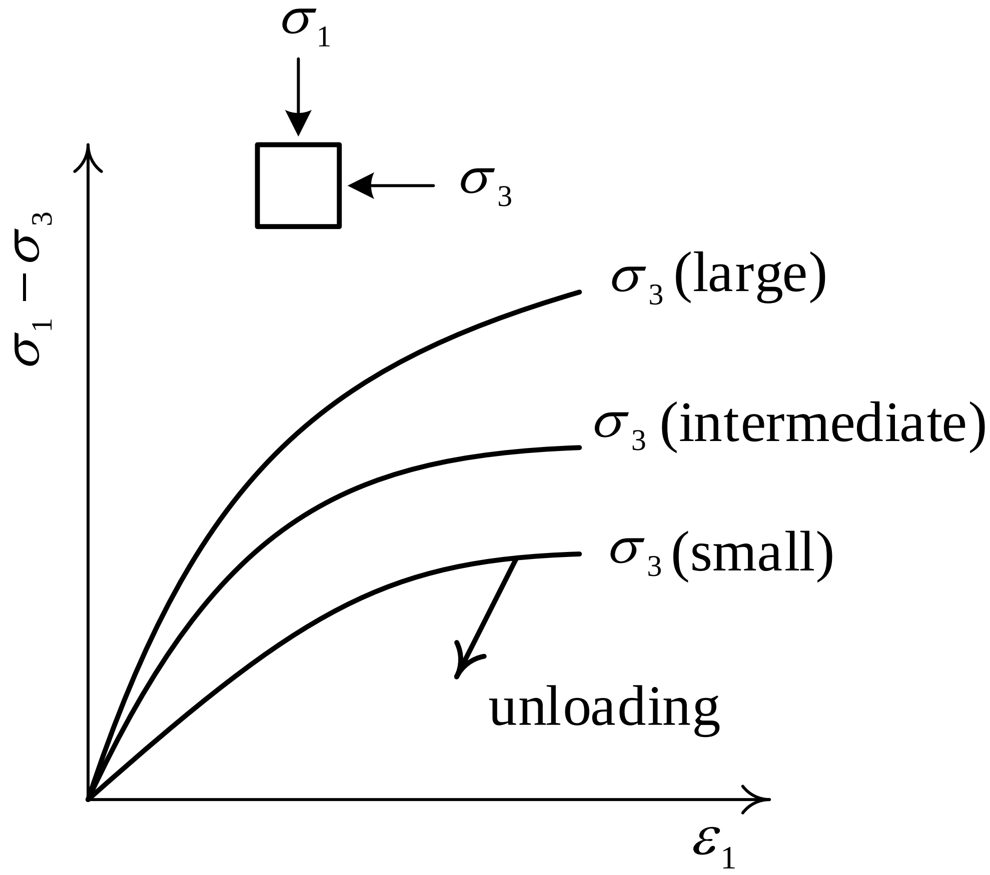

FIGURE 8.12 Typical stress-strain relations of soils

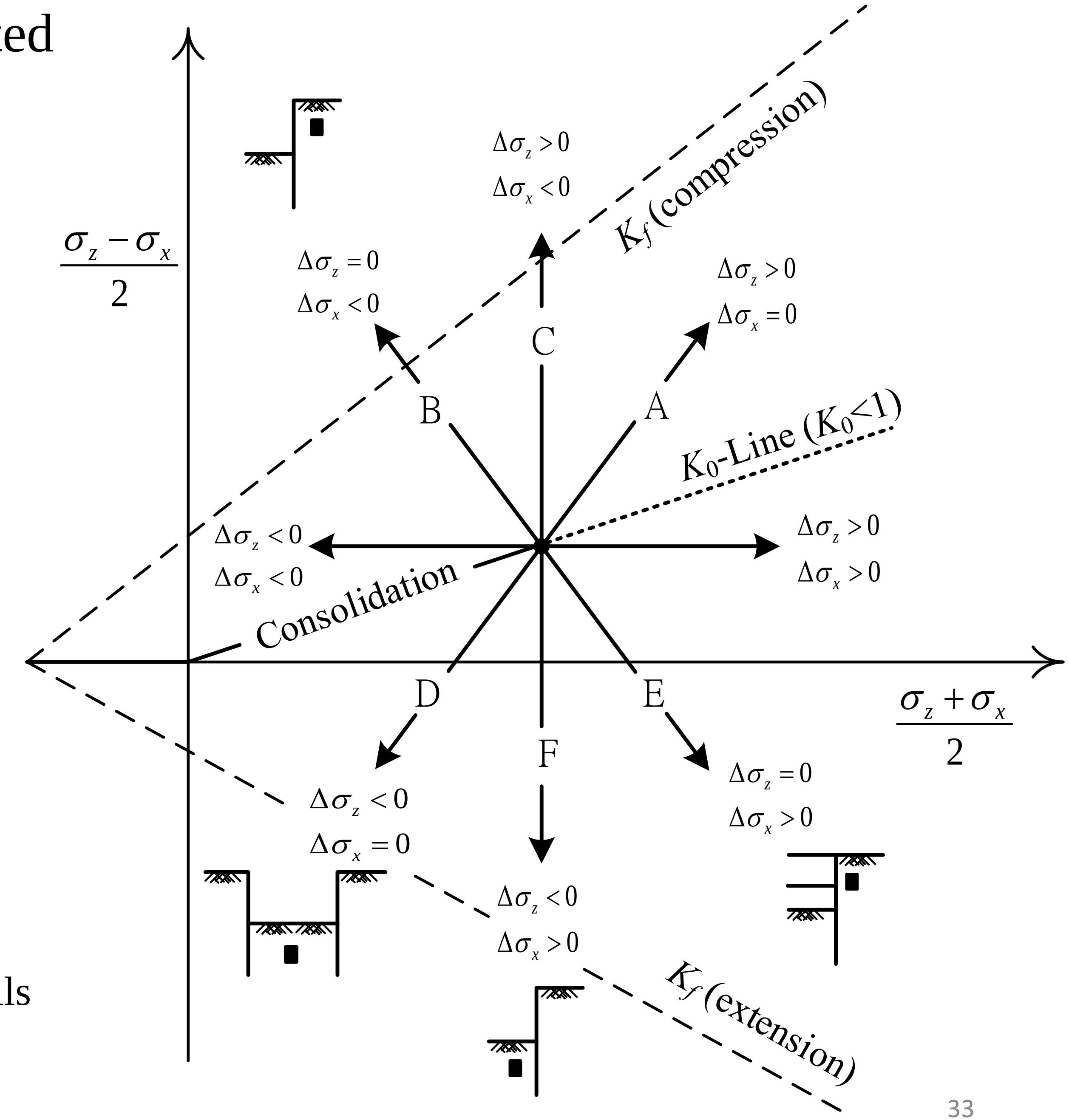

8.4.1 Mohr-Coulomb (MC) model – linear elastoplastic model

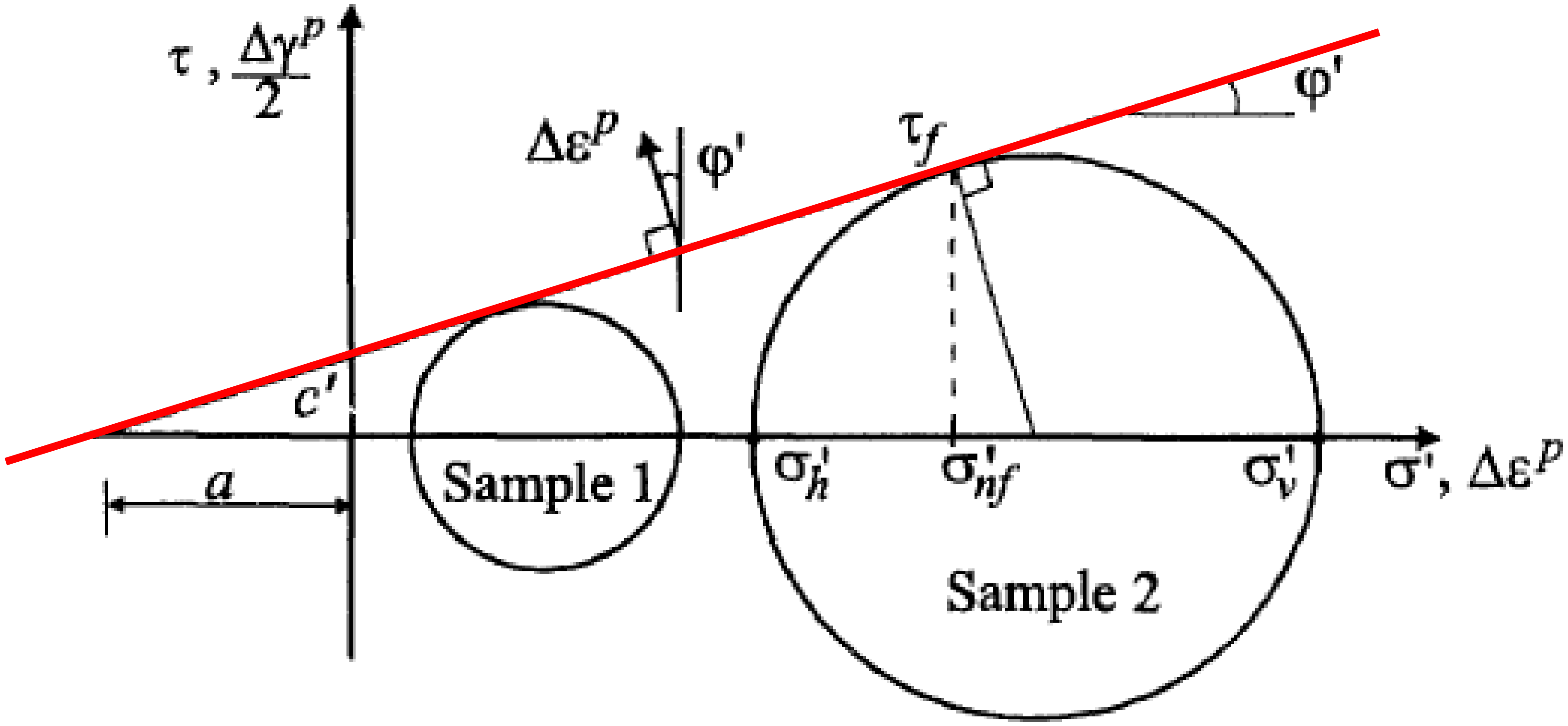

$$\tau_f = c' + \sigma'_{nf} \tan\varphi'$$

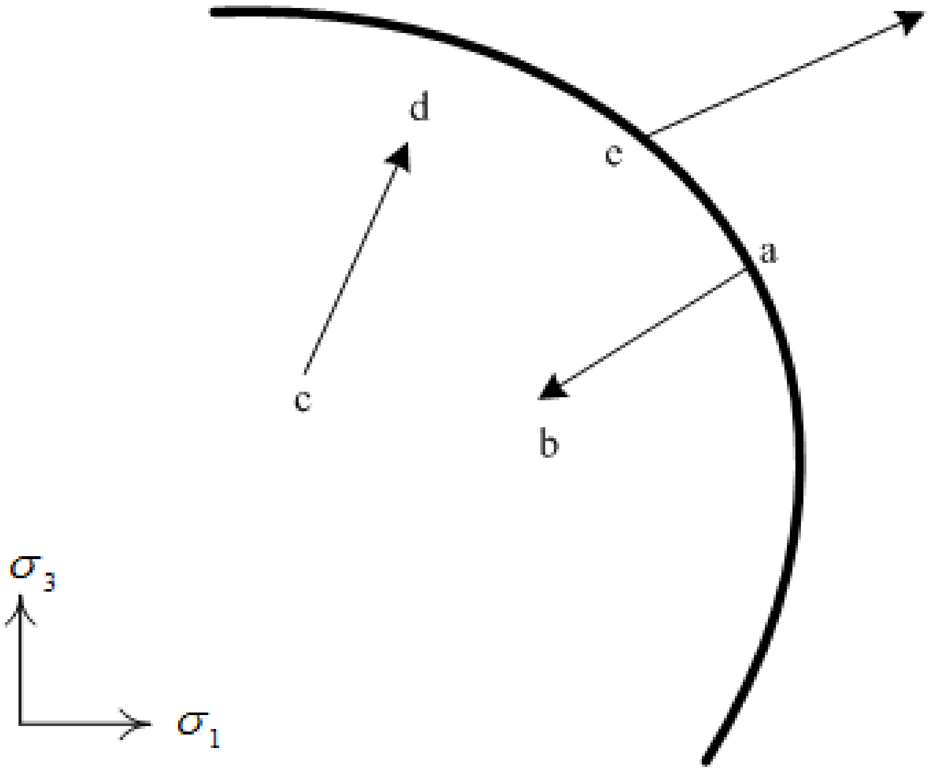

Y is fixed and defined by the Mohr-Coulomb failure criterion

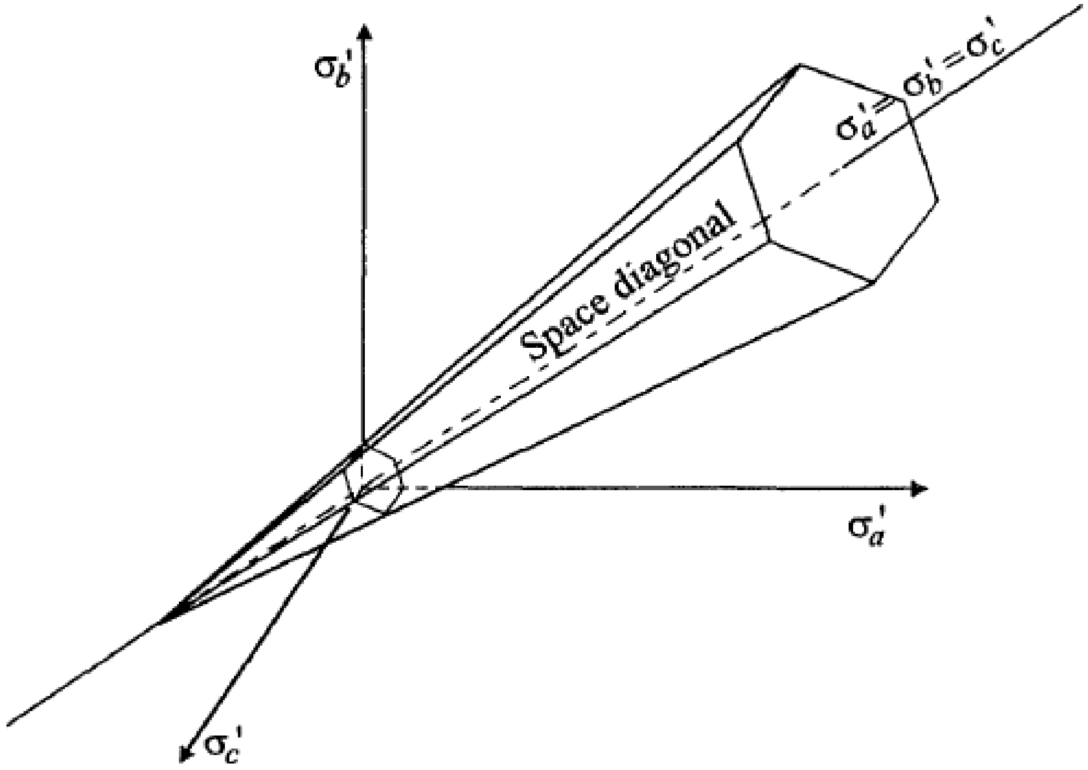

Mohr-Coulomb yield surface

$$[K_E] = \int_{vol} [B]^T [D][B] dV \qquad (8.6)$$

$$\{\Delta\sigma\} = \left([D^e] - [D^p]\right)\{\Delta\varepsilon\} = [D^{ep}]\{\Delta\varepsilon\}$$

(8.15)

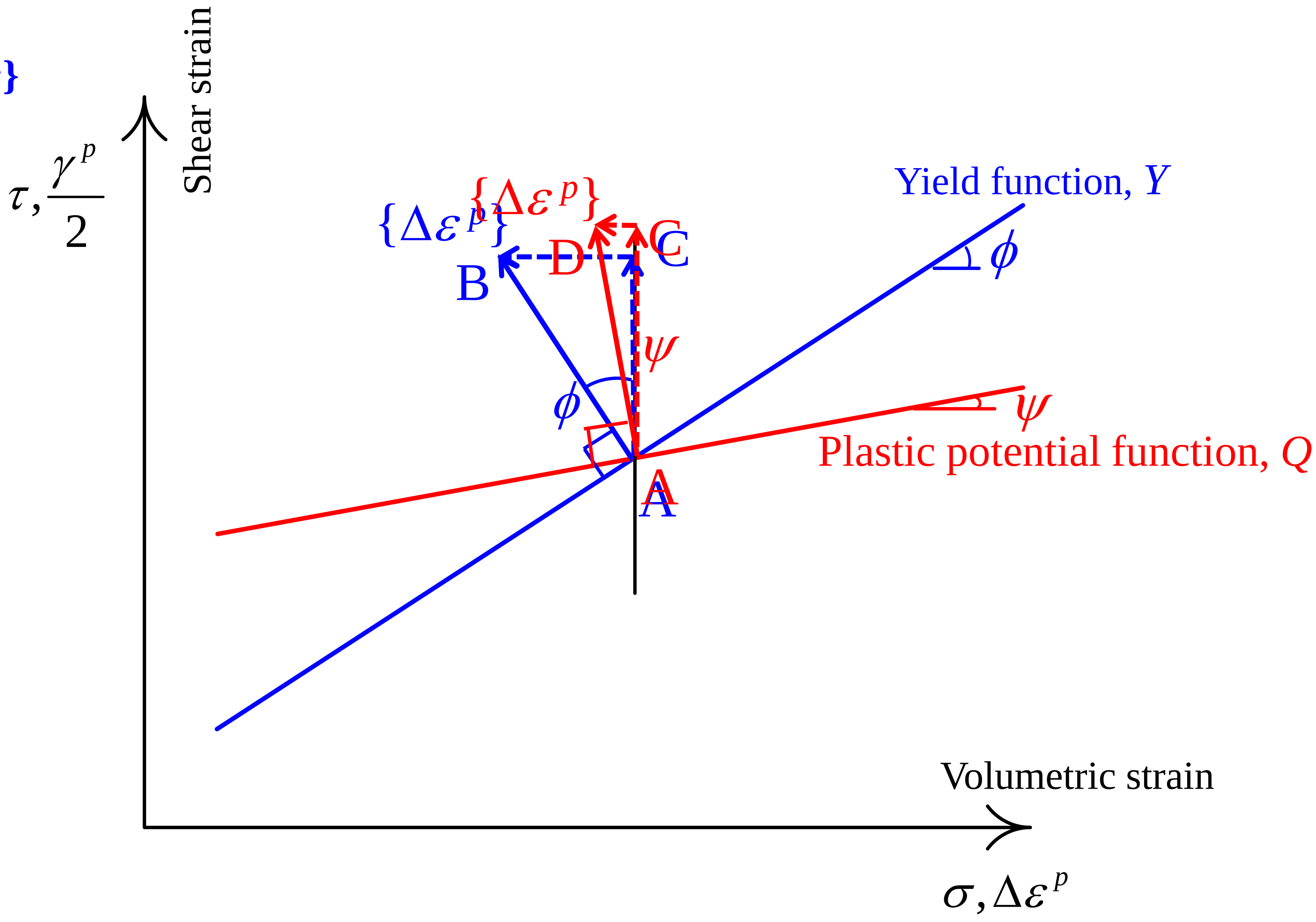

FIGURE 8.13 Yield function and plastic potential function for the Mohr-Coulomb model

If $\psi = \phi'$, $Y = Q$, associated flow rule.

If $\psi < \phi'$, non-associated flow rule. As ψ reduces, less dilation is generated.

If $\psi = 0$, zero plastic dilation (i.e., no plastic volume change) occurs

$$\{\Delta\sigma\} = \{[D] - [D^p]\}\{\Delta\varepsilon\} = [D^{ep}]\{\Delta\varepsilon\} \qquad (8.15)$$

Required parameters: c', ϕ', E', μ', ψ

Two drawbacks:

(1)The magnitude of the plastic volumetric strain (i.e., the dilation) is much larger than that observed in real soils for the associated flow rule.

(2) Once the soil yields, it will dilate for ever. Real soil may dilate initially when the stress state meets the failure surface, and will often reach a constant volume condition at large strain, that is, zero incremental plastic volumetric strains

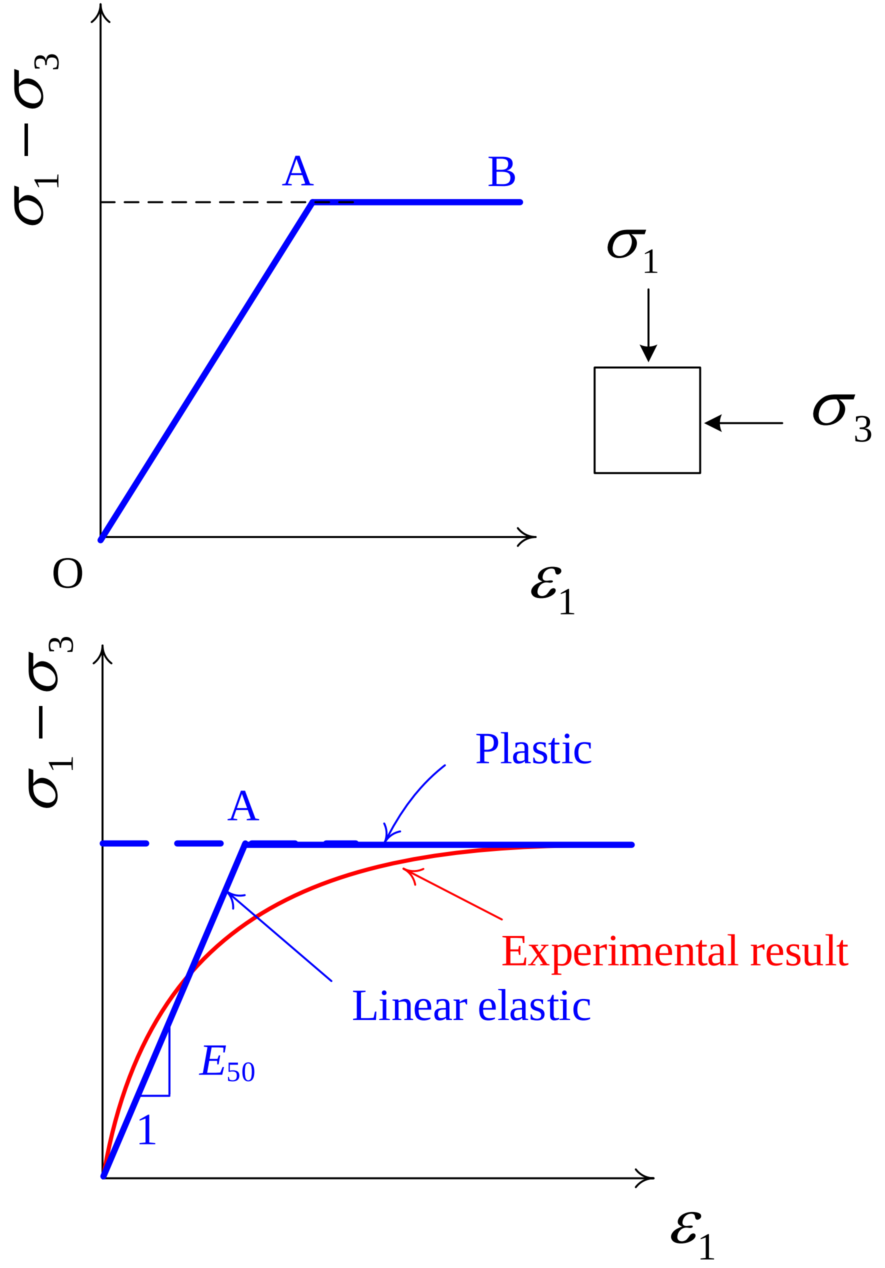

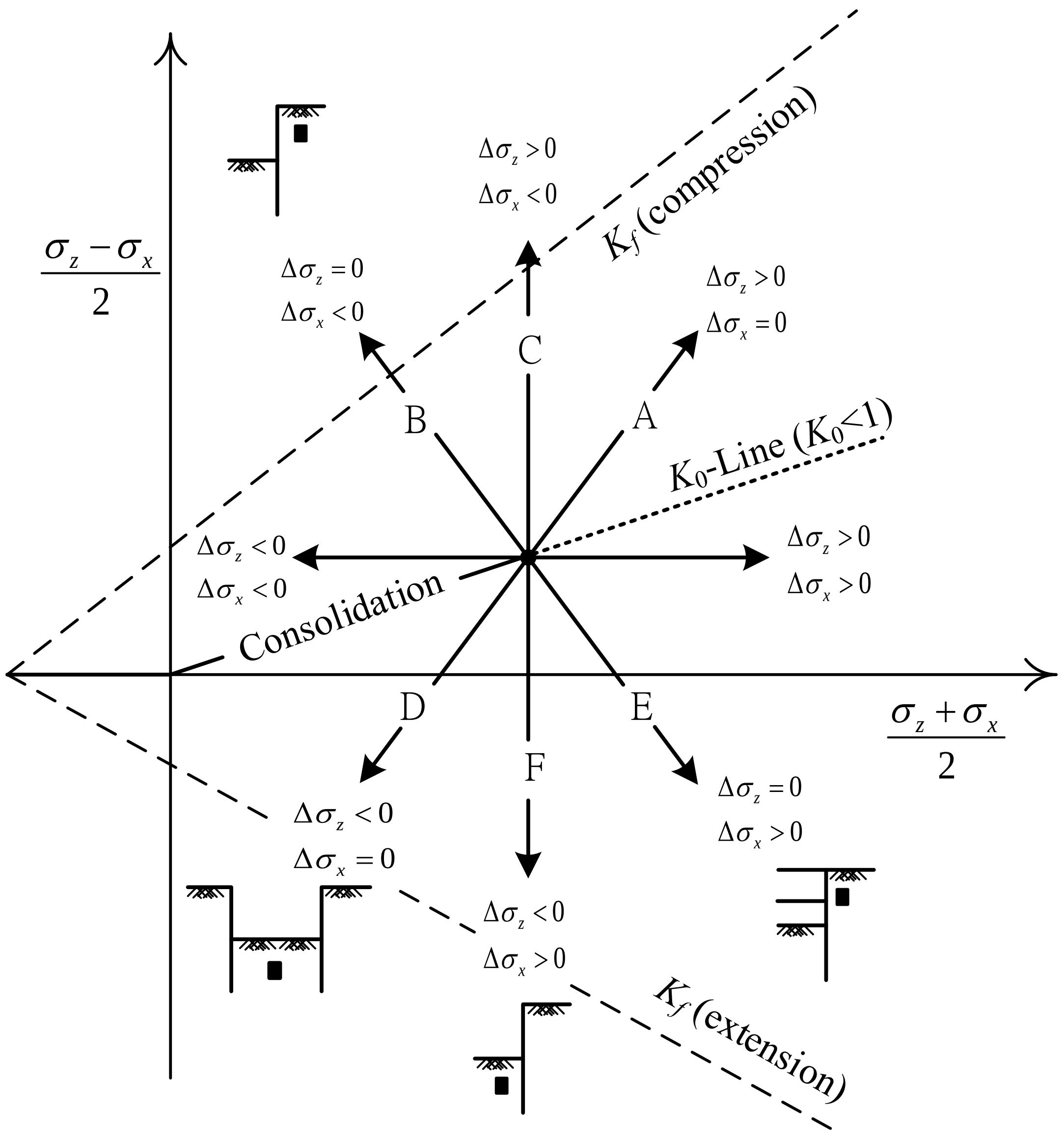

FIGURE 14 Mohr-Coulomb model

Undrained Analysis

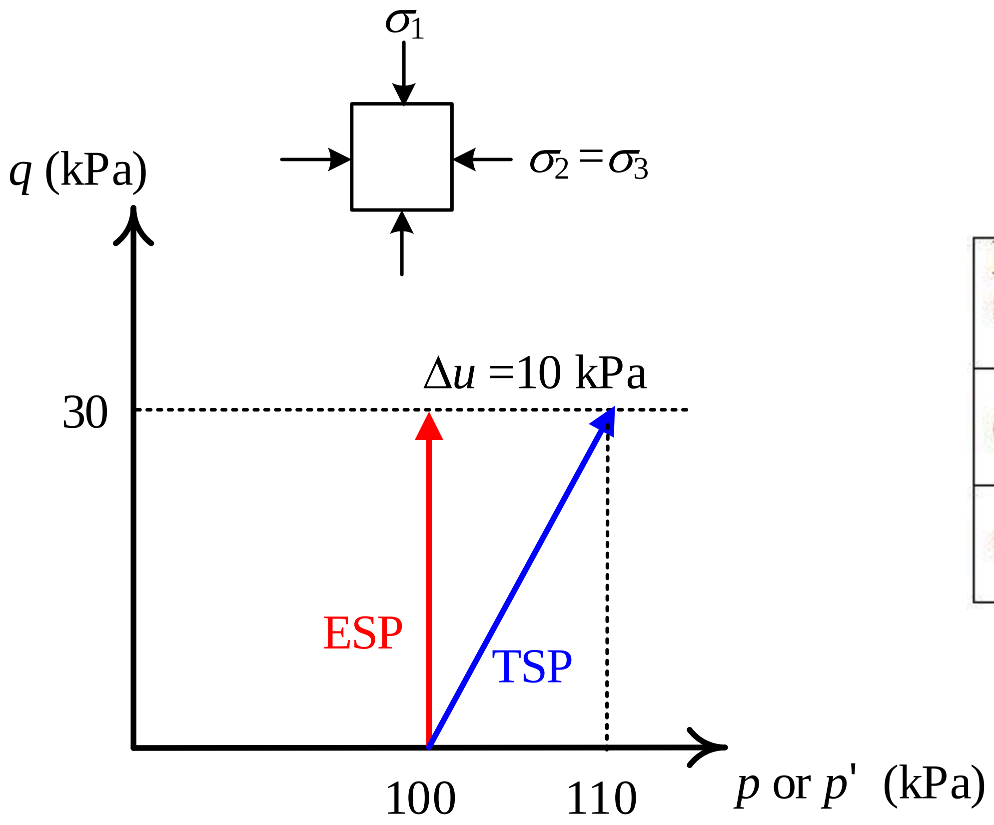

p=(σ_1+σ_2+σ_3)/3, q=(σ_1−σ_3)

Loading stage	σ_1 (kPa)	σ_2 (kPa)	σ_3 (kPa)	p (kPa)	p' (kPa)	q (kPa)
Consolidation	100	100	100	100	100	0
Shearing	130	100	100	110	100	30

FIGURE 8.15 Effective stress path and total stress path of an elastic material in triaxial CD tests

MC Undrained A: c', ϕ', E', μ', ψ

MC Undrained B: s_u, $\phi = 0$, E', μ', ψ

$$\{\Delta\sigma\} = \left([D^e] - [D^p]\right)\{\Delta\varepsilon\} = [D^{ep}]\{\Delta\varepsilon\} \qquad (8.15)$$

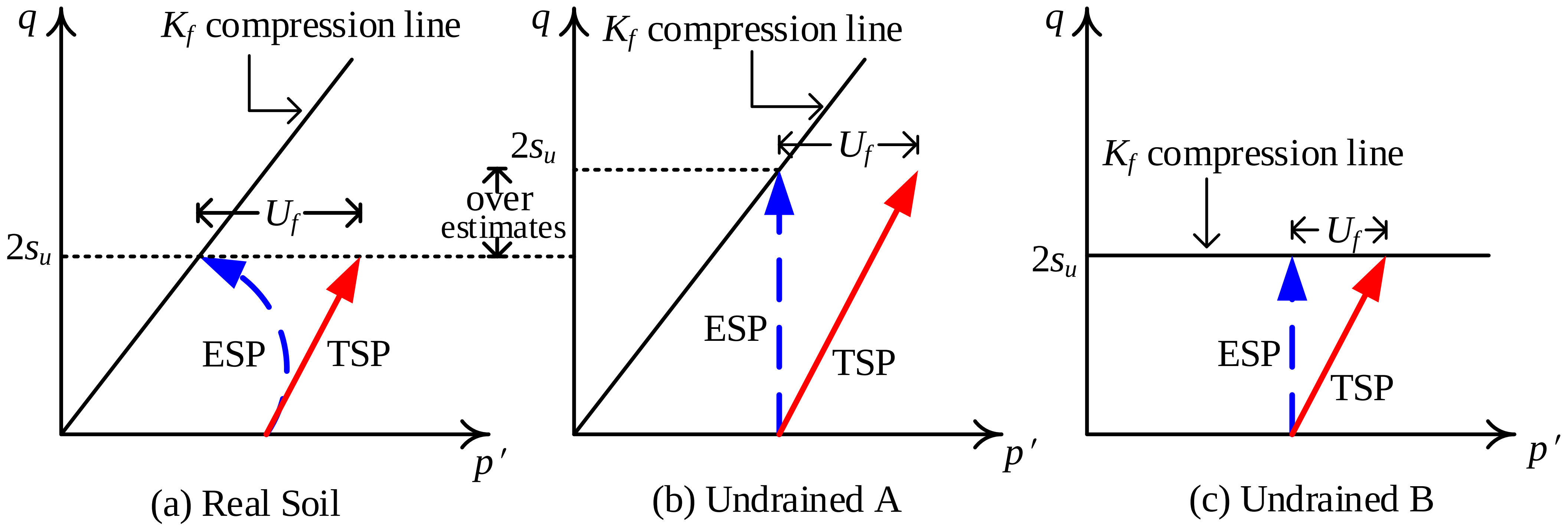

FIGURE 8.16 Stress path of a real soil and MC model
(a) real soil (b) stress path for MC undrained A model (b) stress path from MC undrained B model

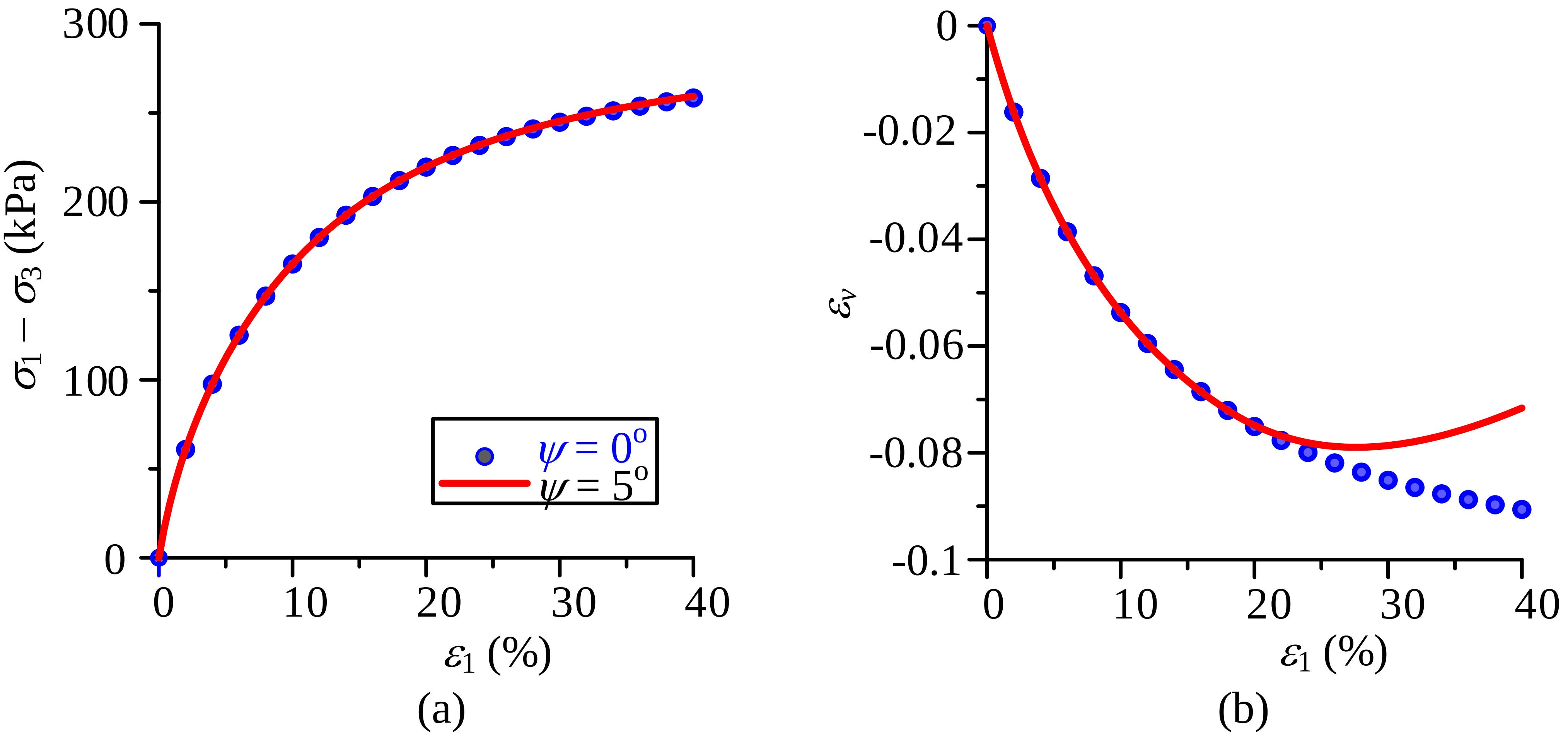

FIGURE 8.17   Stress-strain behavior of saturated clay computed from the MC model in drained shear conditions

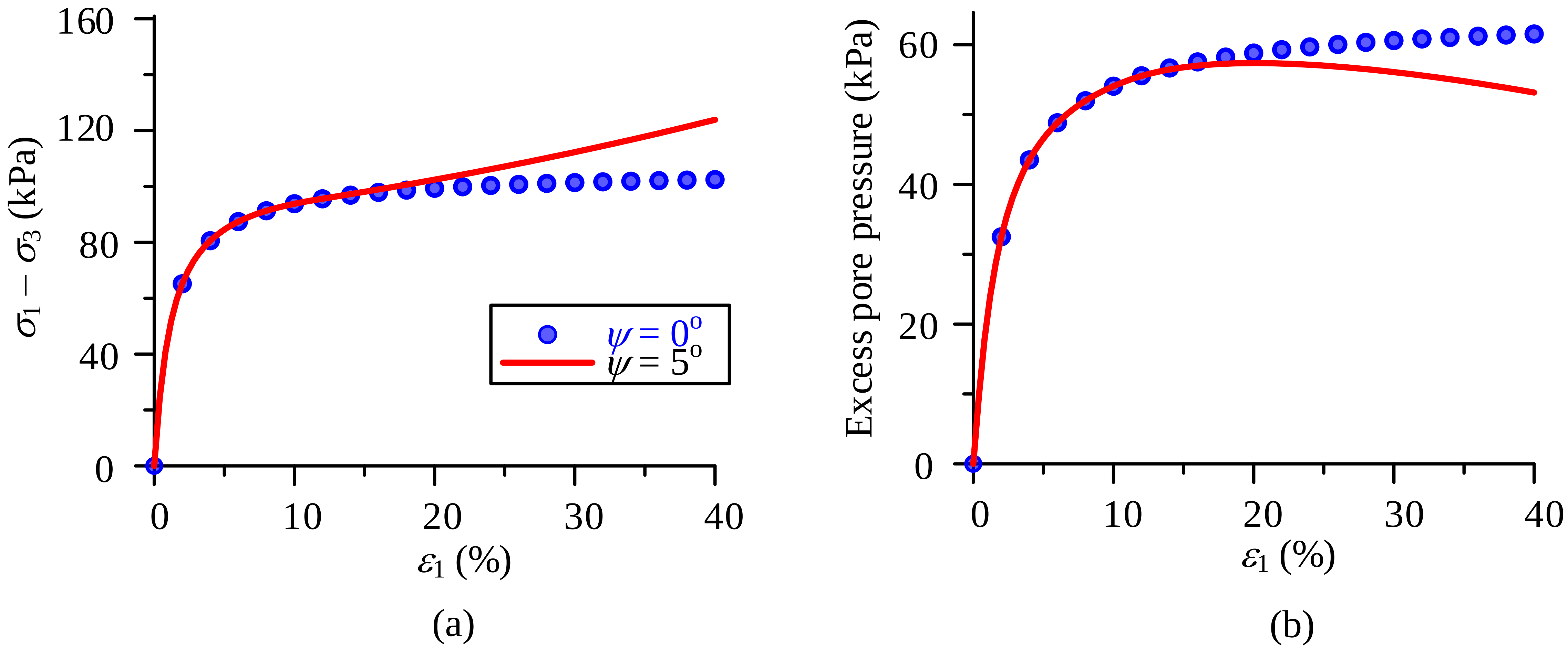

FIGURE 8.18 Stress-strain behavior of saturated clay computed from the MC model in undrained shear conditions

8.4.2 Duncan and Chang (DC) model – nonlinear elastic model

Duncan and Chang (1970)

$$q = \frac{\varepsilon_1}{\frac{1}{E_i} + \frac{\varepsilon_1}{q_a}} \qquad (8.23)$$

q =deviator stress

$q = \sigma_1 - \sigma_3$; σ_1 and σ_1 are major and minor principal stresses, respectively

ε_1 = the strain in the direction of major principal stress

E_i = initial tangent modulus

$q_a = (\sigma_1 - \sigma_3)_{ult}$ =asymptote of the stress-strain curve, representing the ultimate strength

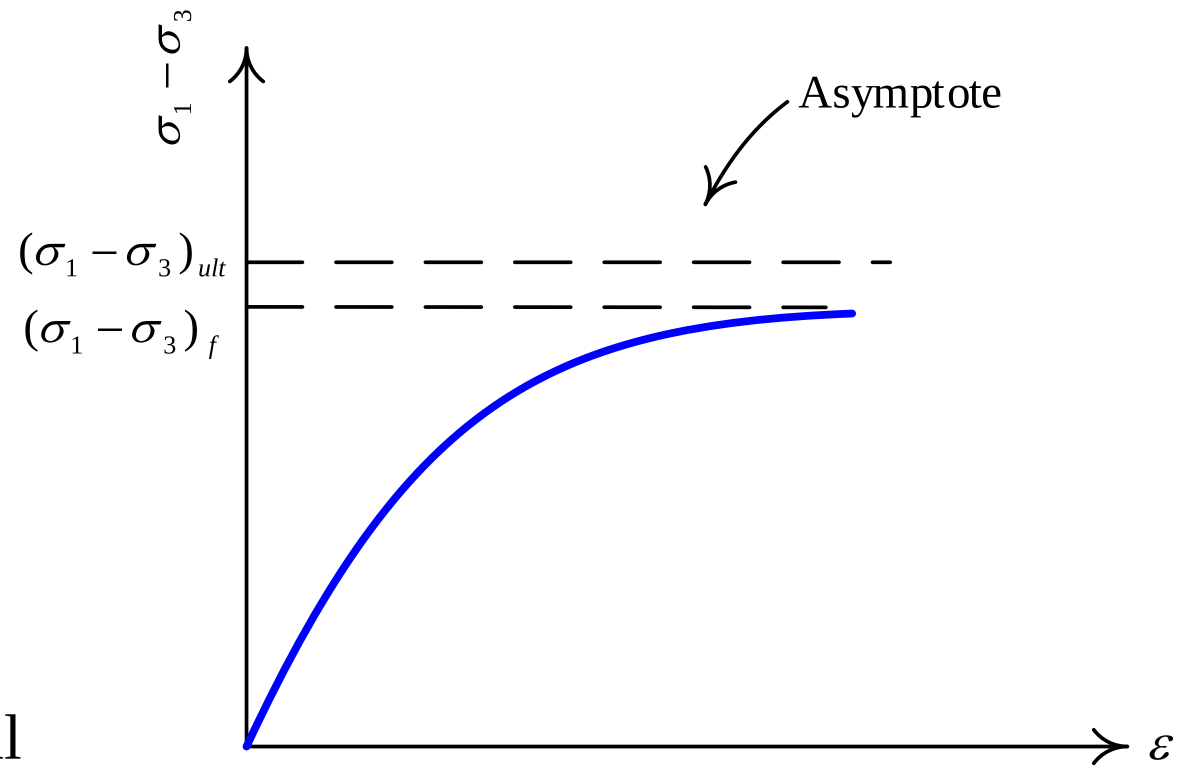

FIGURE 8.19 Duncan and Chang's (DC) model

$$E_i = KP_a\left(\frac{\sigma_3}{P_a}\right)^n \qquad (8.24)$$

P_a= atmospheric pressure = 101.3 kN/m^2
K= dimensionless stiffness modulus number
n= dimensionless stiffness modulus exponent.

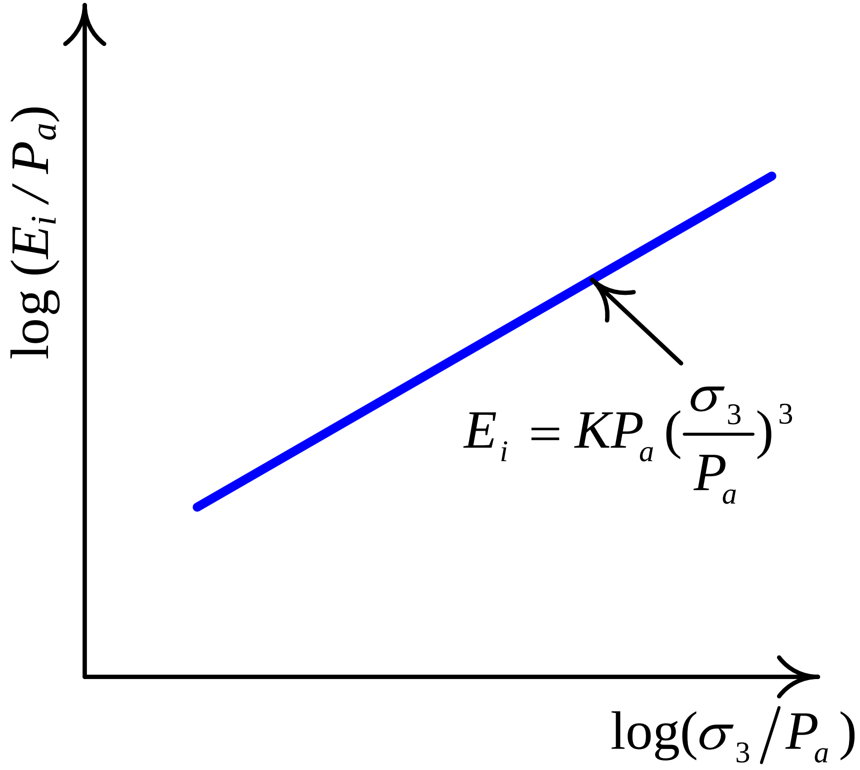

FIGURE 8.20 Relation between the initial Young's modulus and confining pressure

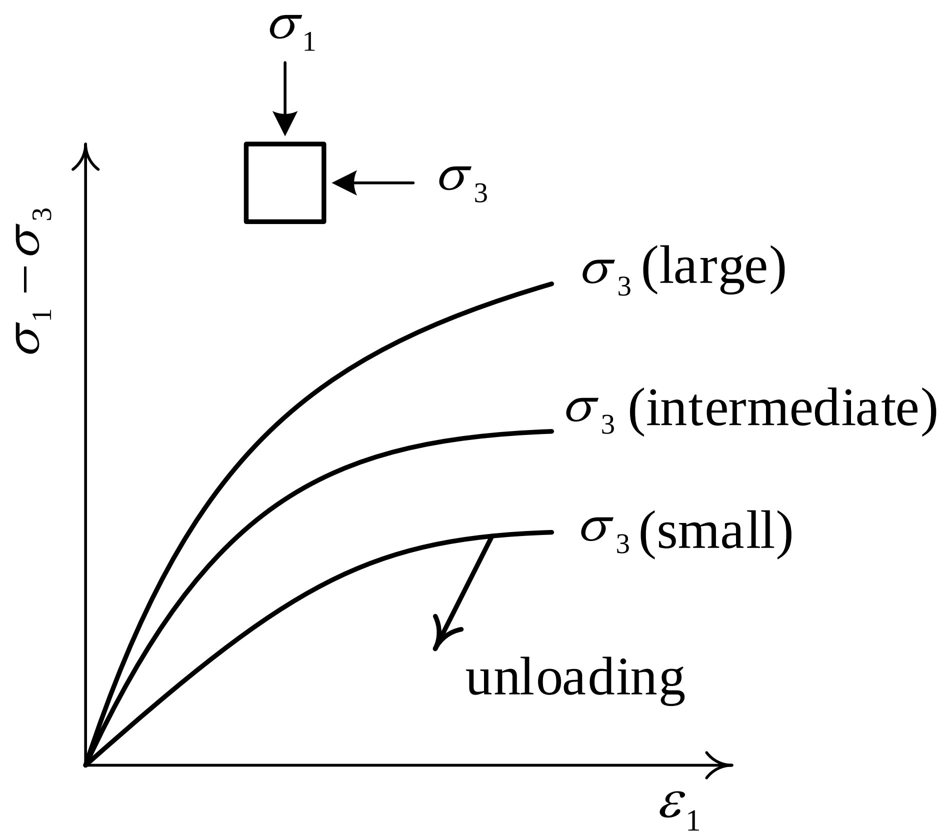

FIGURE 8.12 Typical stress-strain relations of soils

$$q_f = R_f q_a$$

$$q_a = (\sigma_1 - \sigma_3)_{ult}$$

$$q_f = (\sigma_1 - \sigma_3)_f$$

R_f = failure ratio. For most types of soil, R_f ranges between 0.5 to 0.9

According to the Mohr-Coulomb failure theory,

$$q_f = \frac{2c\cos\phi + 2\sigma_3 \sin\phi}{1 - \sin\phi} \qquad (8.26)$$

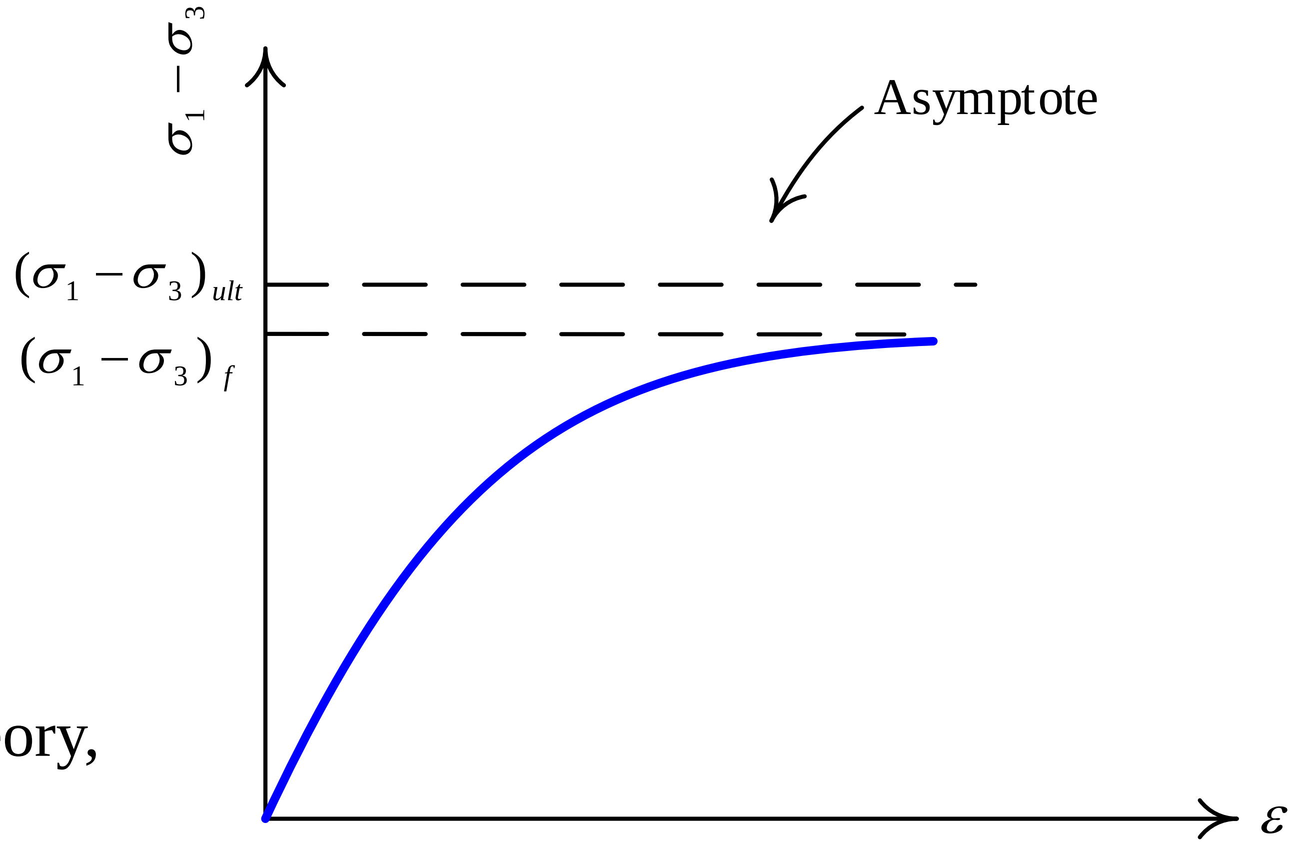

FIGURE 8.19 Duncan and Chang's (DC) model

$$\phi = \phi_0 - \Delta\phi \log_{10}\left(\frac{\sigma_3}{P_a}\right) \qquad (8.27)$$

ϕ_0=angle of shear resistance when σ_3=1 atm=101.3 kN/m^2

Substitute Eqs. 8.24, 8.25, and 8.26 in Eq. 8.23, and differentiate with respect to strain, and then we can obtain the tangent elastic modulus E_t for any stress state

$$E_t = \left[1 - \frac{R_f(1-\sin\phi)(\sigma_1-\sigma_3)}{2c\cos\phi + 2\sigma_3\sin\phi}\right]^2 KP_a\left(\frac{\sigma_3}{P_a}\right)^n$$

$$= \left[1 - R_f \cdot SL\right]^2 KP_a\left(\frac{\sigma_3}{P_a}\right)^n$$

Stress level $SL = q/q_f$

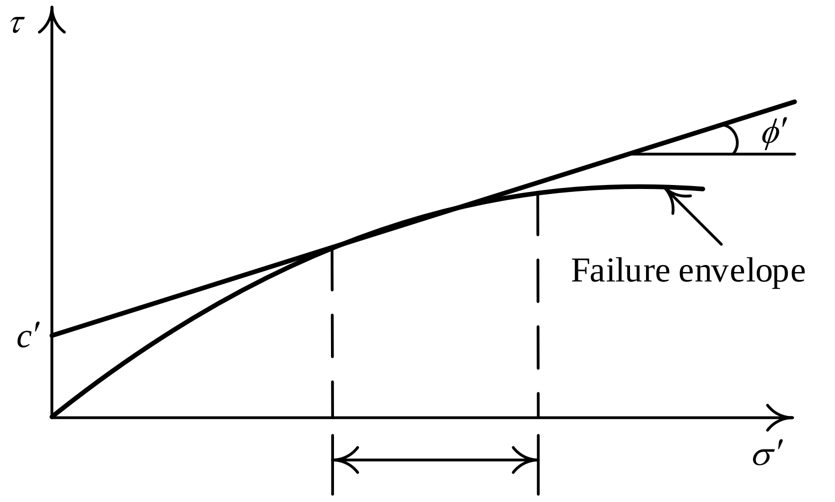

FIGURE 2.9 Apparent cohesion and friction angle for sand

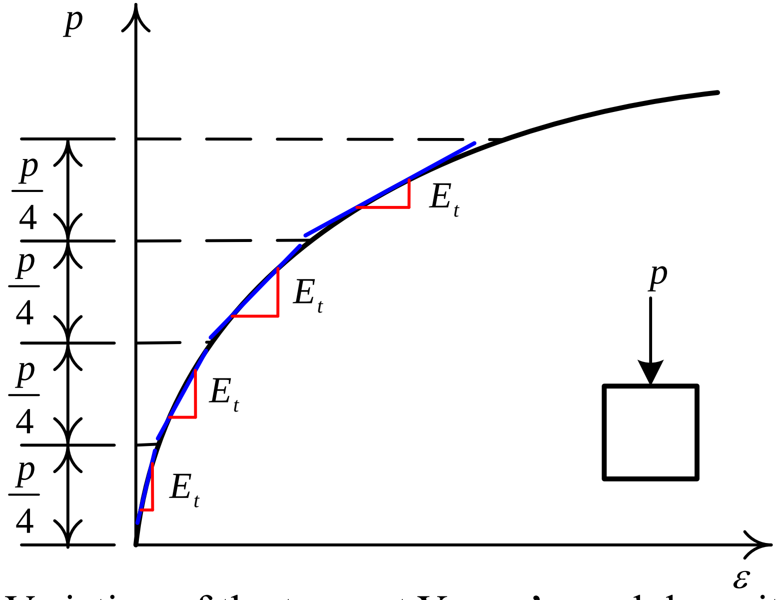

FIGURE 8.22 Variation of the tangent Young's modulus with strain

In the FEM analysis:

In numerical analysis, loading is first divided into many sub-loading. Therefore, even the soil stress-strain relation is nonlinear, the stress-strain relation at each sub-load stage can be treated as linear elastic, in which Young's modulus can be expressed by $\boldsymbol{E_t}$

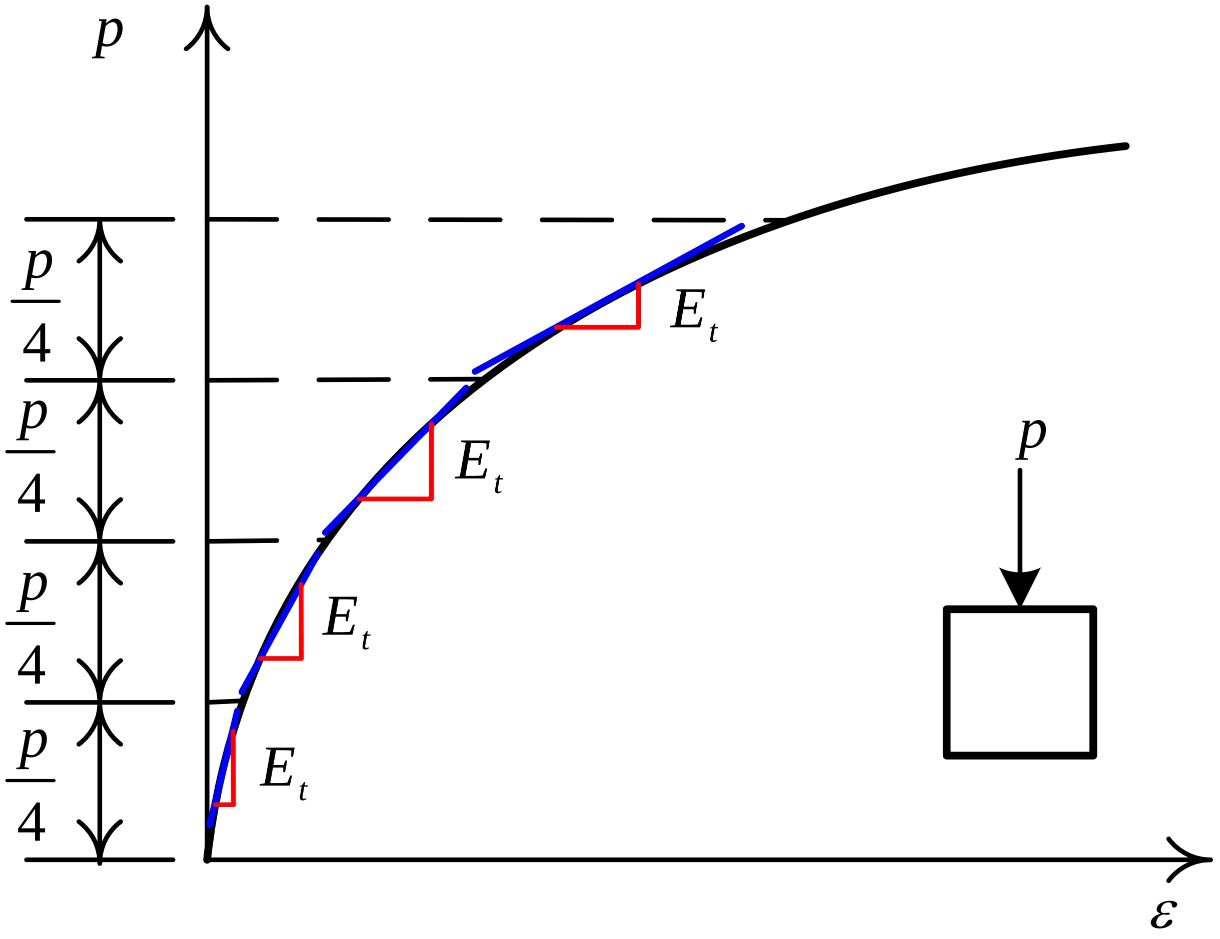

FIGURE 8.22 Variation of the tangent Young's modulus with strain

$$E_{ur} = K_{ur} P_a \left(\frac{\sigma_3}{P_a} \right)^n \qquad (8.29)$$

K_{ur}= dimensionless unloading/reloading stiffness modulus number.

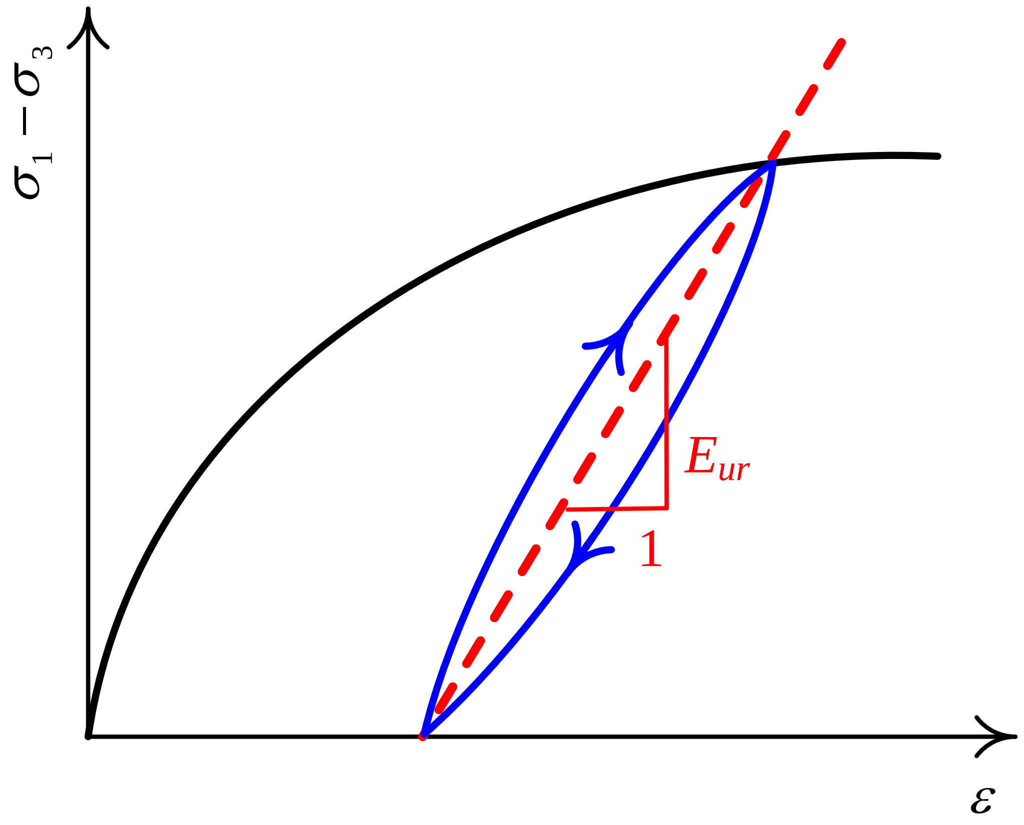

FIGURE 8.21 Unloading-reloading Young’s modulus

According to Eqs. 8.1 and 8.6, to establish the stiffness matrix of an element, the required parameters are ***E* (*E_t* or *E_{ur}*) and *μ***

$$\{\sigma\} = [D]\{\varepsilon\} \qquad (8.1)$$

$$[K_E] = \int_{vol} [B]^T [D][B] dV \qquad (8.6)$$

The stiffness matrix at a stress level or at a stress state can then be obtained. The required parameters are:

c, ϕ_0, $\Delta\phi$, K, n, K_{ur}, R_f, μ

Duncan and Chang's model is often categorized as **the elastic model**

8.4.3 Modified Cam-clay (MCC) model -- critical state model

The critical state of soil refers to the state where volumetric strain is not further produced with the increase of shear strain at large shear strain. The critical state is usually either the failure state or the ultimate state.

Assuming in the laboratory **triaxial test condition**:

$$p' = \frac{1}{3}(\sigma'_1 + \sigma'_2 + \sigma'_3) \qquad (8.30)$$

$$q = \sigma'_1 - \sigma'_3 \qquad (8.31)$$

σ_1, σ_2, and σ_3 are the major, intermediate and minor principal stresses.

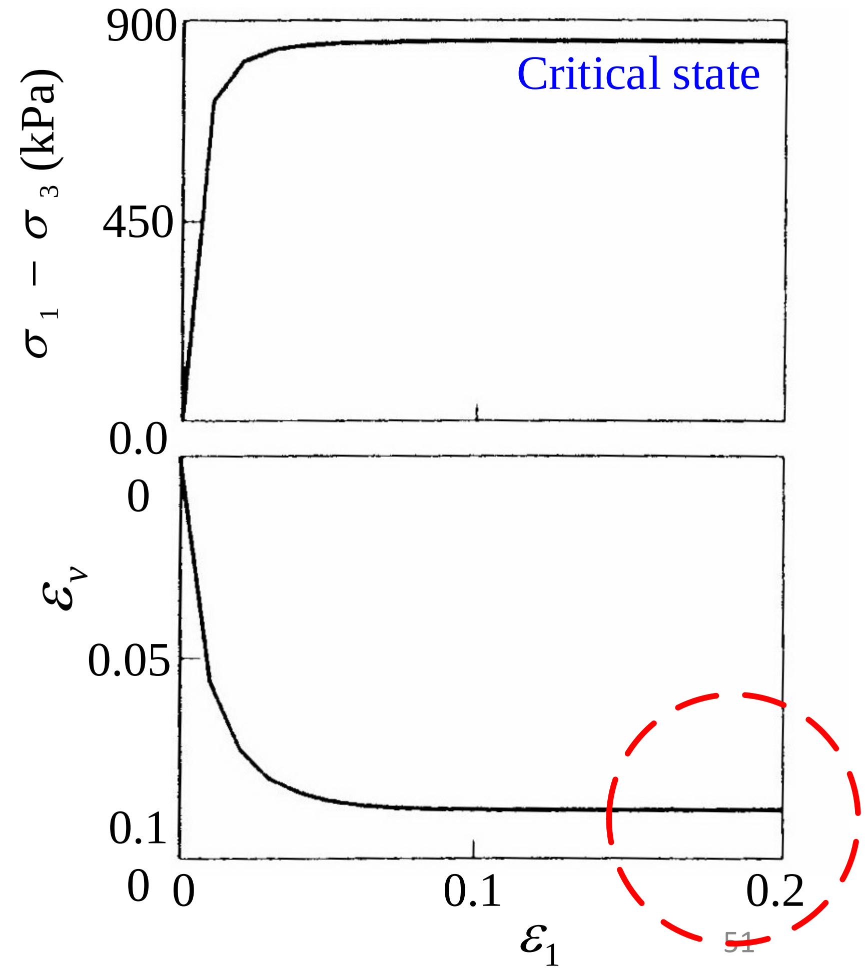

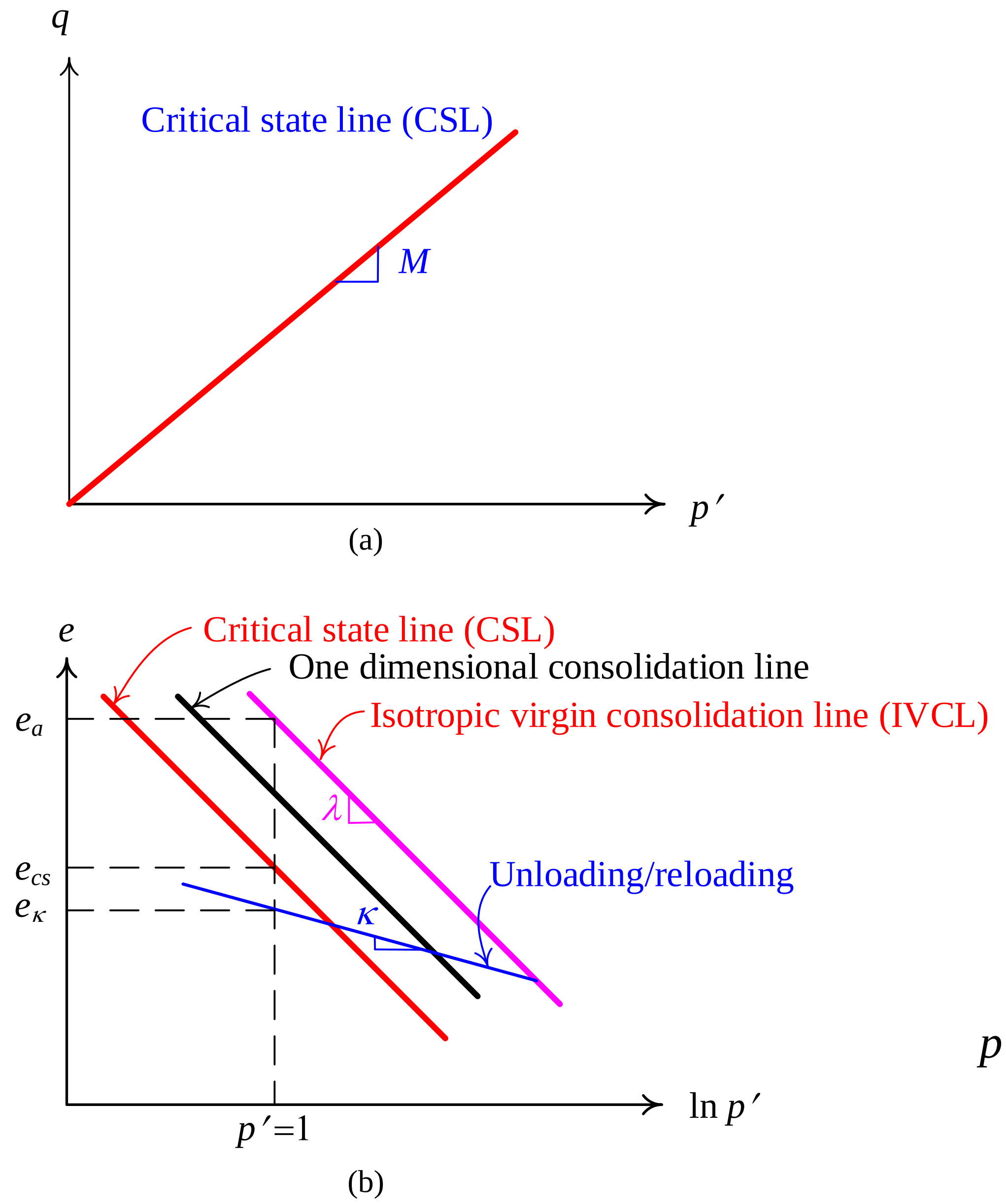

FIGURE 8.23 Definitions of various parameters in critical soil mechanics

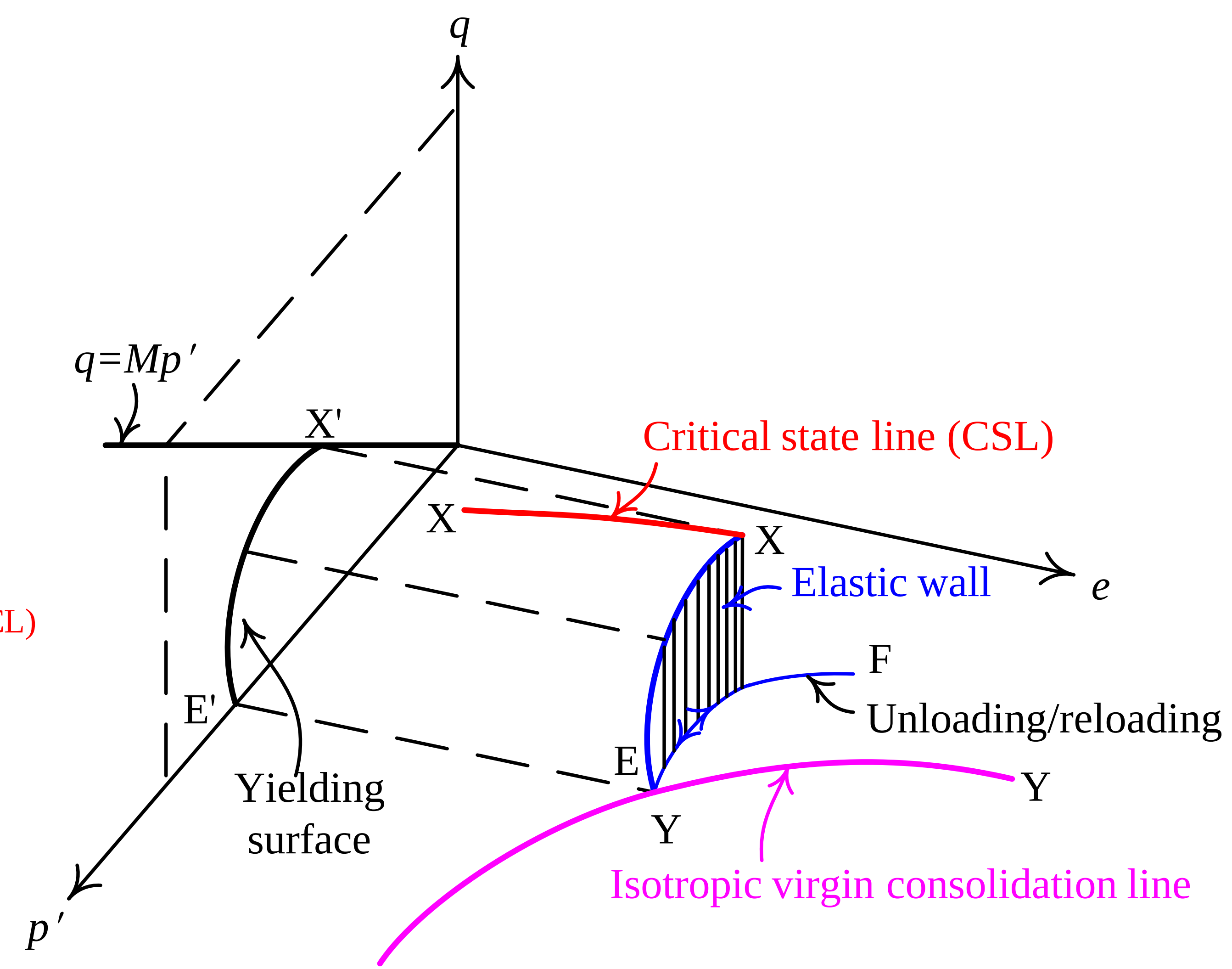

FIGURE 8.24 State boundary surface

The critical state line:

$$q = Mp' \tag{8.32}$$

$$e = e_{cs} - \lambda \ln p' \tag{8.33}$$

Combined Eq. 8.32 with the definition of p' and q, the friction constant, M, is given by

$$M = \frac{6\sin\phi'}{3-\sin\phi'} \tag{8.34}$$

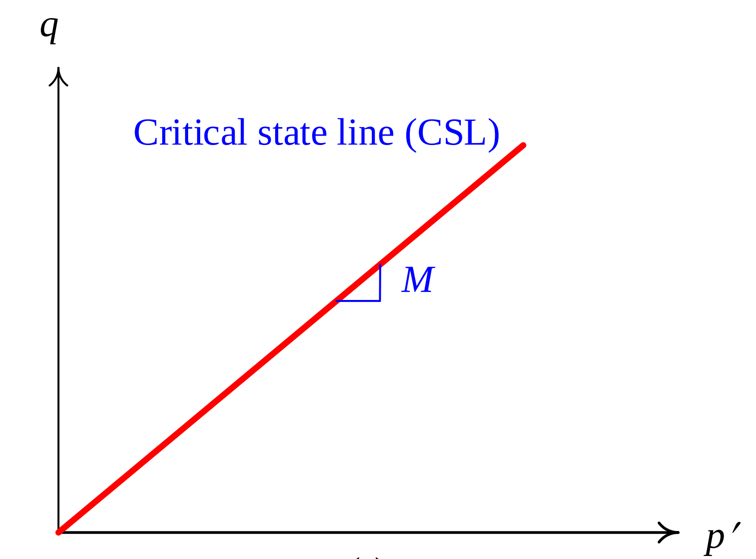

(a)

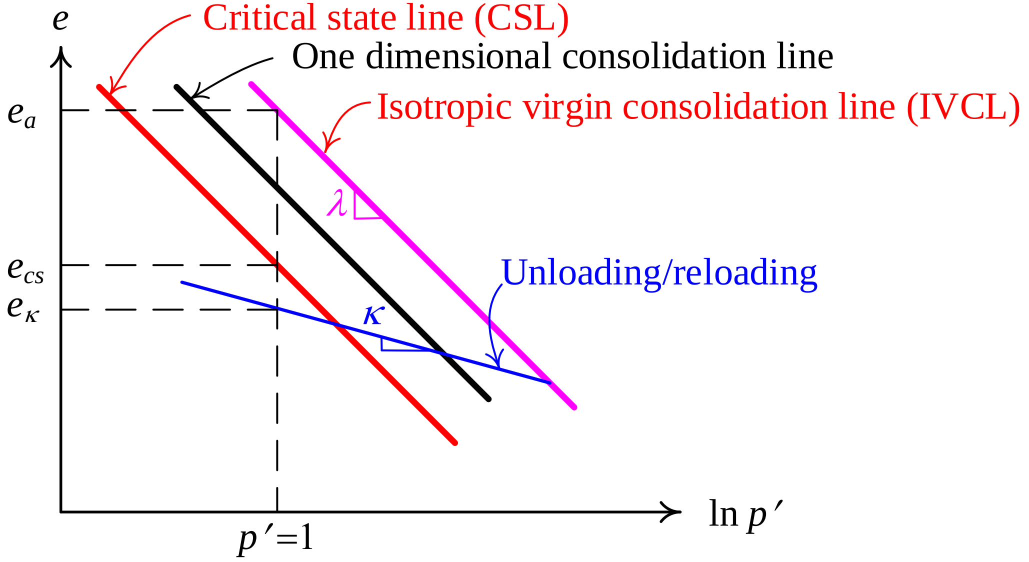

(b)

Isotropic virgin consolidation line:

$$e = e_a - \lambda \ln p' \qquad (8.35)$$

The unloading/reloading equation

$$e = e_\kappa - \kappa \ln p' \qquad (8.36)$$

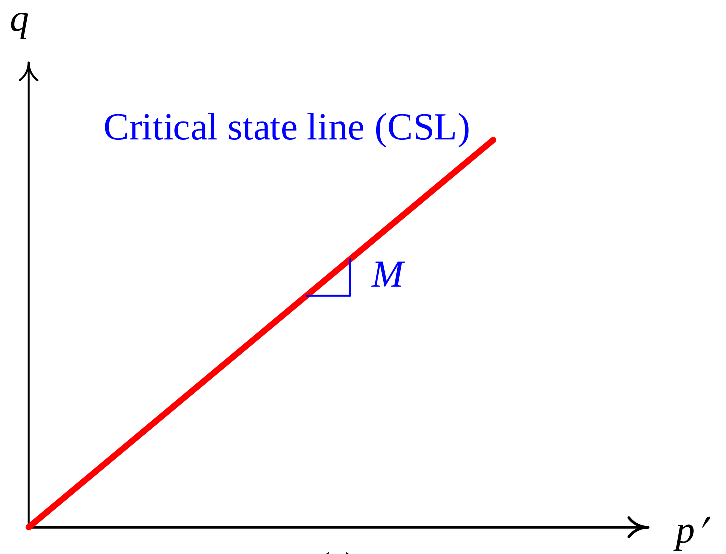

(a)

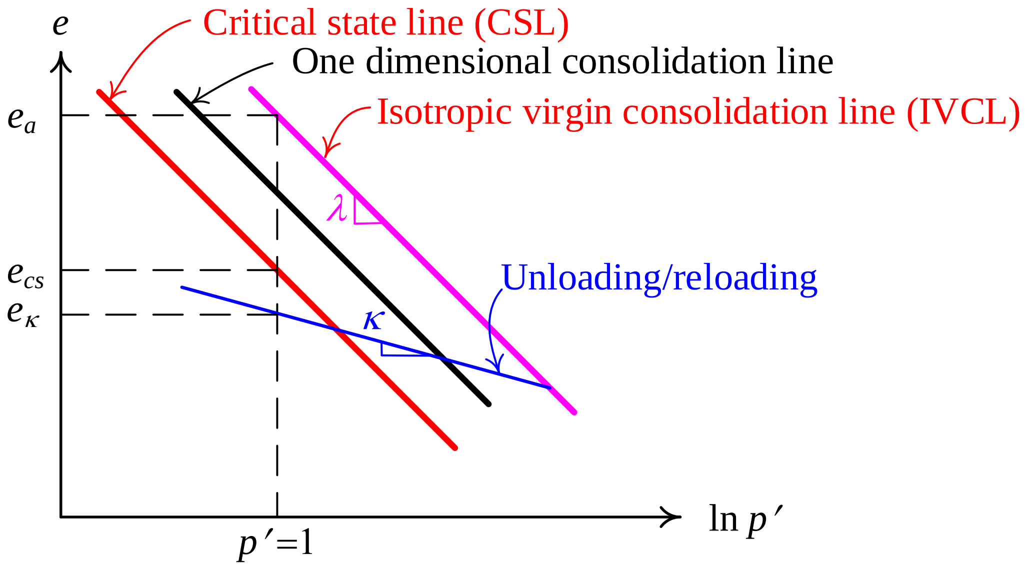

(b)

The state boundary surface with the MCC model:

$$\frac{p'}{p_e} = \left(\frac{M^2}{M^2 + q^2 / p'^2} \right)^{(1-\kappa/\lambda)} \qquad (8.37)$$

$$p_e = \exp\left(\frac{e_a - e}{\lambda} \right) \qquad (8.38)$$

The yield surface :

$$p' = p'_0 \left(\frac{M^2}{M^2 + q^2 / p'^2} \right) \qquad (8.39)$$

p'_0 is the p'-value when $q = 0$

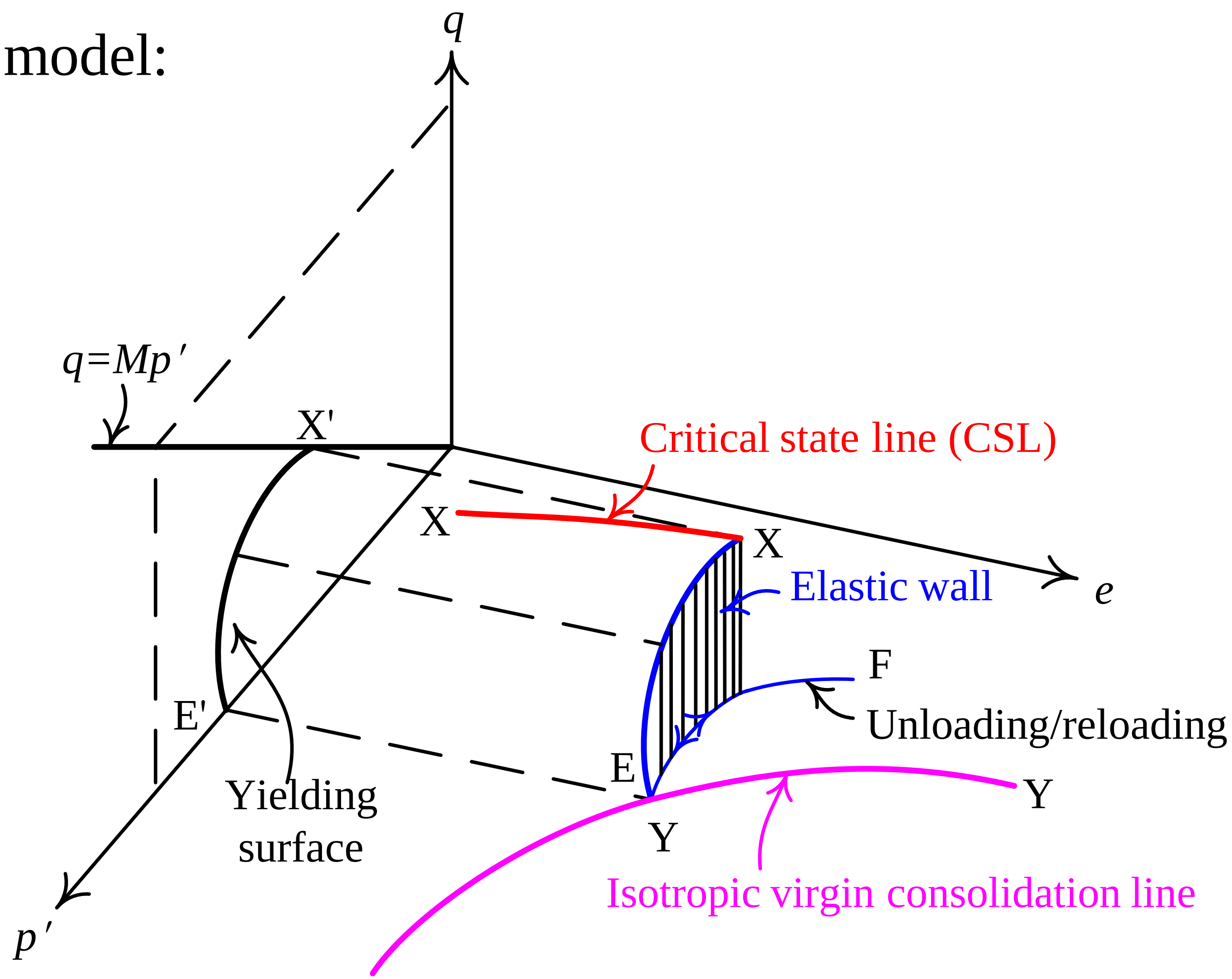

The parameters related to the state boundary surface or the yielding surface are

***M* (or ϕ') , λ , κ**

If the MCC model is adopted as the yielding function, the required input parameters are ***M* (or ϕ'), λ , κ ,** plus elastic constants **E'_{ur} and μ'_{ur}** that form the elastic constitutive matrix **[D^e]**

$$\{\Delta\sigma\} = \left([D^e] - [D^p]\right)\{\Delta\varepsilon\} = [D^{ep}]\{\Delta\varepsilon\} \qquad (8.15)$$

$$[D^{ep}] = [D^e] - [D^p] \qquad (8.16)$$

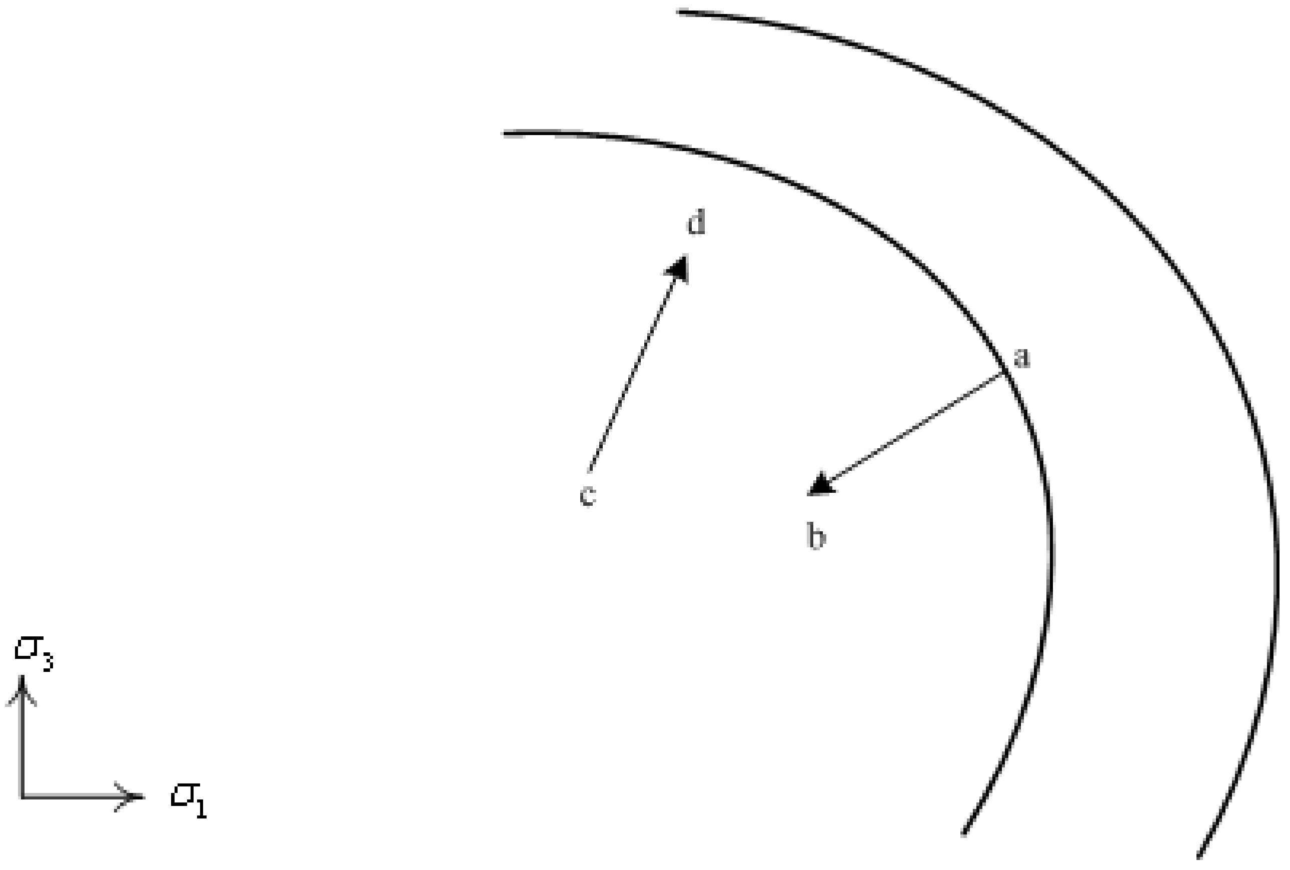

Y is enlarged with the stress state
and defined by MCC model

8.4.4 Hardening soil (HS) model --- nonlinear elastoplastic model

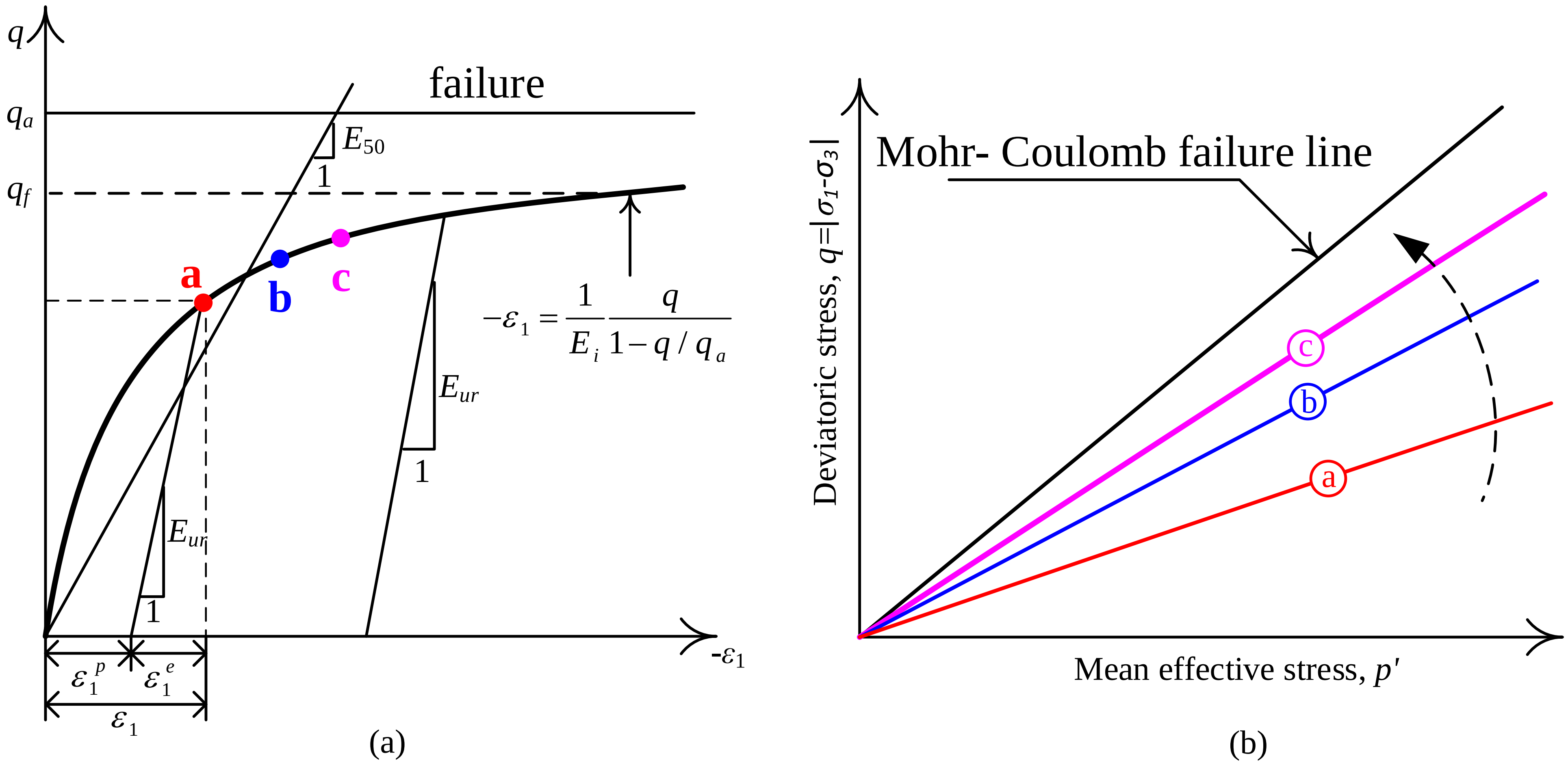

FIGURE 8.25 Hardening soil model (a) stress-strain curve by a hyperbola (b) shear yield surface (tension in positive)

Schanz et al. (1999) derived the yield function for the soil subject to shear as

$$Y_s = \frac{2 - R_f}{E'_{50}} \frac{q}{1 - q/q_a} - \frac{2q}{E'_{ur}} - \gamma^p \qquad (8.40)$$

E'_{50} is the tangent Young's modulus corresponding stress level=50%,

γ^p is the plastic strain function

The rest parameters such as q , q_a , q_f , R_f , E'_{ur} are exactly the same as those in the DC model

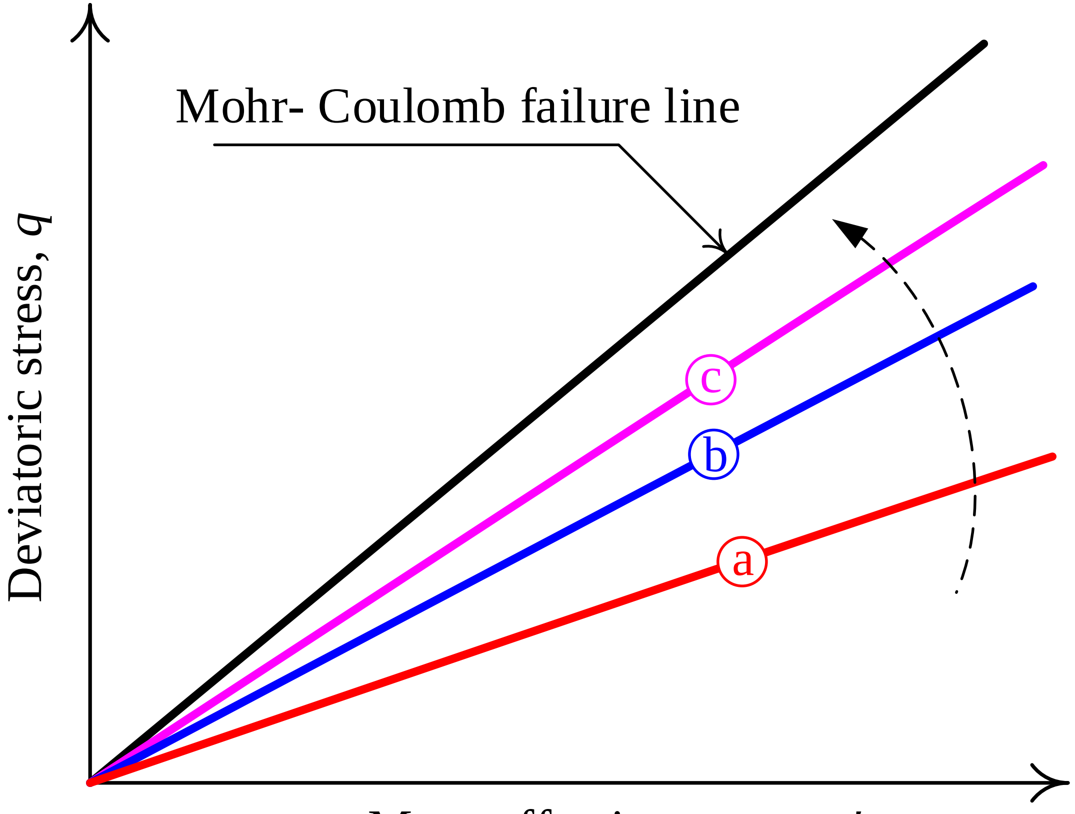

(b)

$$E'_{50} = E'^{\,ref}_{50}\left(\frac{c'\cot\phi' + \sigma'_3}{c'\cot\phi' + p'^{\,ref}}\right)^m \qquad (8.41)$$

$$E_i = KP_a\left(\frac{\sigma_3}{P_a}\right)^n \qquad (8.24)$$

$$E'_{ur} = E'^{\,ref}_{ur}\left(\frac{c'\cot\phi' + \sigma'_3}{c'\cot\phi' + p'^{\,ref}}\right)^m \qquad (8.42)$$

$p'^{\,ref}$ is the reference pressure, which is similar to the atmospheric pressure P_a in the DC model; usually sets $p'^{\,ref}$ =100 stress unit

$E'^{\,ref}_{50}$ = reference Young's modulus

$E'^{\,ref}_{ur}$ = reference unloading/reloading Young's modulus

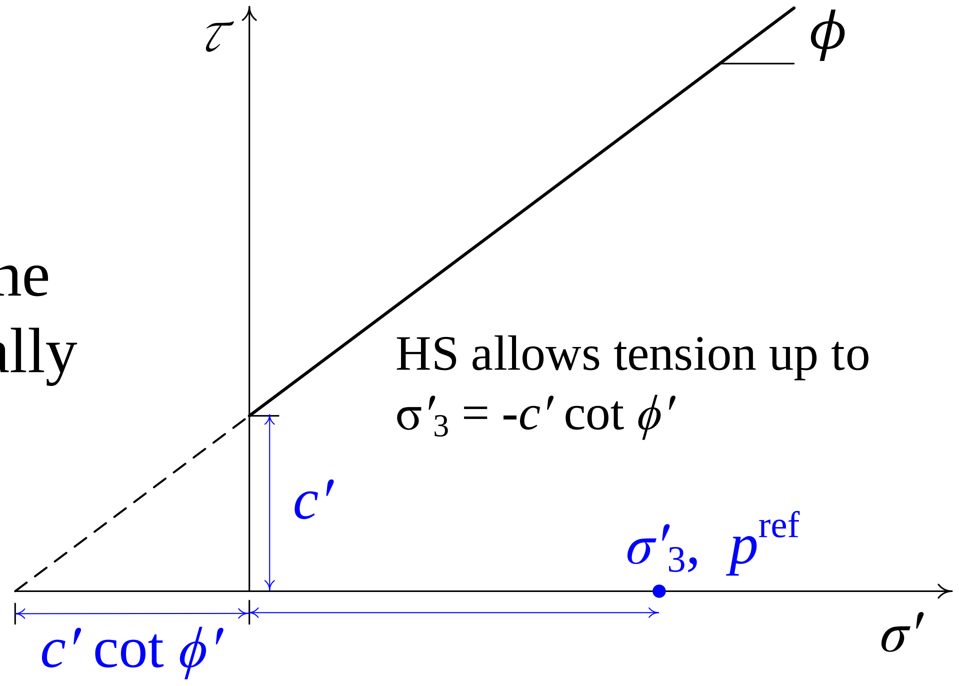

FIGURE 8.26 Reference tangent Young's modulus considering the effect of cohesion

$$E'_{oed} = E'^{\,ref}_{oed}\left(\frac{c'\cot\phi' + \sigma'_1}{c'\cot\phi' + p'^{\,ref}}\right)^m = E'^{\,ref}_{oed}\left(\frac{c'\cos\phi' + \sigma'_3\sin\phi' / K_{0,NC}}{c'\cos\phi' + p'^{\,ref}\sin\phi'}\right)^m \qquad (8.43)$$

$E'^{\,ref}_{oed}$ = reference tangent oedometer Young's modulus

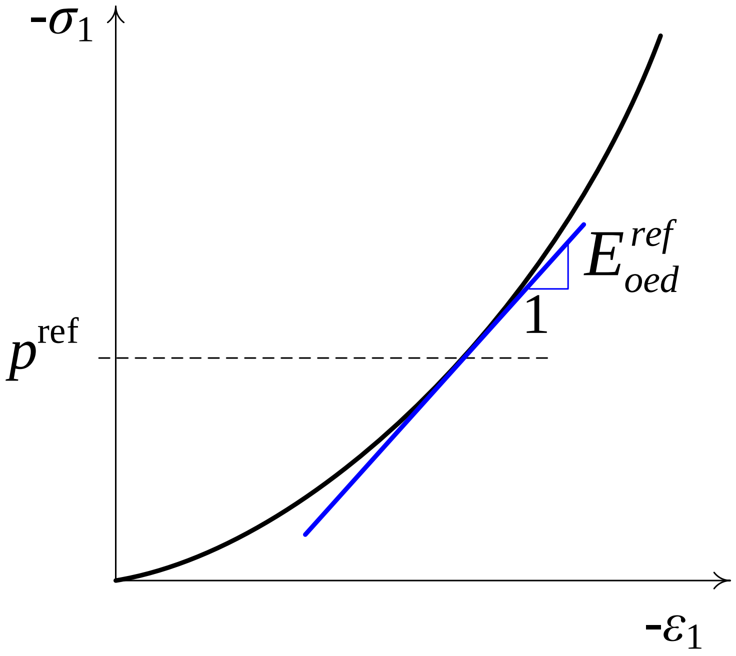

FIGURE 8.28 Reference oedometer Young's modulus

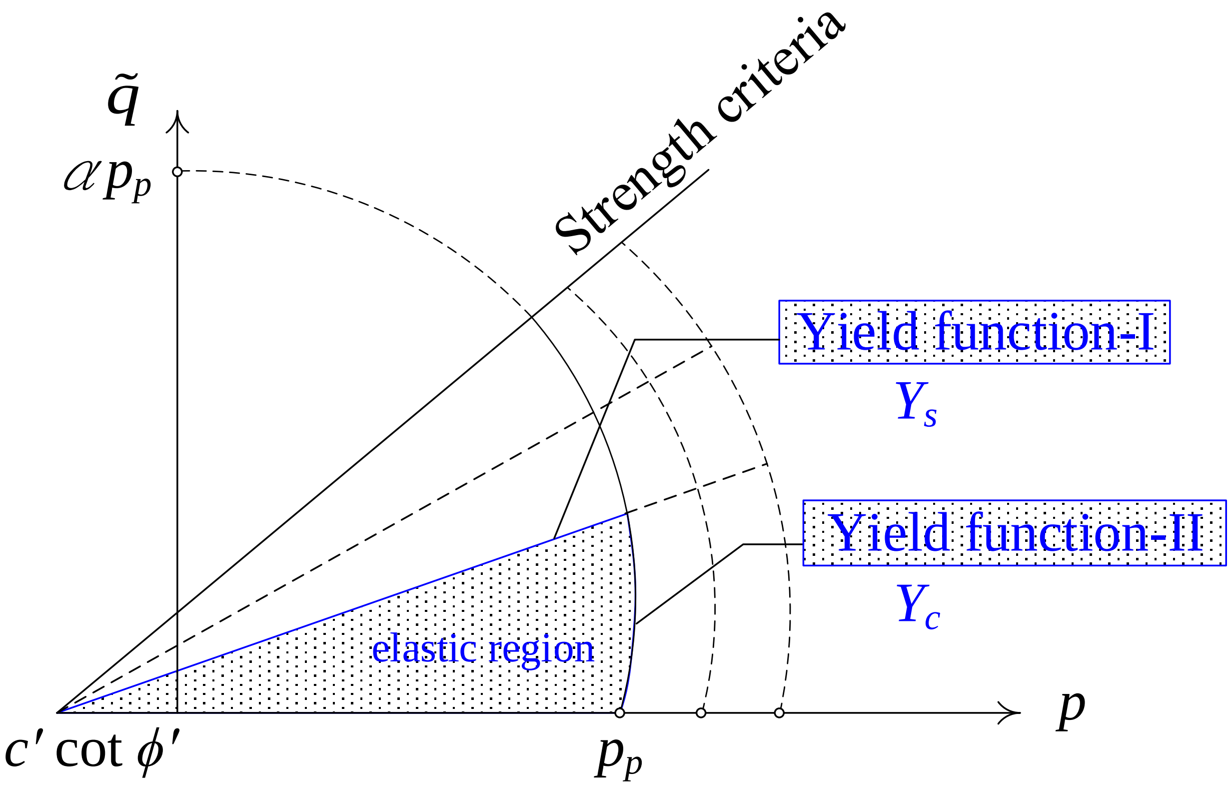

FIGURE 8.27 Yield surfaces used in the hardening soil model

Use the mobilized friction angle (ϕ'_m) and dilation angle (ψ_m) to represent the shear stress and dilation behavior of the soil at various stages

$$\sin\phi'_m = \frac{\sigma'_1 - \sigma'_3}{\sigma'_1 + \sigma'_3 - 2c'\cot\phi'} \qquad (8.44)$$

$$\sin\psi_m = \frac{\sin\phi'_m - \sin\phi'_{cv}}{1 - \sin\phi'_m \sin\phi'_{cv}} \qquad (8.45)$$

ϕ'_{cv} is the friction angle at the critical state or at the state of constant volume

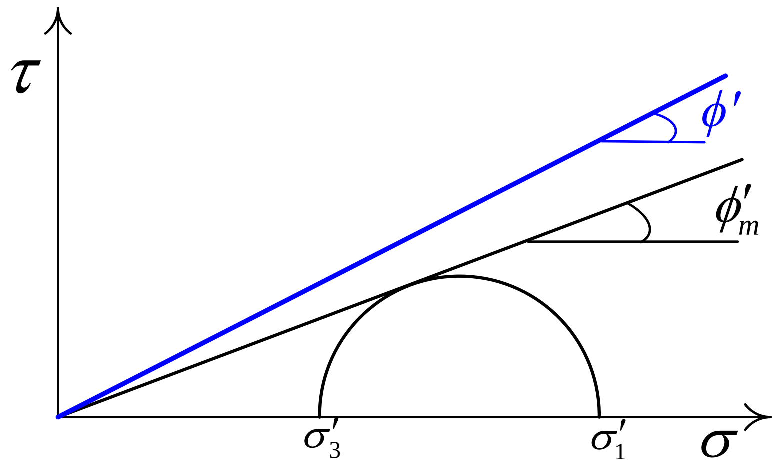

FIGURE 8.29 mobilized friction angle

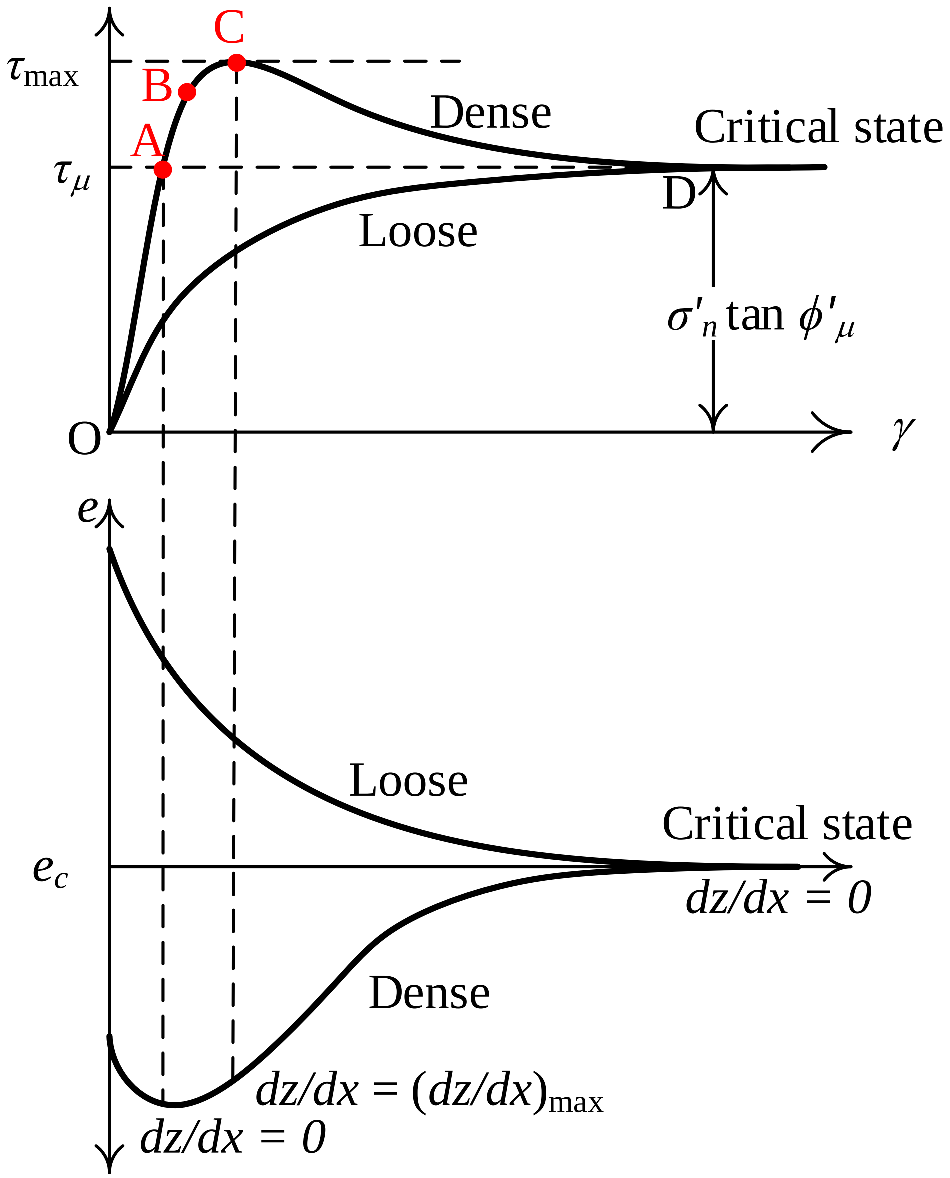

FIGURE 2.8 Rowe's theory

When the soil is at failure, $\phi'_m = \phi'$, and $\psi_m = \psi$, substitute those values into Eq. 8.45, we can obtain

$$\sin\psi = \frac{\sin\phi' - \sin\phi'_{cv}}{1 - \sin\phi' \sin\phi'_{cv}} \qquad (8.46)$$

Move ϕ'_{cv} to the left hand side (Eq. 8.46), and make a necessary simplification, then

$$\sin\phi'_{cv} = \frac{\sin\phi' - \sin\psi}{1 - \sin\phi' \sin\psi} \qquad (8.47)$$

Therefore, as long as the ϕ' and ϕ' is known, the ϕ'_{cv} can be obtained from Eq. 8.47, and the ϕ'_m and ψ_m can be obtained from Eqs. 8.44 and 8.45, respectively.

The HS model requires $\boxed{E'_{ur}\ (\text{or } E'^{ref}_{ur}),\ \mu'_{ur}}$, $\boxed{c', \phi', R_f, p'^{ref}, E'_{ur}\ (\text{or } E'^{ref}_{ur}),\ E'_{50}\ (\text{or } E'^{ref}_{50}),}$ $\boxed{E'_{oed}(\text{or } E'^{ref}_{oed}),\ m,\ K_{0,NC},\ p'_c}$, ψ

• A good case history, **TNEC** is used in evaluation of the performance of the above models

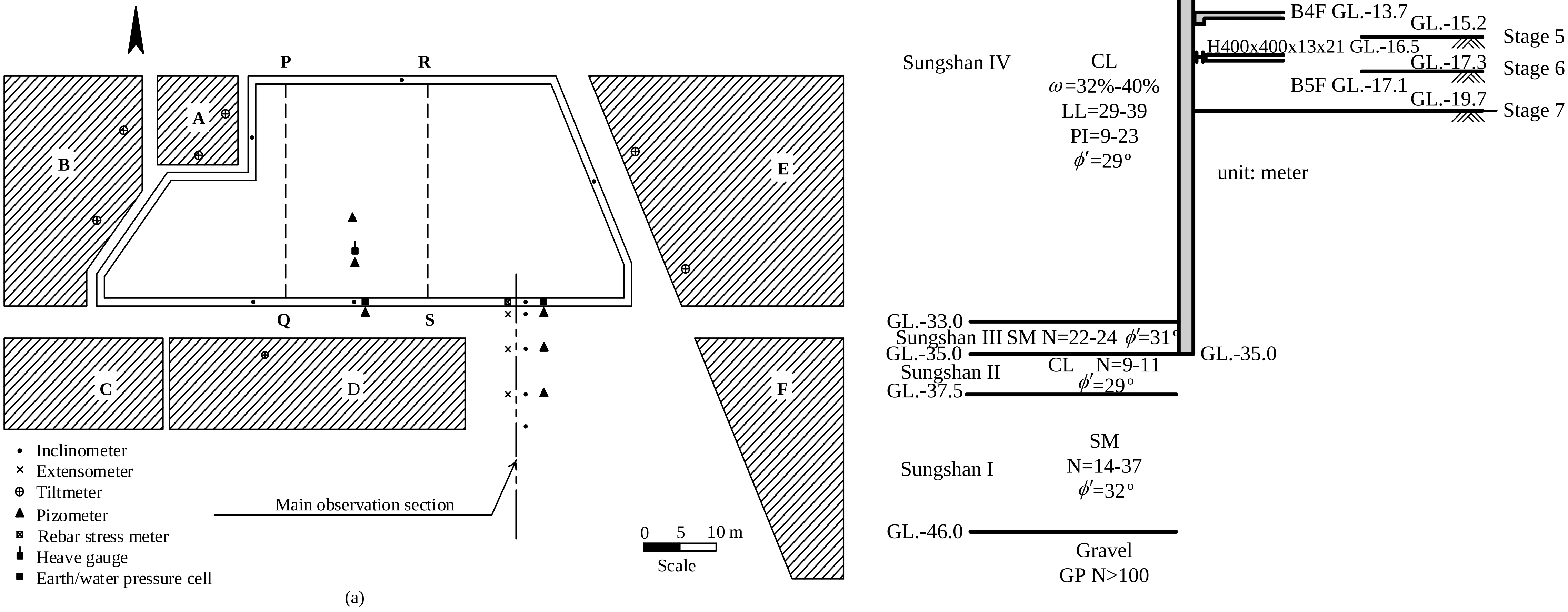

Figure 3.34

Parameters for the lateral support

Stage	Type	A(m^2)	t(m)	s(m)	E(MPa)	μ
1	steel	0.012	-	8	210000	0.2
2	slab	-	0.15	-	21000	0.15
3	slab	-	0.15	-	21000	0.15
4	slab	-	0.15	-	21000	0.15
5	slab	-	0.15	-	21000	0.15
6	steel	0.0219	-	3.4	210000	0.2

Note : s= spacing distance between struts ; t = thickness of slab

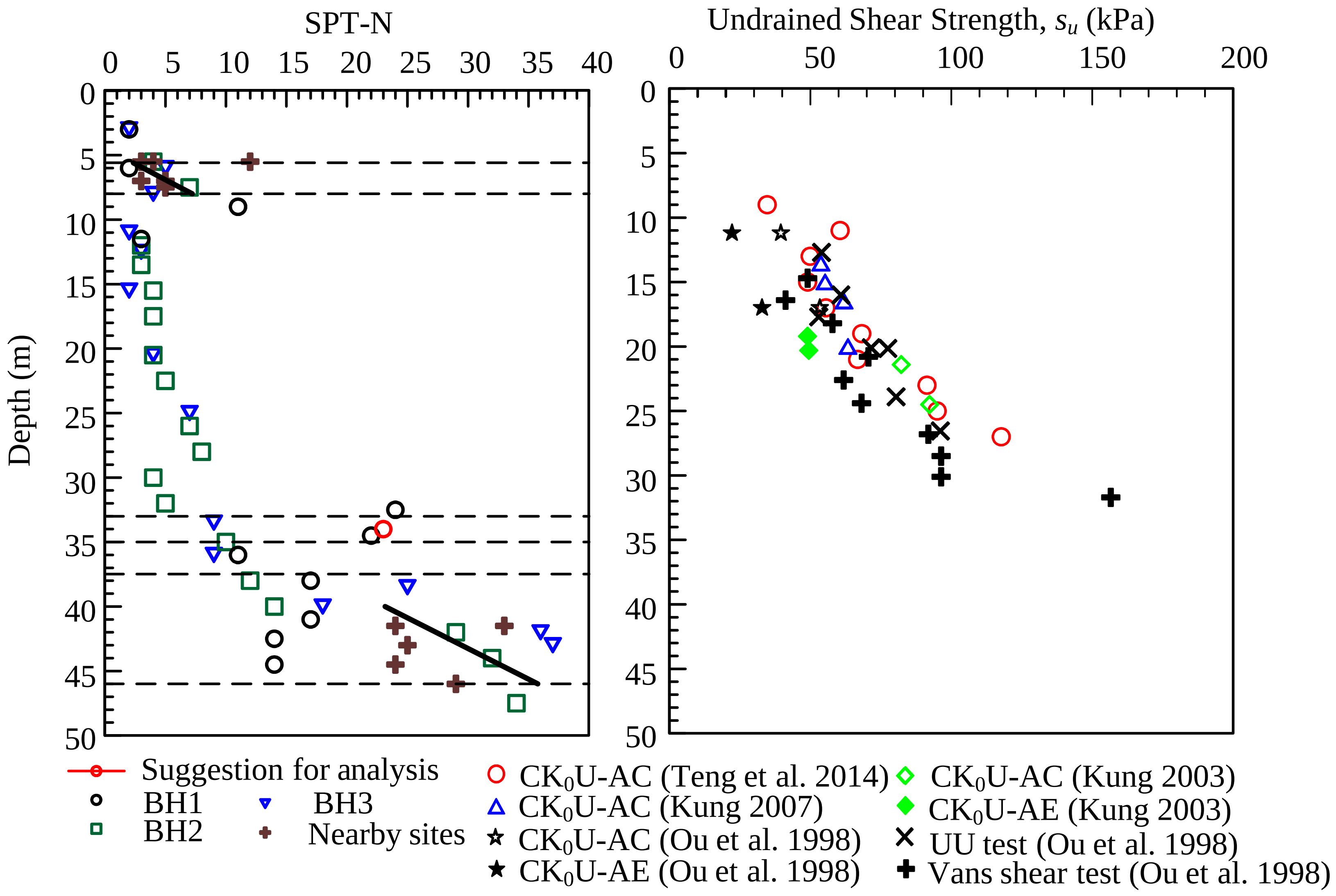
SPT-N
Undrained Shear Strength, s_u (kPa)
Depth (m)
Suggestion for analysis
BH1
BH3
BH2
Nearby sites
CK_0U-AC (Teng et al. 2014)
CK_0U-AC (Kung 2007)
CK_0U-AC (Ou et al. 1998)
CK_0U-AE (Ou et al. 1998)
CK_0U-AC (Kung 2003)
CK_0U-AE (Kung 2003)
UU test (Ou et al. 1998)
Vans shear test (Ou et al. 1998)

FIGURE B.1

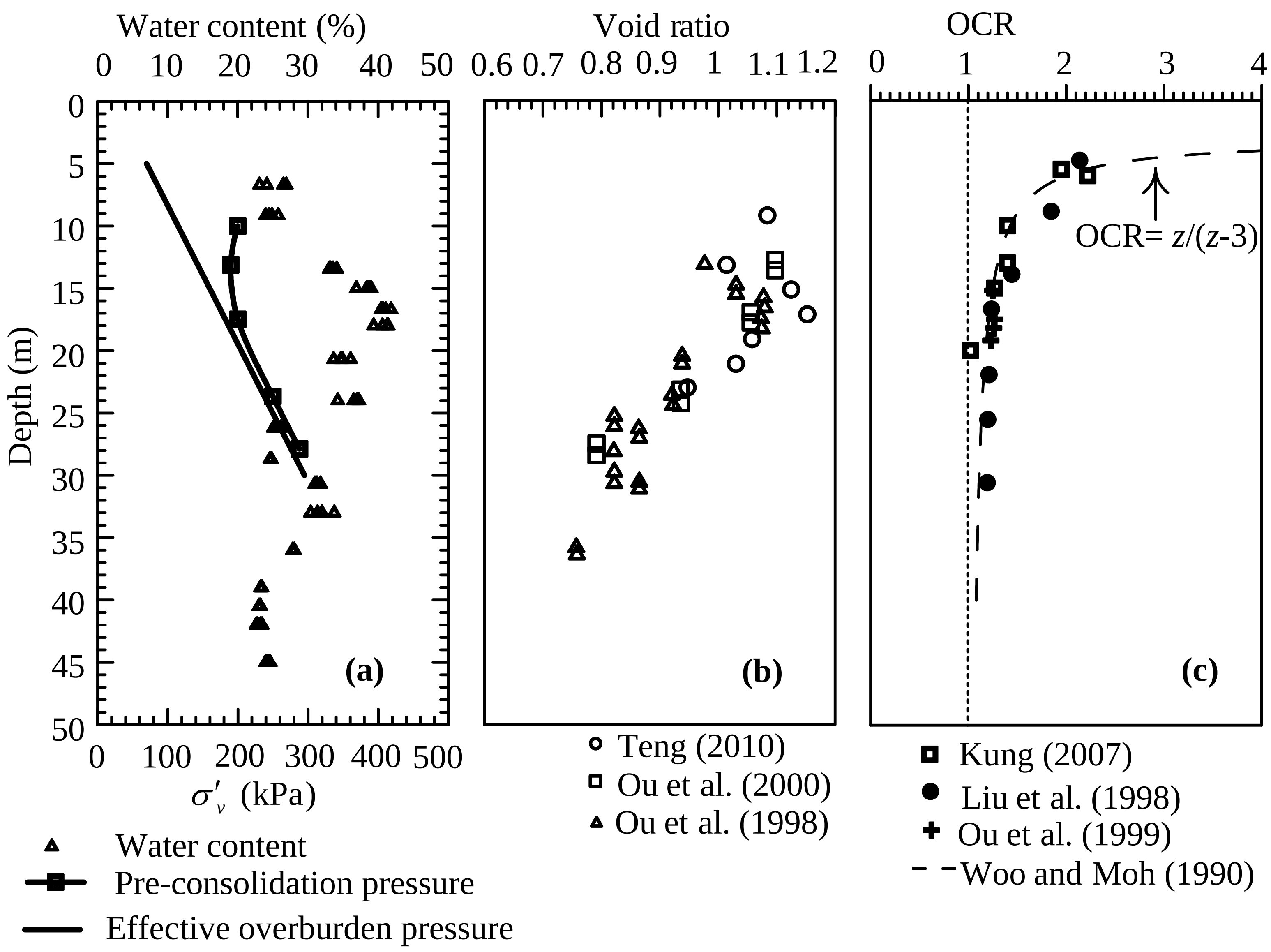

Water content (%)
0 10 20 30 40 50
Void ratio
0.6 0.7 0.8 0.9 1 1.1 1.2
OCR
0 1 2 3 4
Depth (m)
0 5 10 15 20 25 30 35 40 45 50
0 100 200 300 400 500
σ'_v (kPa)
(a)
(b)
(c)
OCR= z/(z-3)
Water content
Pre-consolidation pressure
Effective overburden pressure
Teng (2010)
Ou et al. (2000)
Ou et al. (1998)
Kung (2007)
Liu et al. (1998)
Ou et al. (1999)
Woo and Moh (1990)

FIGURE B.2

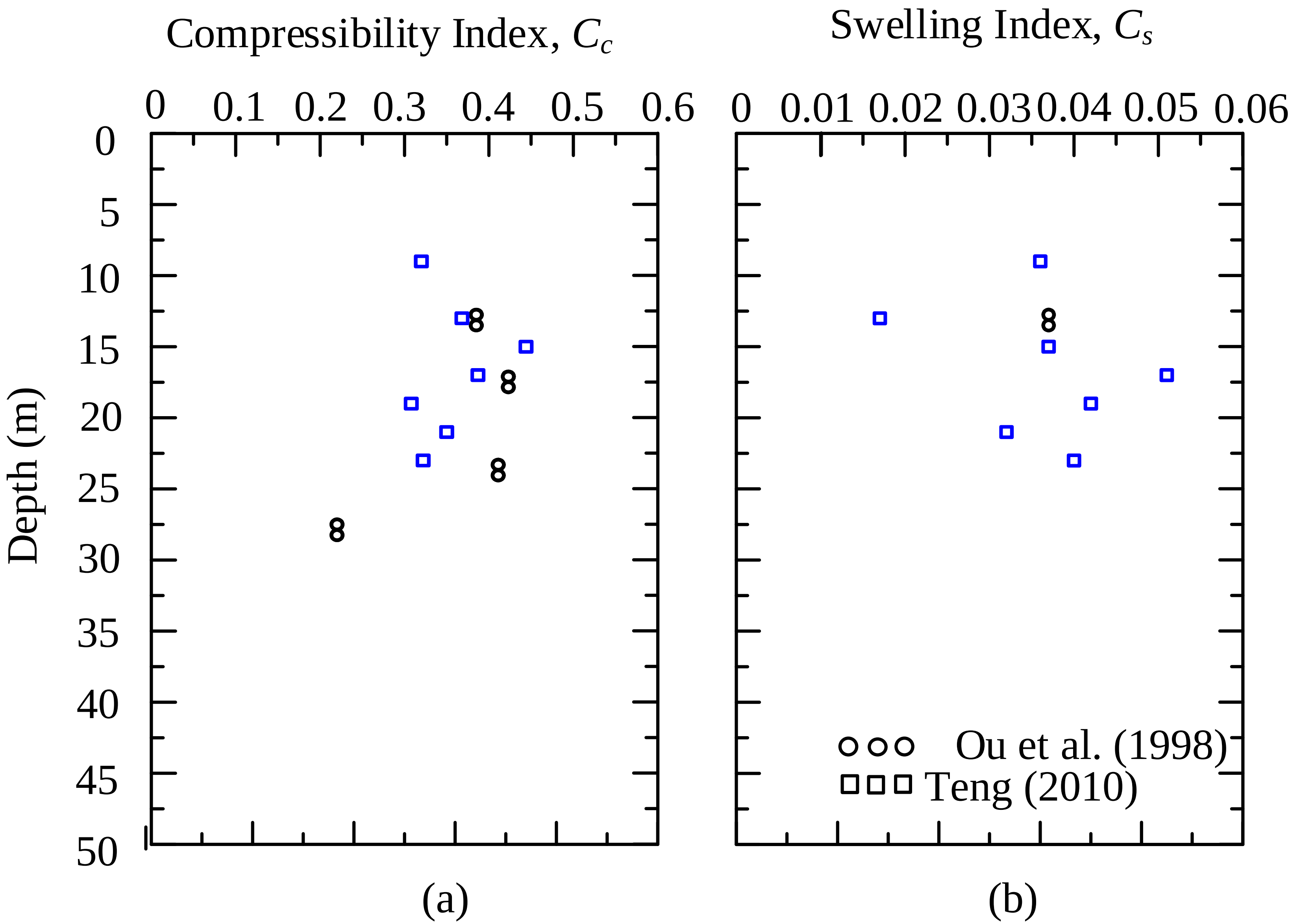

Compressibility Index, C_c
0
0.1
0.2
0.3
0.4
0.5
0.6
Swelling Index, C_s
0
0.01
0.02
0.03
0.04
0.05
0.06
Depth (m)
0
5
10
15
20
25
30
35
40
45
50
Ou et al. (1998)
Teng (2010)
(a)
(b)

FIGURE B.3

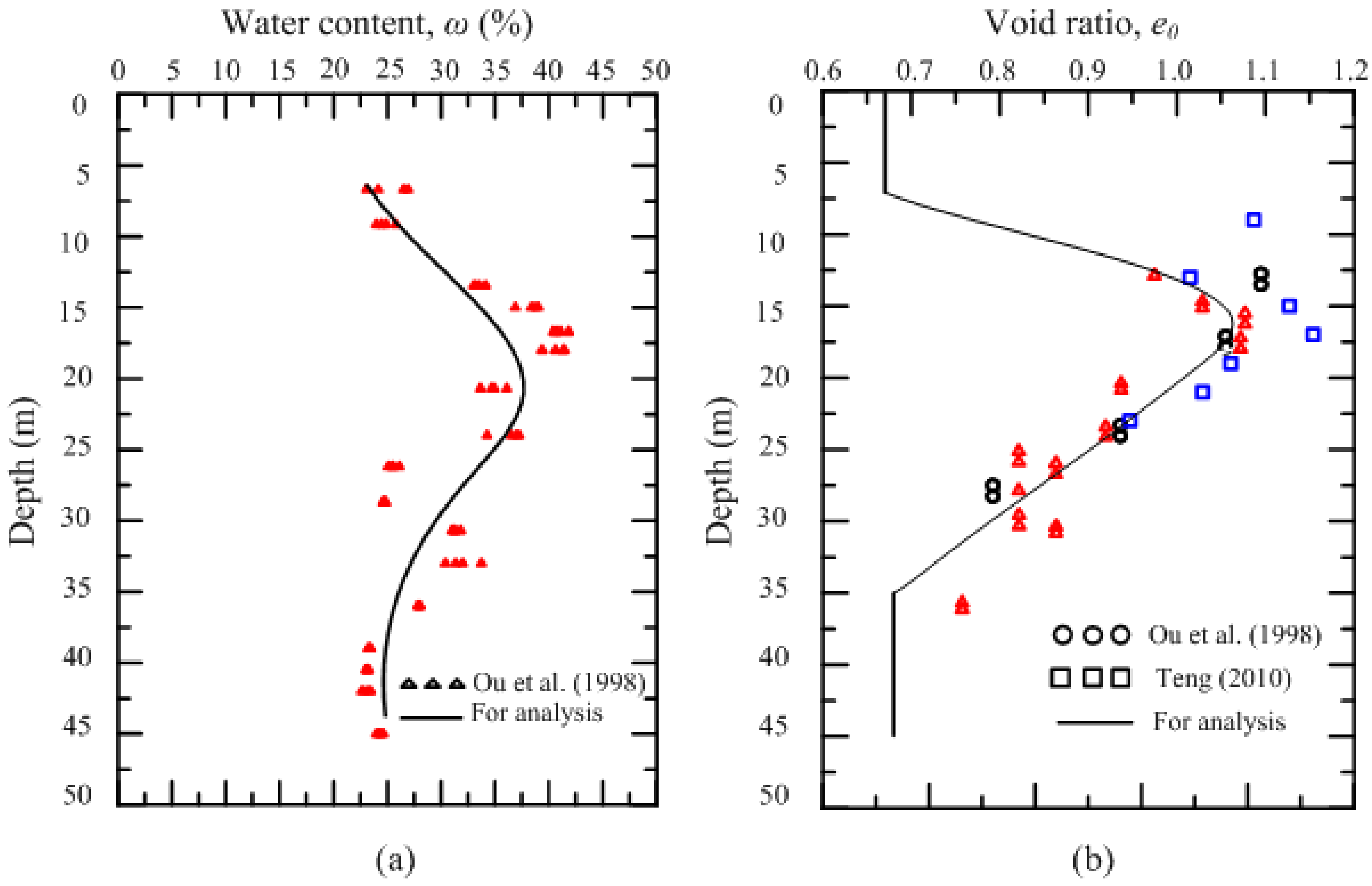

The variation of (a)water content and (b)initial void ratio with depth

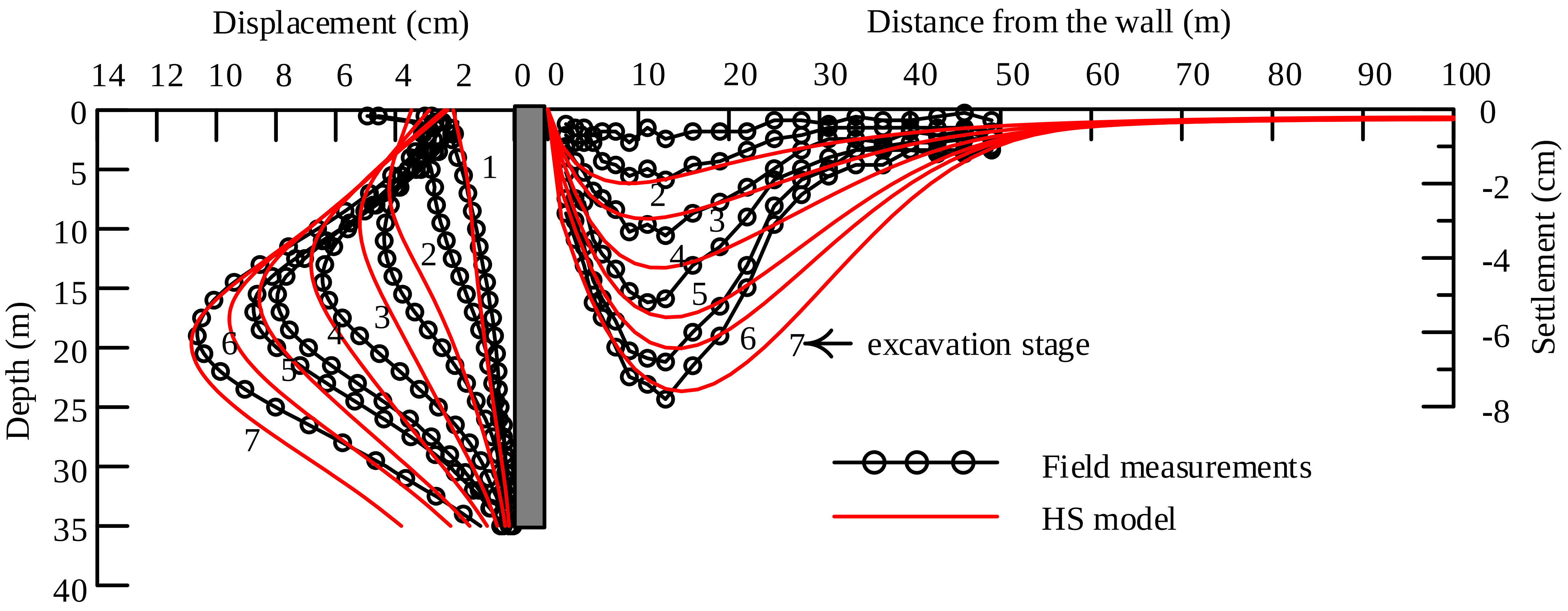

FIGURE 8.30 Results from the HS model for the TNEC case with field measurements

8.4.5 Small strain model

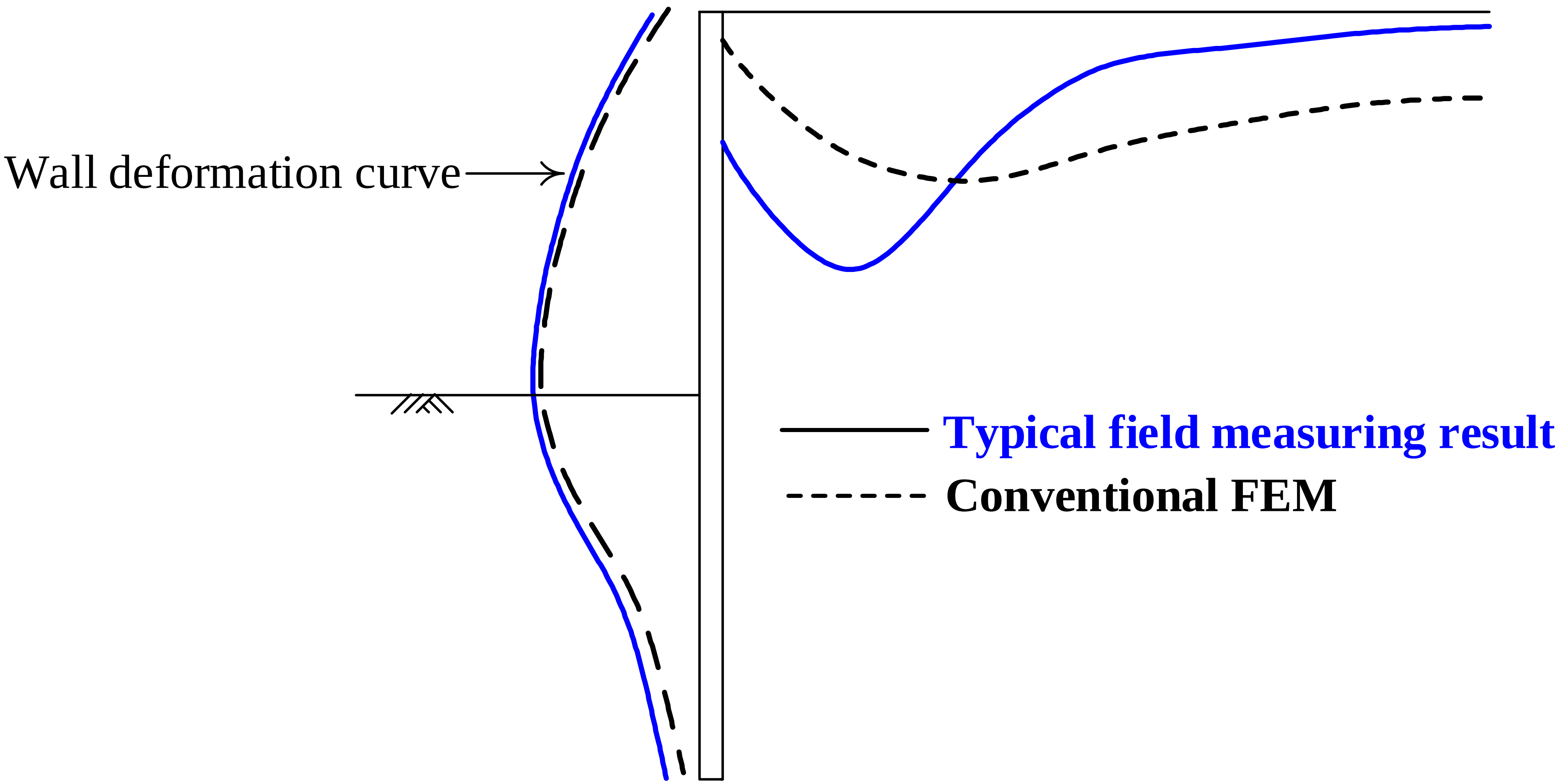

FIGURE 8.31 Wall deflection and surface settlement computed from a typical conventional finite element method

Smith et al. (1992)

Area 1: 10^{-7} to 10^{-5}; linear elastic, high stiffness

Area 2: <10^{-4}; linear elastic, stiffness decreases rapidly

Area 3: a plastic strain is generated

Area 4: When the strain reaches Y3, the soil deformations and plastic strain are all increased and a large amount of deformation is generated.

Y3 is often called initial yield surface

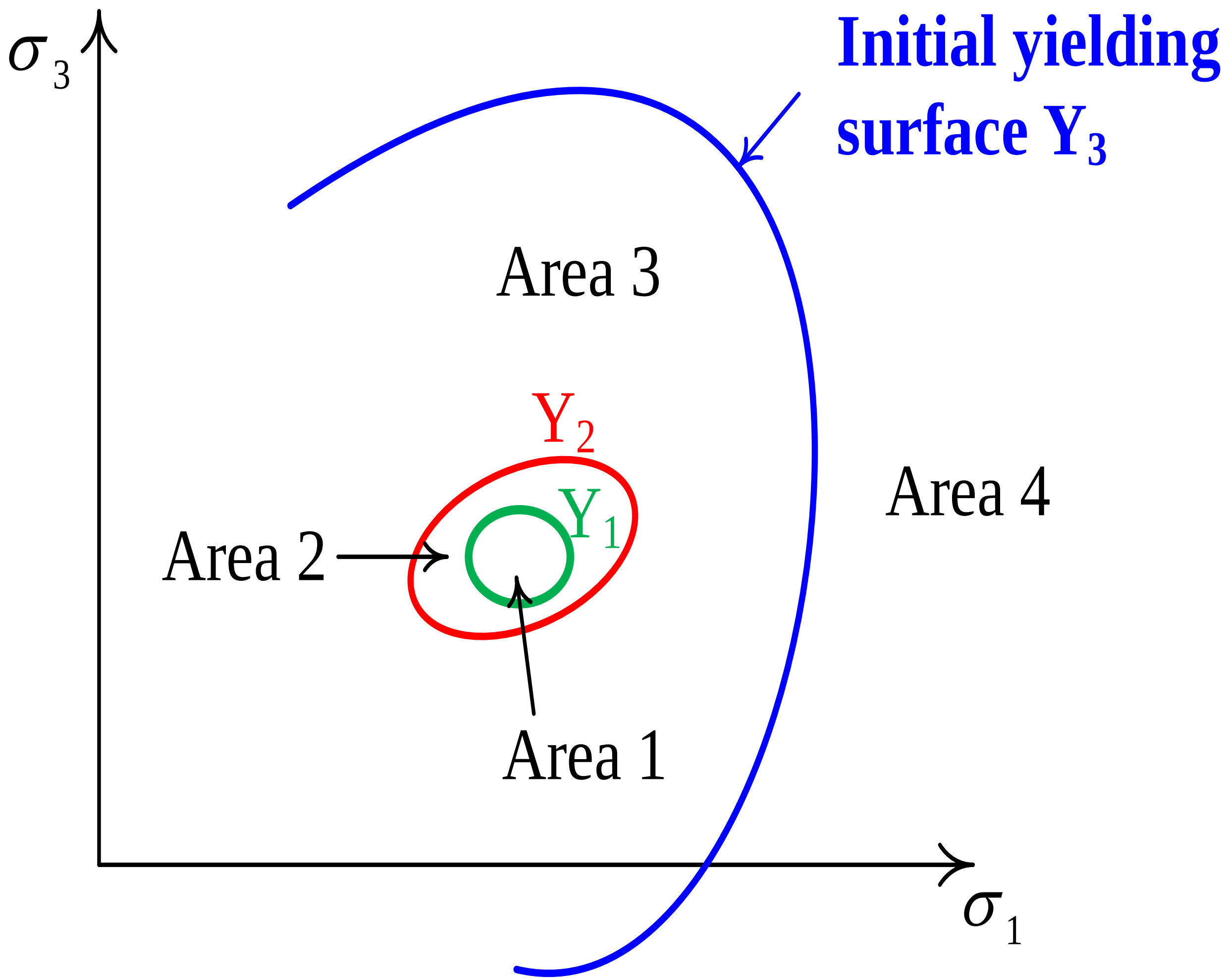

FIGURE 8.32 Yield surfaces at different strains of clay soils

Additional Soil Parameters :

- the initial or very small-strain shear modulus G_0
- the shear strain level $\gamma_{0.7}$ at which the secant shear modulus G_s is reduced to about 70% of G_0

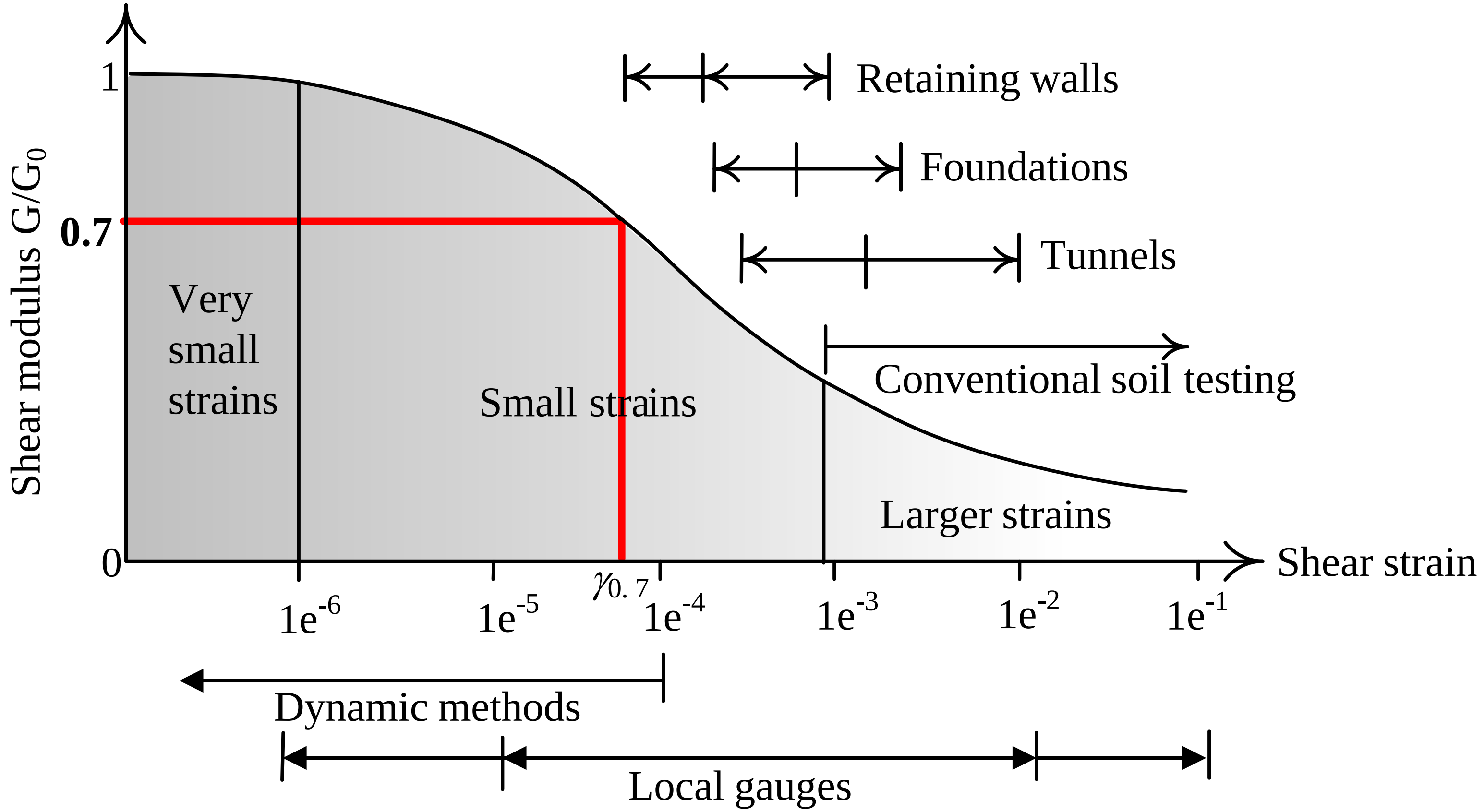

FIGURE 8.33 Shear modulus degraded with shear strain

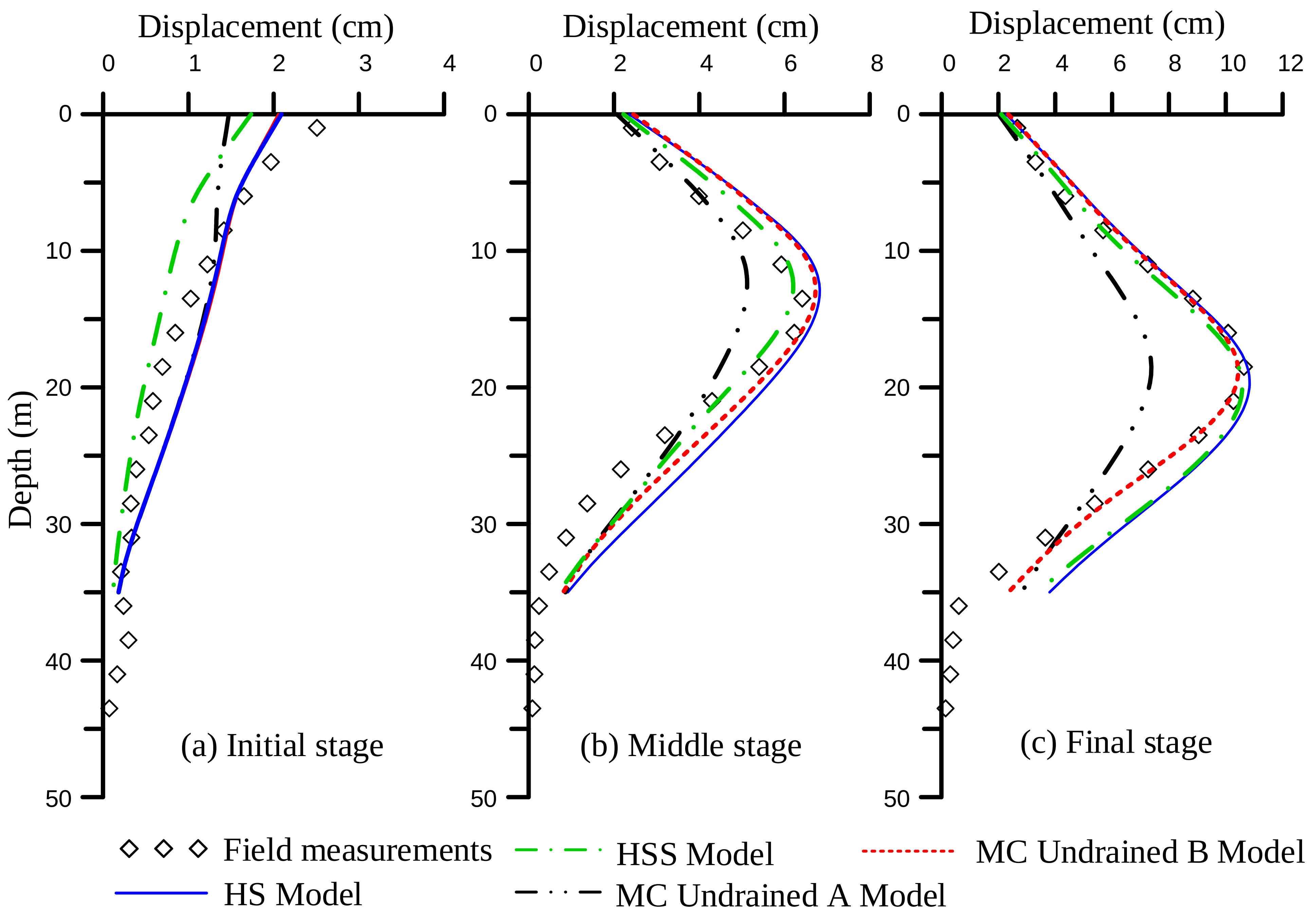

Displacement (cm)
0
1
2
3
4
Displacement (cm)
0
2
4
6
8
Displacement (cm)
0
2
4
6
8
10
12
0
10
20
30
40
50
Depth (m)
(a) Initial stage
(b) Middle stage
(c) Final stage
Field measurements
HS Model
HSS Model
MC Undrained A Model
MC Undrained B Model

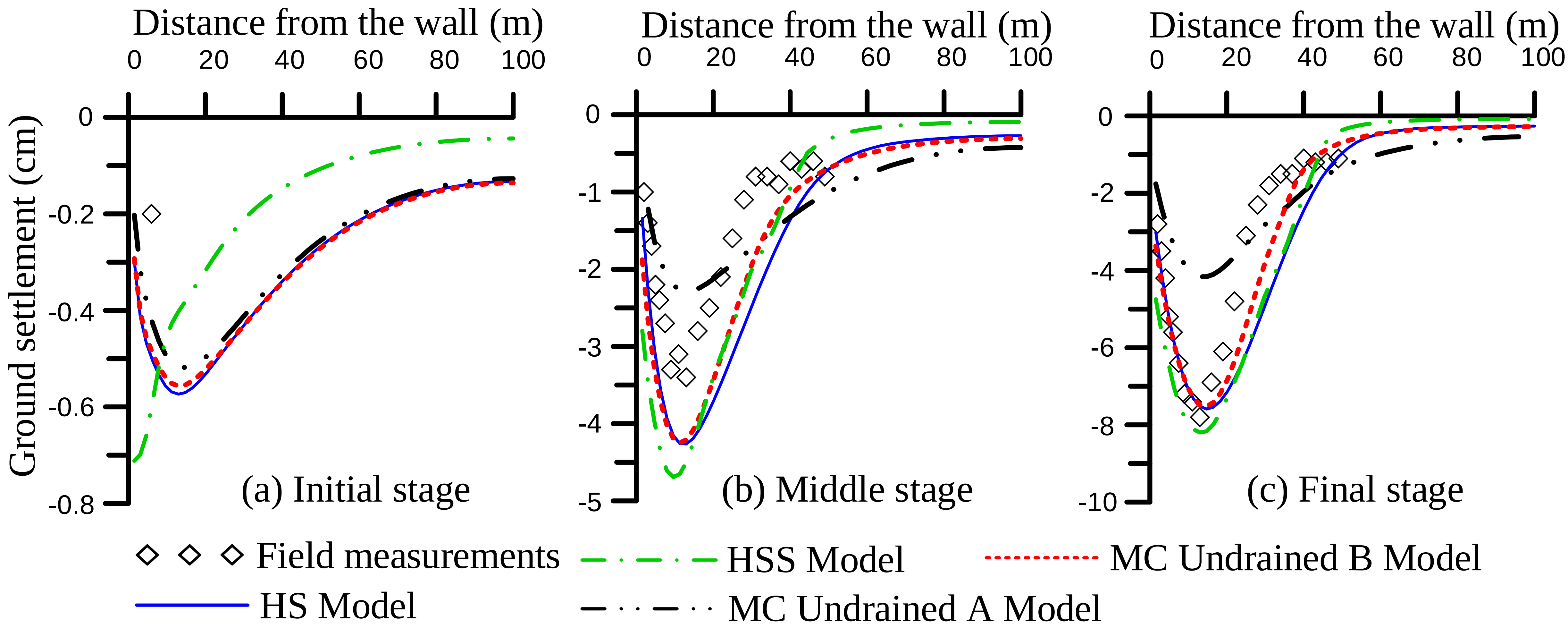

Distance from the wall (m)
0
20
40
60
80
100
Ground settlement (cm)
0
-0.2
-0.4
-0.6
-0.8
(a) Initial stage
-1
-2
-3
-4
-5
(b) Middle stage
-2
-4
-6
-8
-10
(c) Final stage
Field measurements
HSS Model
MC Undrained B Model
HS Model
MC Undrained A Model

PLAXIS suggested:

$$\gamma_{0.7} = \frac{1}{9G_0}[2c'(1+\cos 2\phi') - \sigma_1'(1+K_0)\sin 2\phi']$$

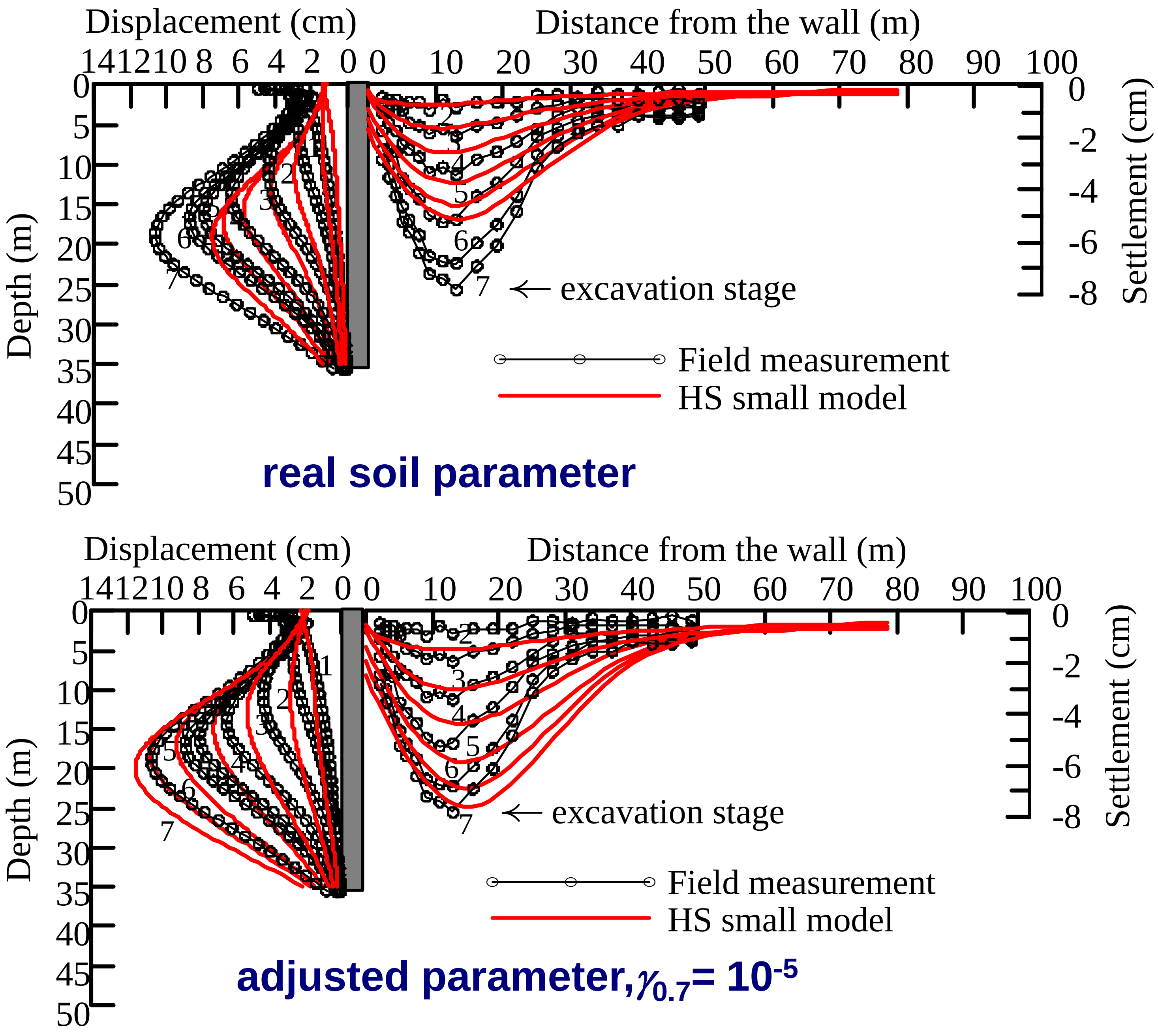

FIGURE 8.34 the HSS model for TNEC case

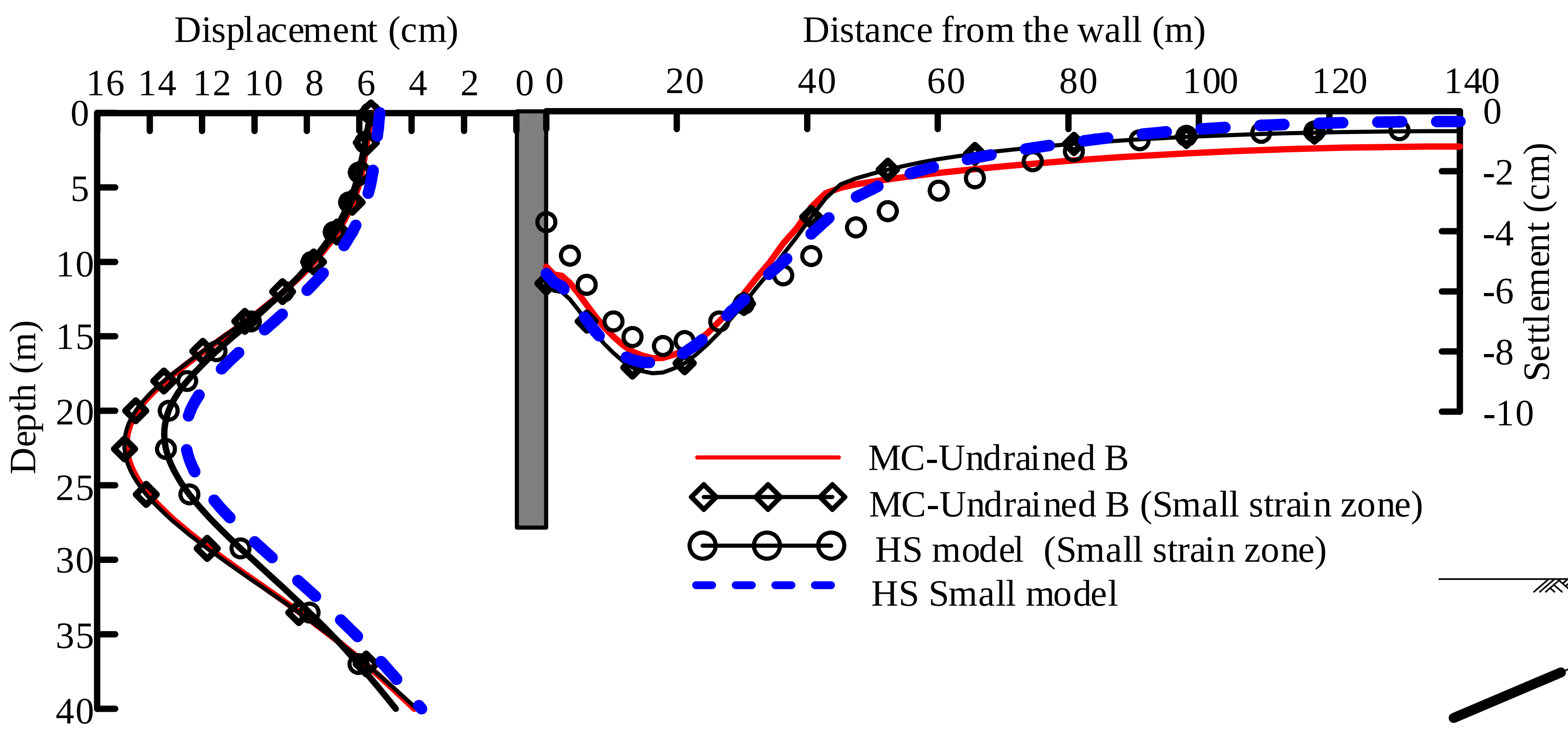

FIGURE 8.35 The HS, HSS, and MC undrained B models for an excavation in 80 m thick soft clay at the final stage

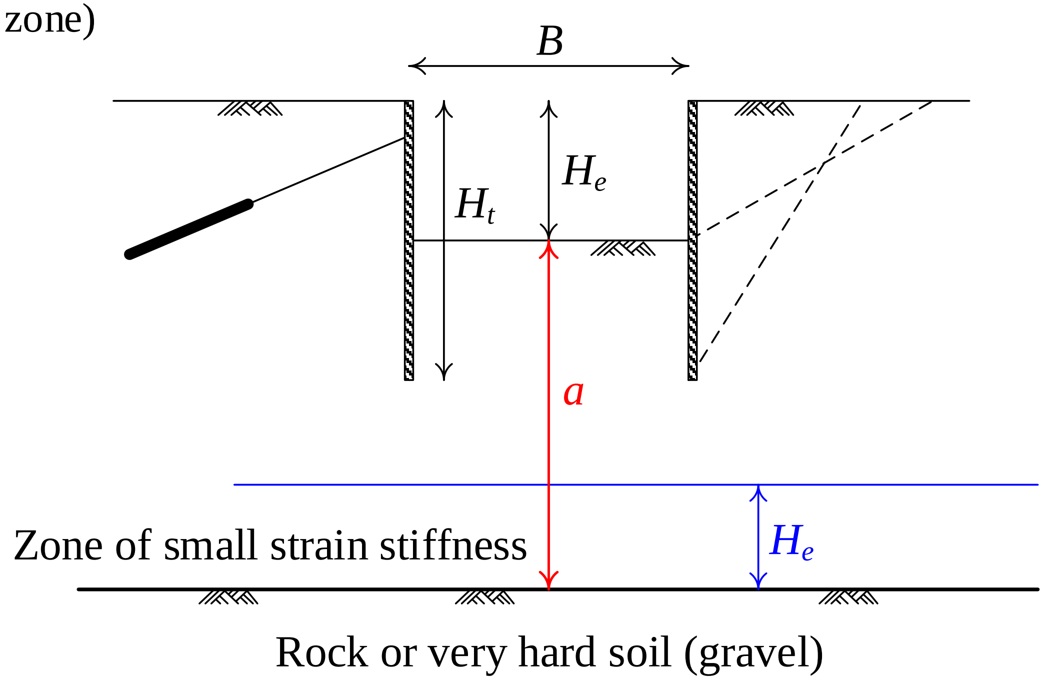

FIGURE 8.43 Distance of finite element mesh boundary (Waterman, 2009)

Stress path dependent total stress model

TNEC

Deep clay

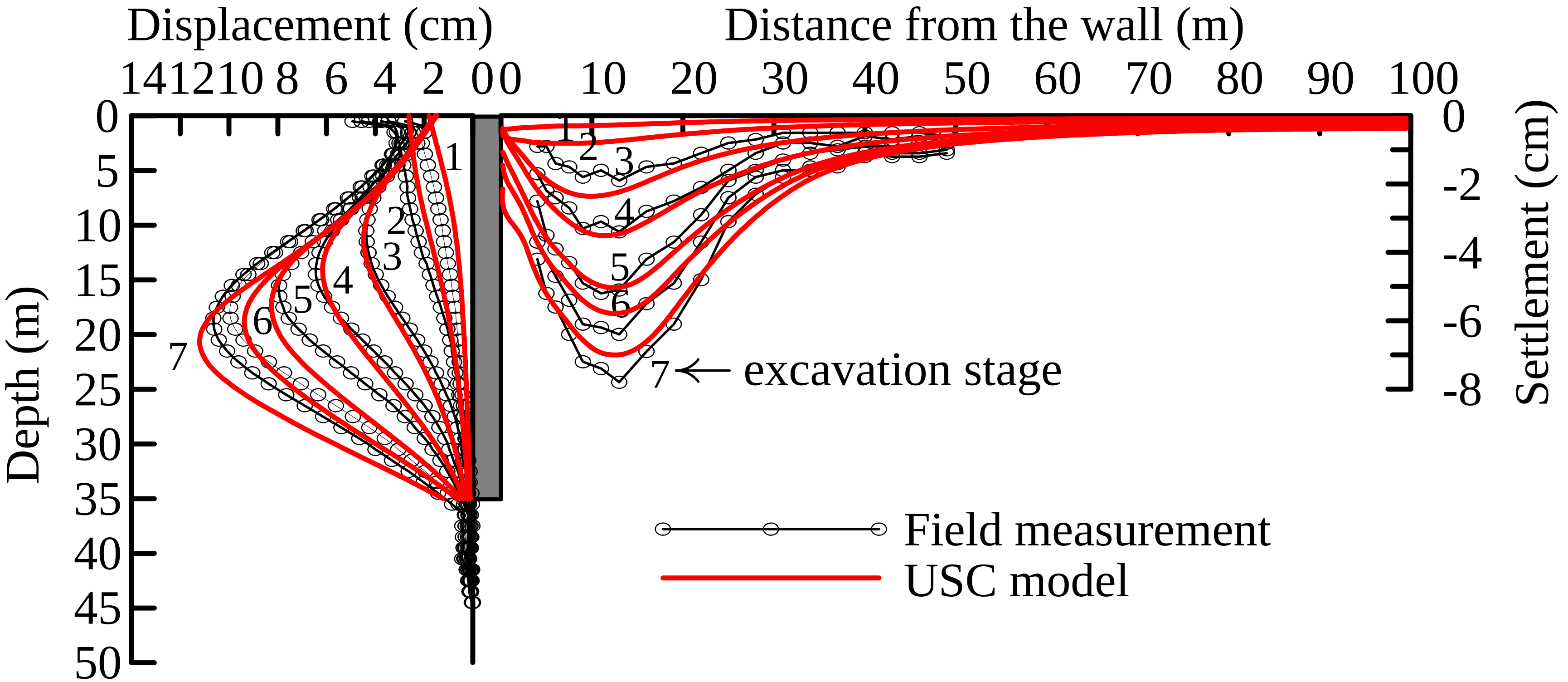

FIGURE 8.36 Comparison of wall deflections and surface settlements computed from using the USC model for the TNEC case with field measurements.

8.5 Determination of soil parameters

Effective shear strength parameters: c', ϕ'

Undrained (or total) shear strength parameters: s_u, $\phi=0$

(All refer to Sections 2.5 and 2.6)

The MCC model: E'_{ur}, μ'_{ur}, M (or ϕ'), λ, κ

$$e = e_\kappa - \kappa \ln p' \qquad (8.36)$$

Differentiate Eq. 8.36 at both sides,

$$de = -\kappa \frac{dp'}{p'} \qquad (8.52)$$

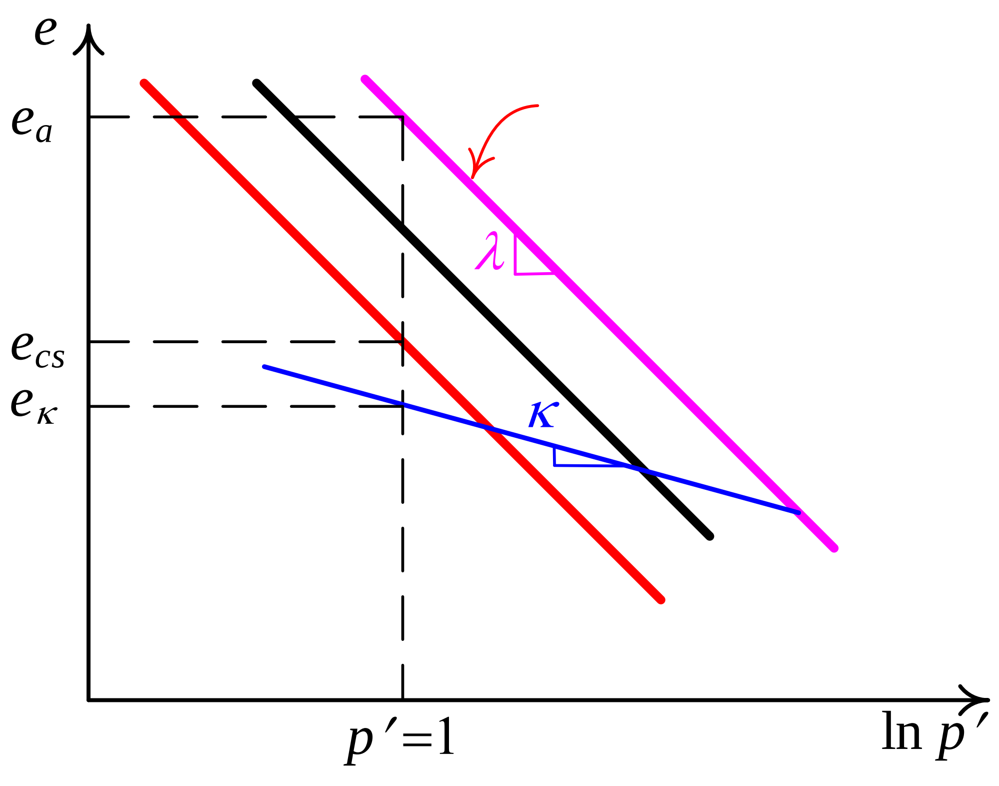

FIGURE 8.23 Definitions of various parameters in critical soil mechanics

$$K'_{ur} = -\frac{dp'}{d\varepsilon_v} = -\frac{dp'}{de/(1+e)} = \frac{(1+e)p'}{\kappa} = \frac{2.303(1+e)p'}{C_s} \qquad (8.53)$$

According to Table 2.13. we have

$$E'_{ur} = 3K'_{ur}(1-2\mu'_{ur}) = \frac{6.909(1+e)(1-2\mu'_{ur})p'}{C_s} \quad (8.54)$$

$$\mu'_{ur} \approx 0.2$$

$$\lambda = \frac{C_c}{2.303} \quad (8.48) \qquad \kappa = \frac{C_s}{2.303} \quad (8.49)$$

Empirical relationship

$$C_s = (\frac{1}{10} \text{ to } \frac{1}{5})C_c \quad (8.50)$$

Analysis of the TNEC case with the MCC model

Depth (m)	γ_t (kN/m^3)	M	υ_{ur}	κ/λ
0 ~ 5.6	18.25	1.2	0.2	0.09
8 ~ 12	18.15	1.16	0.2	0.1
12 ~ 33	18.15	1.16	0.2	0.1 ~ 0.15
35 ~ 37.5	19.13	1.2	0.2	0.14

The parameters e, M, λ, κ are directly from the tests

Comparison

MCC model

The real parameter κ

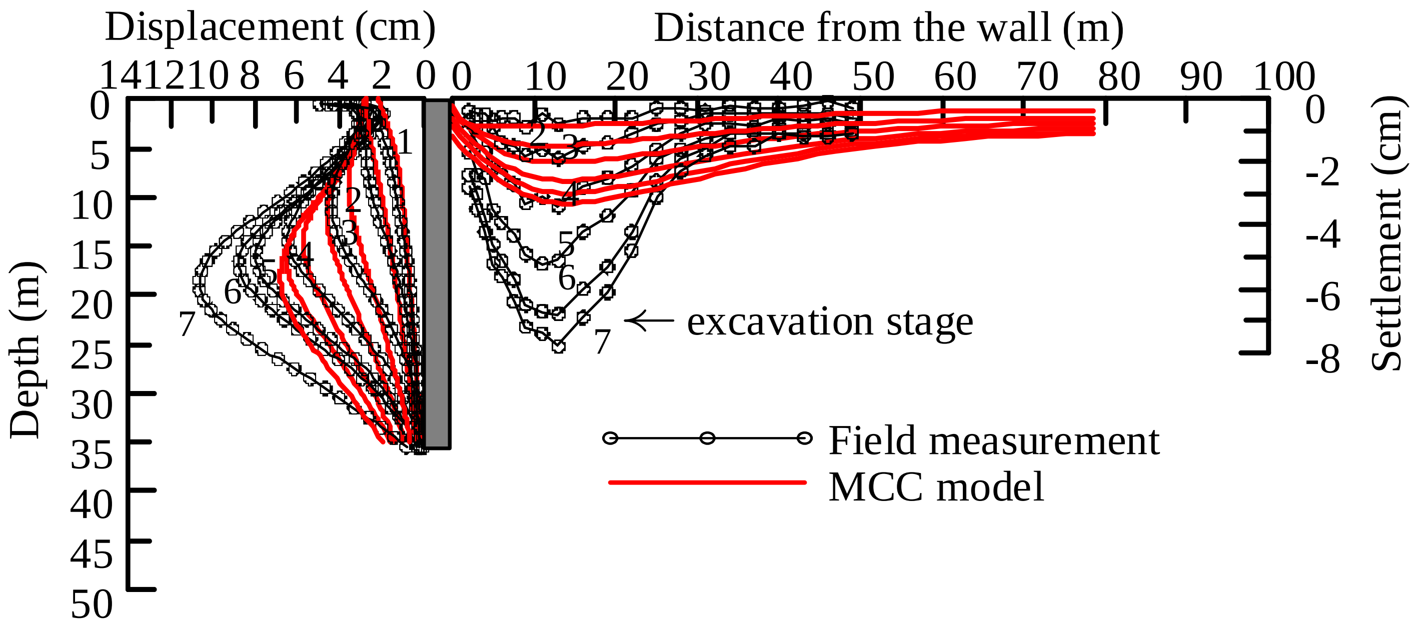

The adjusted parameter κ

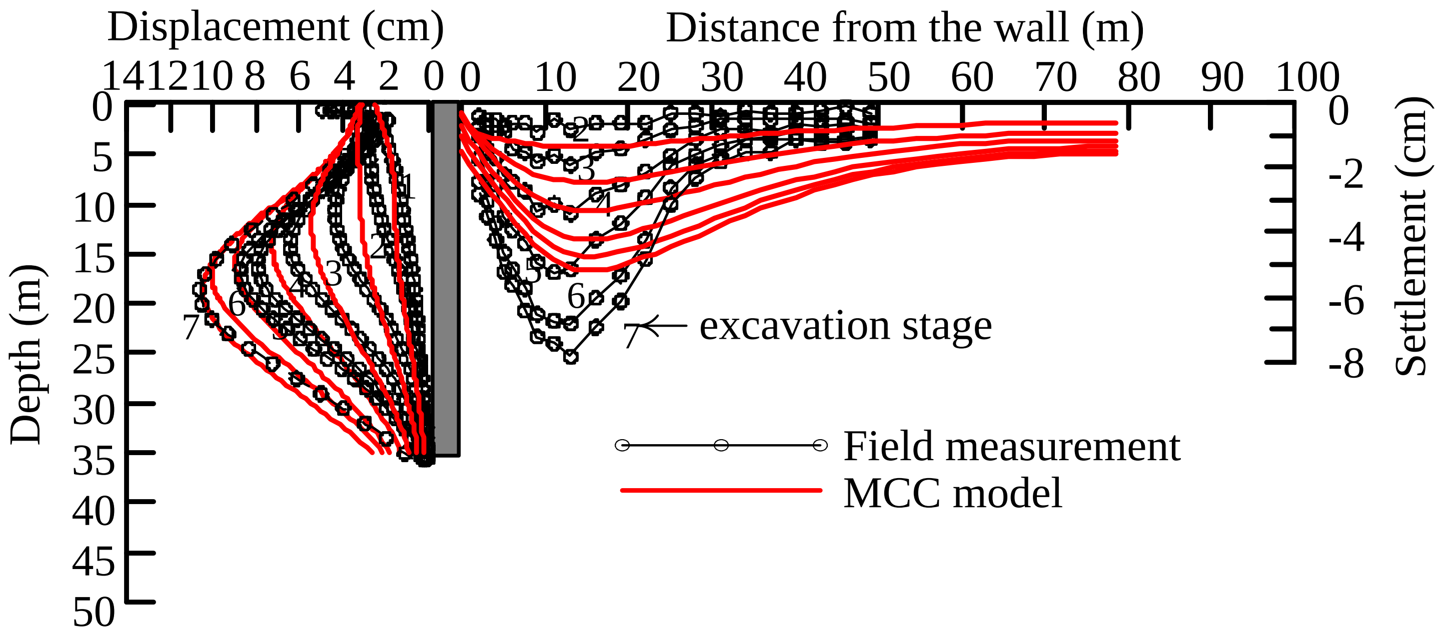

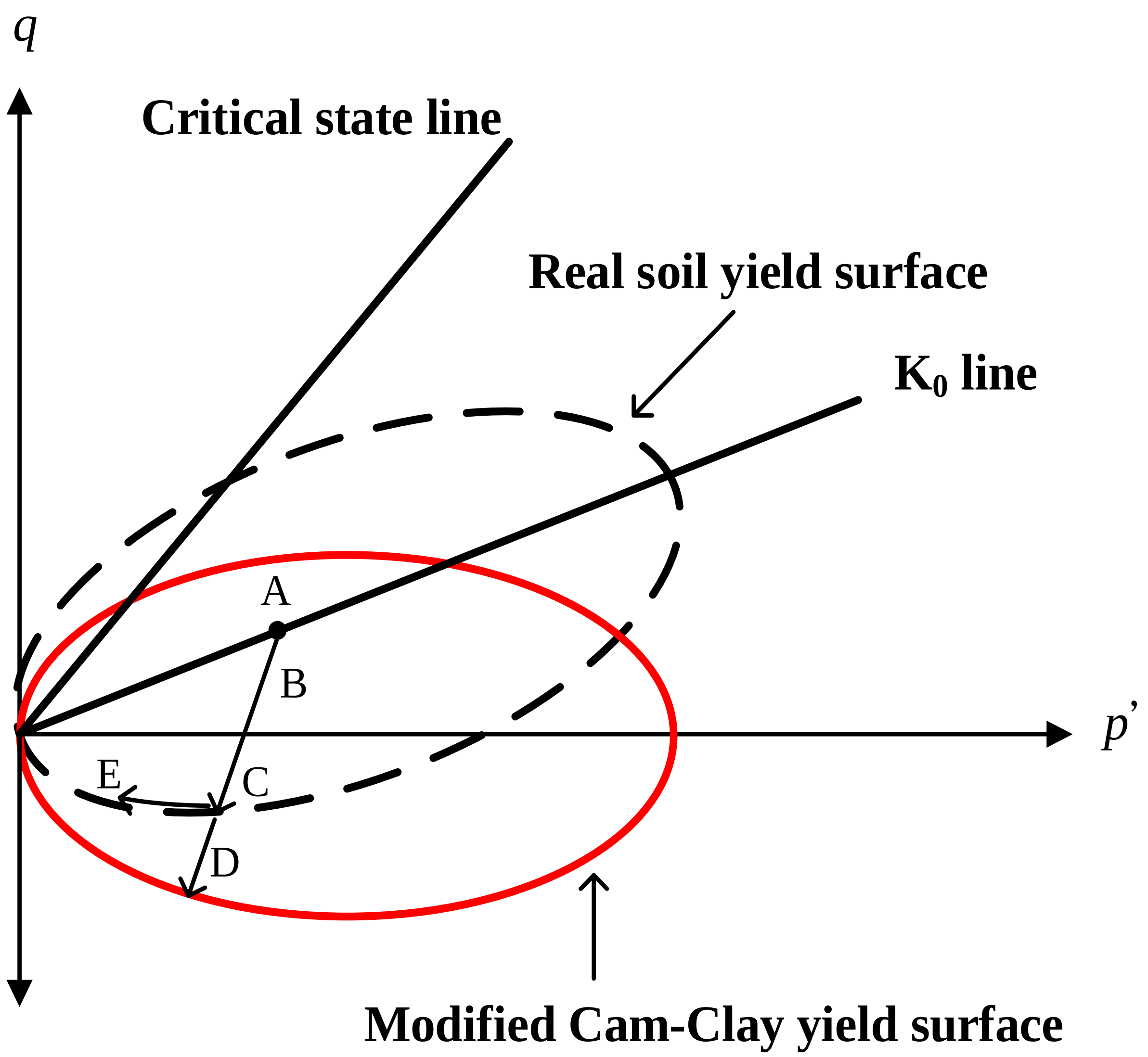

Relationship of stress path in modified Cam-Clay yield surface and yield surface of natural soil

$$C_s = (\frac{1}{5} \text{ to } \frac{1}{4}) C_c \qquad (8.51)$$

Adjusted parameters of undrained material (clay) for the MCC model

Depth (m)	γ_t (kN/m^3)	M	κ	υ_{ur}	κ/λ
0 ~ 5.6	18.25	1.2	–	0.2	0.09
8 ~ 12	18.15	1.16		0.2	0.1
12 ~ 33	18.15	1.16	0.2λ	0.2	0.2
35 ~ 37.5	19.13	1.2	0.2λ	0.2	0.2

The parameters κ is adopted directly from the tests for the soil at a depth of GL0 to GL-12 m and is adjusted to be 0.2λ for the soil below GL-12 m

Comparison

MCC model

The real parameter κ

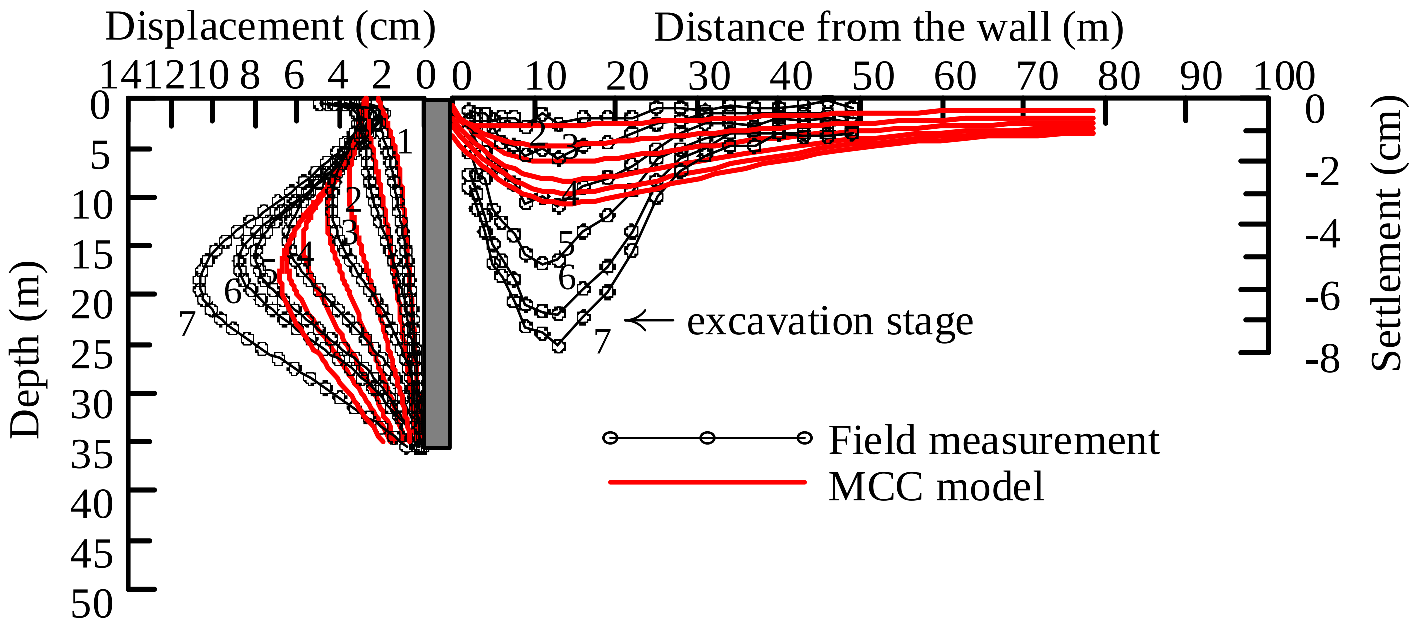

The adjusted parameter κ

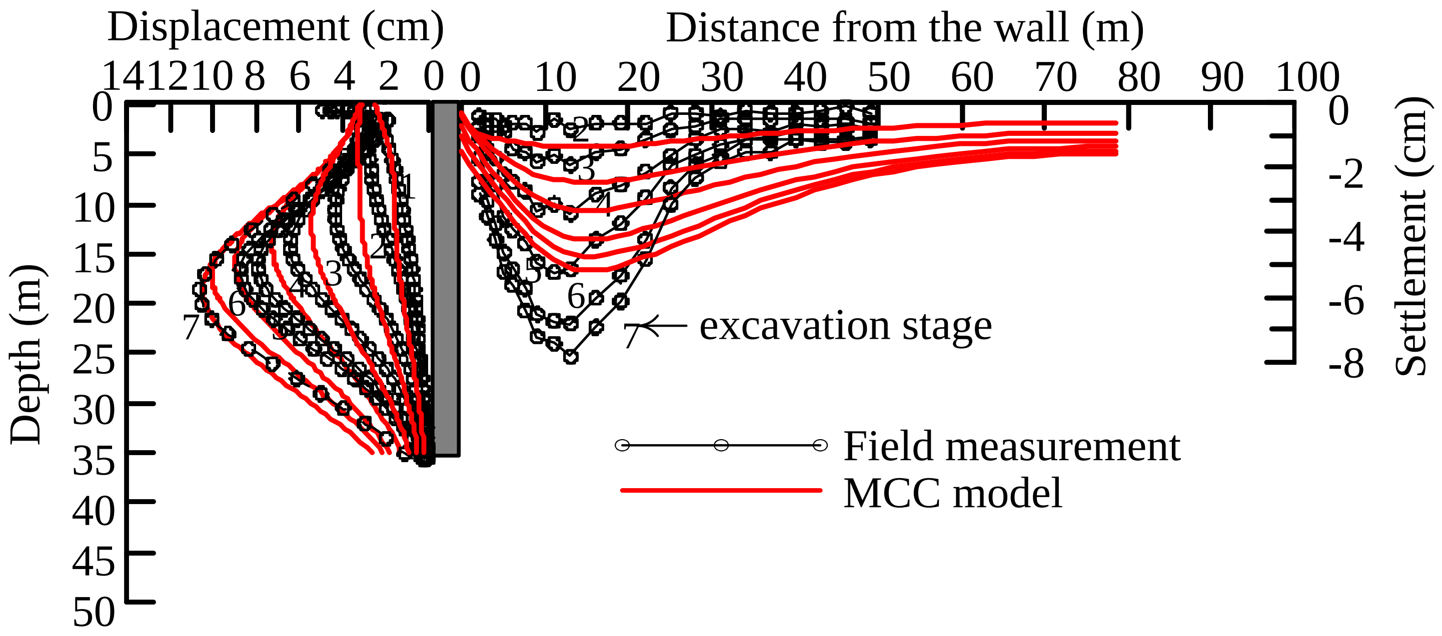

Elastic constants

The HS model requires $\boxed{E'_{ur}\ (\text{or } E'^{ref}_{ur}),\ \mu'_{ur}}$, c', ϕ', R_f, p'^{ref}, E'_{ur} (or E'^{ref}_{ur}), E'_{50} (or E'^{ref}_{50}), E'_{oed} (or E'^{ref}_{oed}), m, $K_{0,NC}$, p'_c, ψ

$$\{\Delta\sigma\} = \left([D^e] - [D^p]\right)\{\Delta\varepsilon\} = [D^{ep}]\{\Delta\varepsilon\} \qquad (8.15)$$

For clay, all the parameters can be obtained by the simulation of triaxial compression tests with unloading/reloading and oedometer tests using the FEM with the HS model.

From correlation:

$$E'_{ur} = 3K'_{ur}(1-2\mu'_{ur}) = \frac{6.909(1+e)(1-2\mu'_{ur})p'}{C_s} \qquad (8.54) \qquad \mu'_{ur} \approx 0.2$$

$$E'^{ref}_{50} = E'^{ref}_{ur}/(3\sim5) = E'^{ref}_{ur}/3.5 \quad \text{(NC Clay)} \qquad E'^{ref}_{50} = E'^{ref}_{ur}/3$$

$$E'^{ref}_{50} = E'^{ref}_{ur}/(2\sim3) = E'^{ref}_{ur}/2.5 \quad \text{(OC Clay)}$$

$$E'^{ref}_{oed} \approx (0.7-1.0)E'^{ref}_{50}$$

$$m \approx 0.9 \qquad R_f = 0.9 \qquad \psi = \phi' - 30^{\text{o}} \quad \text{(Bolton, 1986)}$$

For sand, it is determined to the unloading/reloading Young's modulus (E'_{ur}) first:

$$E'_{ur} = f\,(\text{SPT-}N) \approx (2{,}000 \text{ to } 3{,}000)N \qquad (8.56) \qquad \text{(Khoiri and Ou, 2013)}$$

where E'_{ur} is in kN/m^2, N is SPT-N value

$E'^{\,ref}_{ur}$ can be obtained from
$$E'_{ur} = E'^{\,ref}_{ur}\left(\frac{c'\cot\phi' + \sigma'_3}{c'\cot\phi' + p'^{\,ref}}\right)^m = E'^{\,ref}_{ur}\left(\frac{c'\cos\phi' + \sigma'_3\sin\phi'}{c'\cos\phi' + p'^{\,ref}\sin\phi'}\right)^m \qquad (8.42)$$

$$E'^{\,ref}_{50} = E'^{\,ref}_{ur}/(3\sim5) = E'^{\,ref}_{ur}/3.5 \quad \text{(Loose sand)}$$

$$E'^{\,ref}_{50} = E'^{\,ref}_{ur}/(2\sim3) = E'^{\,ref}_{ur}/2.5 \quad \text{(Dense sand)}$$

$$E'^{\,ref}_{oed} \approx E'^{\,ref}_{50} \qquad m = 0.4 \text{ to } 0.6 \qquad \mu'_{ur} \approx 0.2$$

$$R_f = 0.5\sim0.6 \quad \text{(Wong and Broms, 989)} \qquad \psi = \phi' - 30^{\circ} \quad \text{(Bolton, 1986)}$$

Elastic constants

The HSS model requires $\boxed{E'_{ur}\ (\text{or } E'^{ref}_{ur}),\ \mu'_{ur}}$, c', ϕ', R_f, p'^{ref}, E'_{ur} (or E'^{ref}_{ur}), E'_{50} (or E'^{ref}_{50}), E'_{oed} (or E'^{ref}_{oed}), m, $K_{0,NC}$, p'_c, ψ, G_0, $\gamma_{0.7}$

G_0 is a shear modulus at very small strain, which can be obtained from bender element test, seismic survey, a small strain triaxial test, or from empirical formulas.

$\gamma_{0.7}$ is the shear strain corresponding to G/G_0=0.7

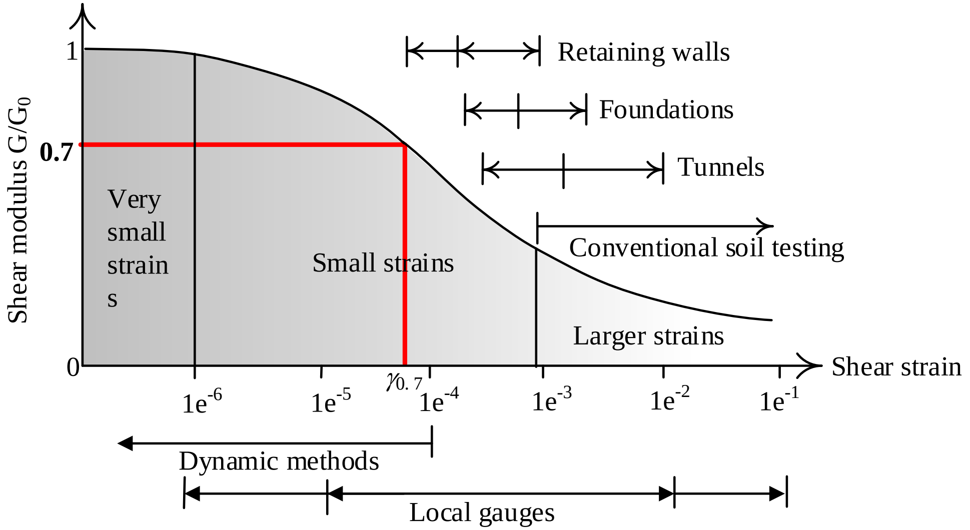

FIGURE 8.33 Shear modulus degraded with shear strain

Using the original Hardin-Drnevich relationship, and related to the model's failure parameters.

$$\gamma_{0.7} \approx \frac{1}{9G_0}\left[2c'(1+\cos(2\varphi')) - \sigma_1'(1+K_0)\sin(2\varphi')\right]$$

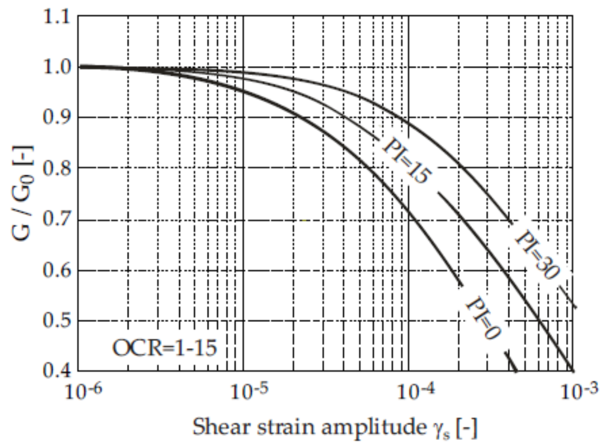

Influence of plasticity index (PI) on stiffness reduction after Vucetic & Dobry (1991).

PLAXIS suggested:

$$\gamma_{0.7} = \frac{1}{9G_0}[2c'(1+\cos 2\phi') - \sigma_1'(1+K_0)\sin 2\phi']$$

Suggested parameter above

Calibrated parameter, $\gamma_{0.7}$= 10^{-5}

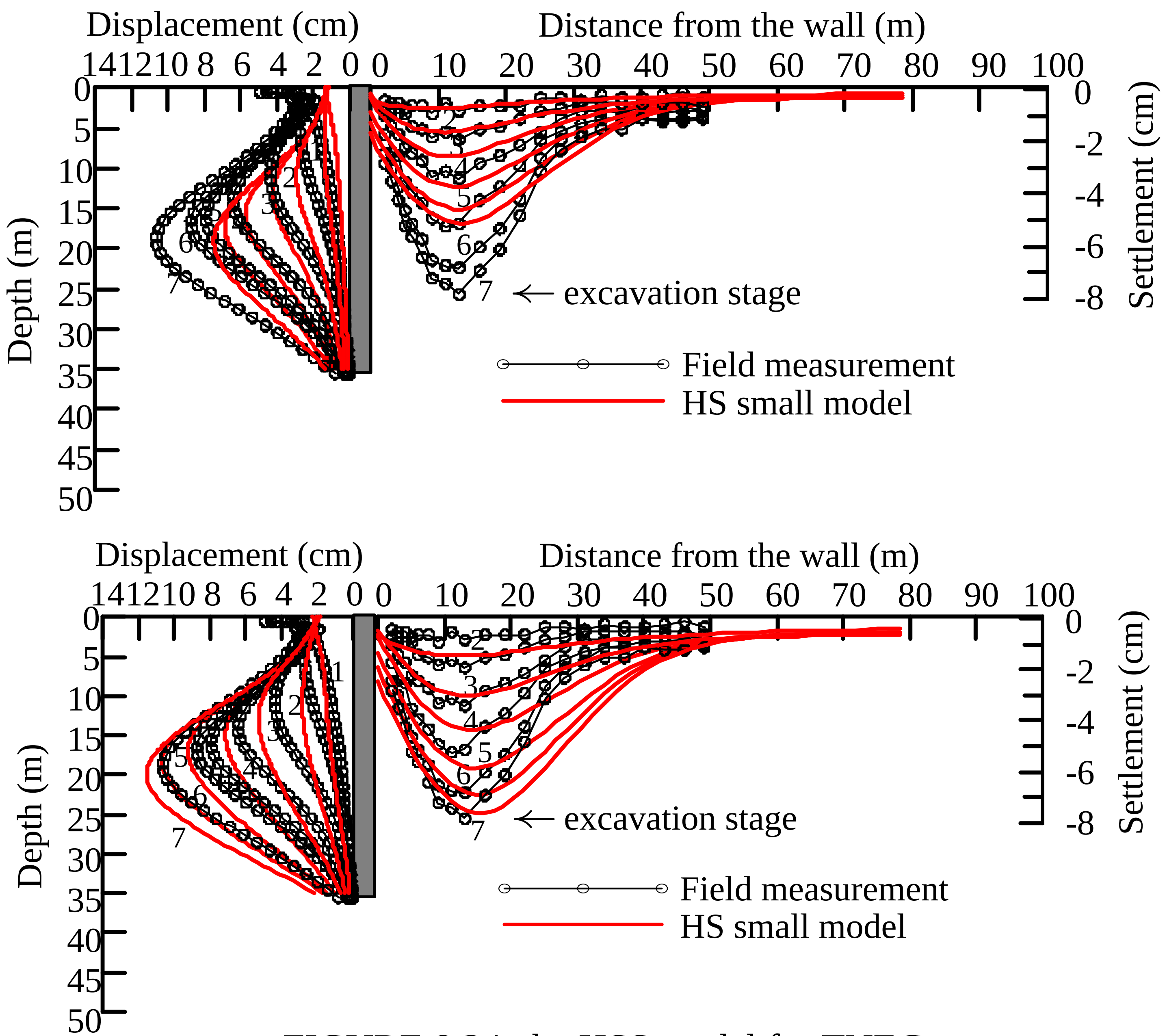

FIGURE 8.34 the HSS model for TNEC case

The MC model for sand, c' and ϕ', E', μ' and ψ.

The dilation angle ψ can be estimated using $\psi = \phi' - 30^{o}$ (Eq. 8.55)

The magnitude of parameters **E' and μ' is related to the stress or loading path**.

The soil in front of the wall is subject to unloading stress path, the E' can be determined following Eq. 8.56, and μ' can be set equal to 0.2.

$$E' = E'_{ur} = (2{,}000 \text{ to } 3{,}000)N \quad (8.56)$$

For the soil subject to **loading stress path** such as the soil behind the wall, the E' is more close to E'_{50}. The relationship of E'_{50} and E'_{ur} as used in the HS model ($E'^{ref}_{50} = E'^{ref}_{ur} / (3 \sim 5)$) can be applied.

The μ' should be in the range of 0.3 to 0.4.

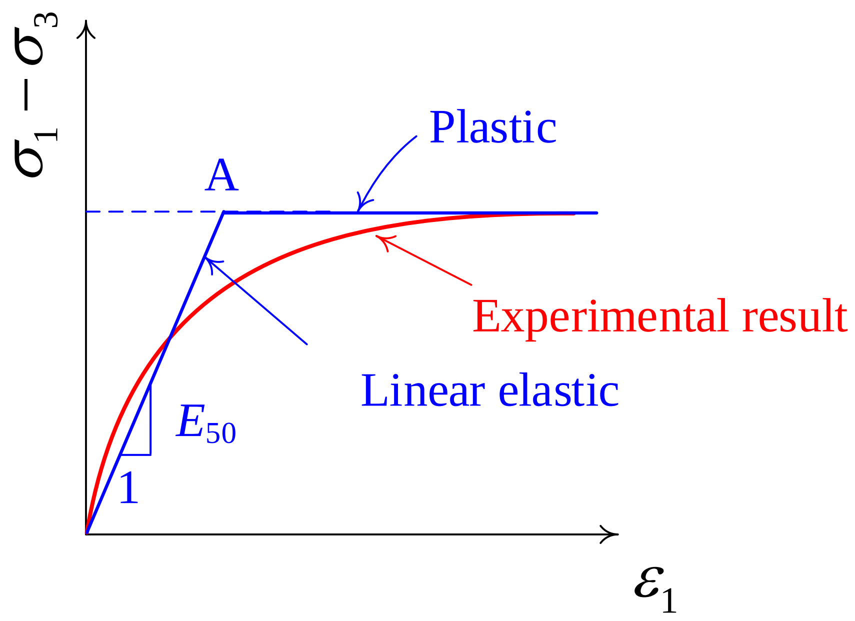

FIGURE 8.14 Mohr-Coulomb model

The MC undrained model B for clay: c' and ϕ', E', μ' and ψ.

$$E' = E'_{ur} \qquad \mu' = \mu'_{ur} \approx 0.2 \qquad \psi = \phi' - 30^{o}$$

The MC undrained model C for clay: s_u, ϕ_u=0, undrained E_u, undrained μ_u

$$\mu_u = 0.5 \;\text{ or }\; 0.495$$

$$G' = \frac{E'}{2(1+\mu')} \qquad (8.57) \qquad\qquad G_u = \frac{E_u}{2(1+\mu_u)} \qquad (8.58)$$

$$E_u = \frac{E'(1+\mu_u)}{(1+\mu')} = \frac{E'_{ur}(1+\mu_u)}{(1+\mu'_{ur})} \qquad (8.59)$$

$E_u/s_u = f$ (PI, OCR)

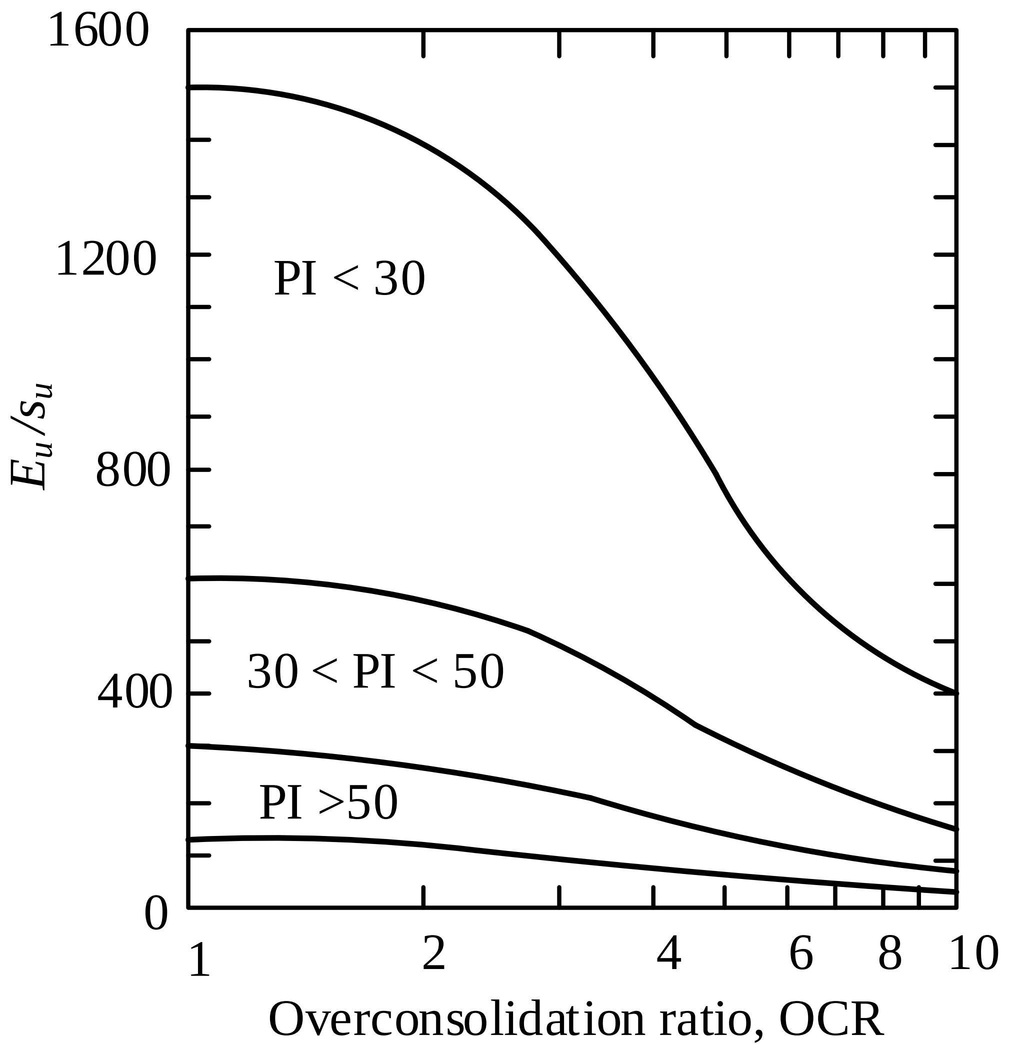

FIGURE 8.37 Relation of E_u/s_u with OCR and PI (redraw from Duncan and Buchignani, 1976)

8.6 Determination of initial stresses

8.6.1 Direct input method

For sloping ground:

$$\sigma'_y = \gamma_m h$$

$$\sigma'_x = K_0 \sigma'_y$$

$$\tau_{xy} = \gamma_m h \sin\alpha / 2$$

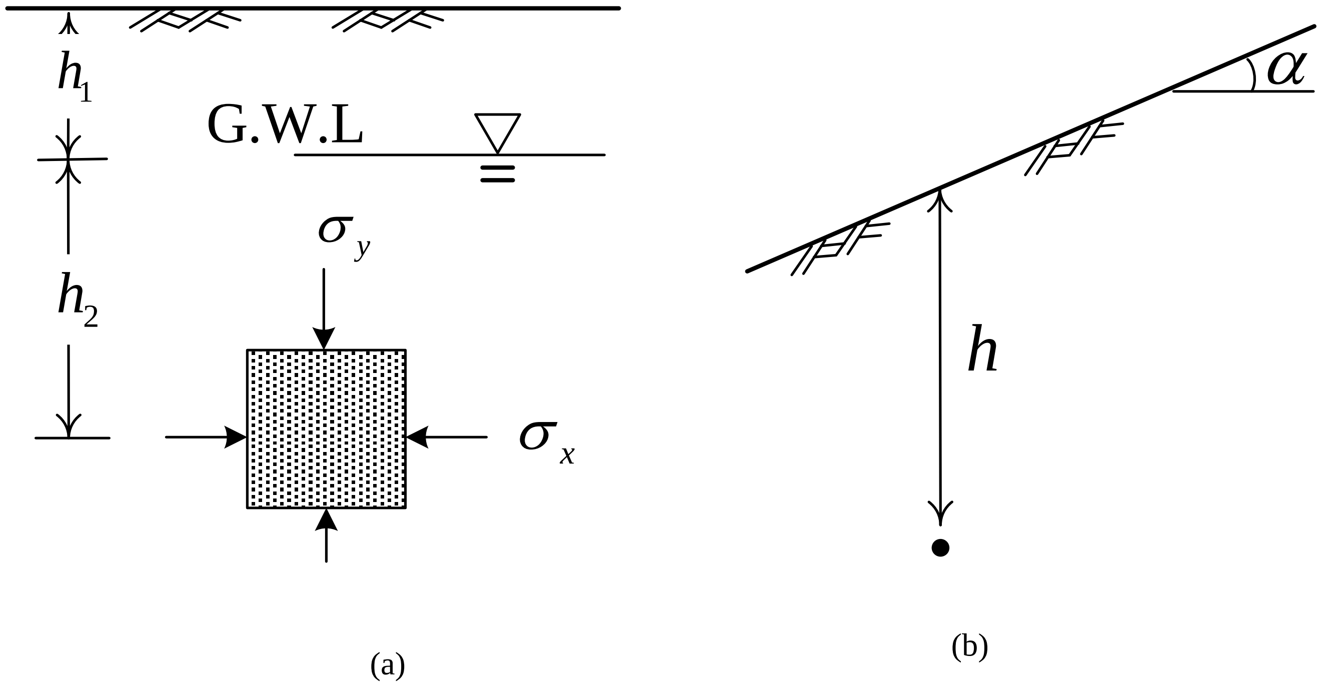

FIGURE 8.38 Initial stresses (a) in the free field (b) in sloping ground

Anisotropic total stress analysis:

$$\sigma_y = \sigma'_y + u\,,\quad \sigma_x = K_0\sigma'_y + u \qquad \bar{K}_0 = \sigma_x / \sigma_y$$

Isotropic total stress analysis:

$$s_u = \frac{s_{uc} + s_{ue}}{2} \qquad (8.59)$$

$$\sigma_y = \sigma_x \qquad K_0(\text{or } \bar{K}_0) = \sigma_x / \sigma_y = 1$$

Equivalent to $\phi = 0$

$$K_0 = 1 - \sin\phi'$$

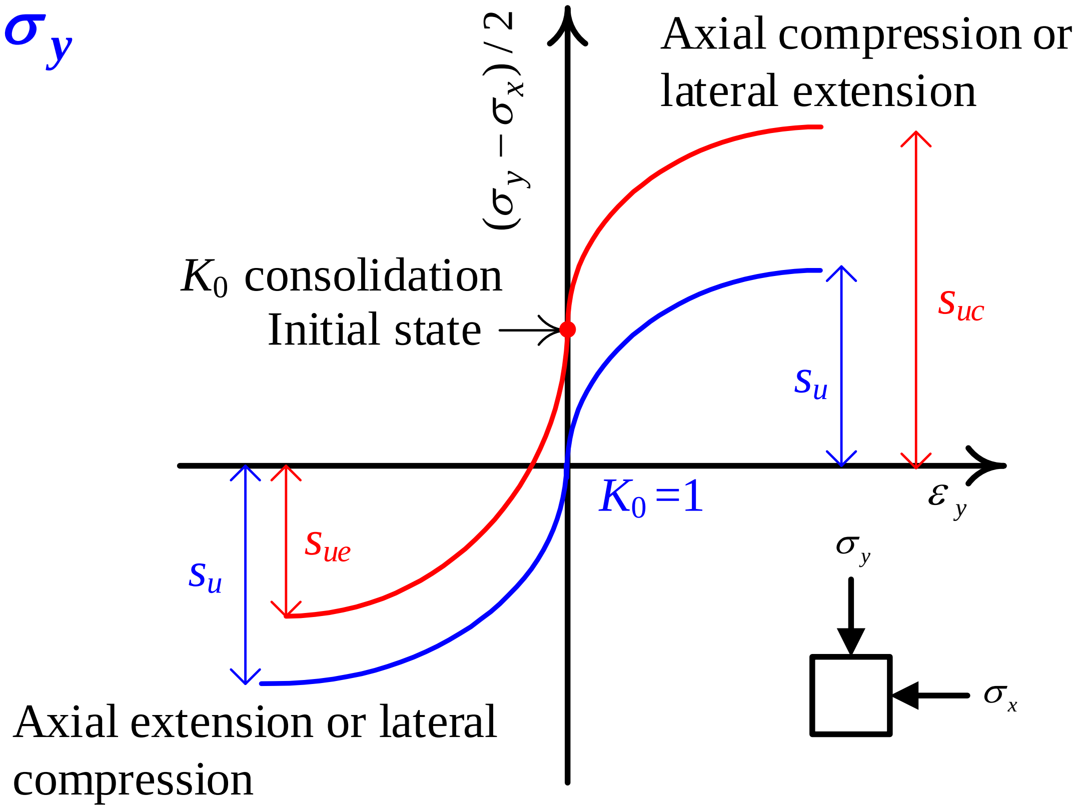

FIGURE 8.39 Calculation of initial stresses with total stress

8.6.2 Gravity generation method

- Change the boundaries of excavations profile to be all rollers
- Assign a suitable μ to each element
- Ignore undrained behavior for the undrained materials in the effective stress analysis
- Apply gravity body force over the whole area and use the standard FEA procedure
- Examine the obtained initial stresses for correctness
- Change the boundaries and the data sets back to what they should be in the formal analysis
- Reset all the induced movements equal to 0

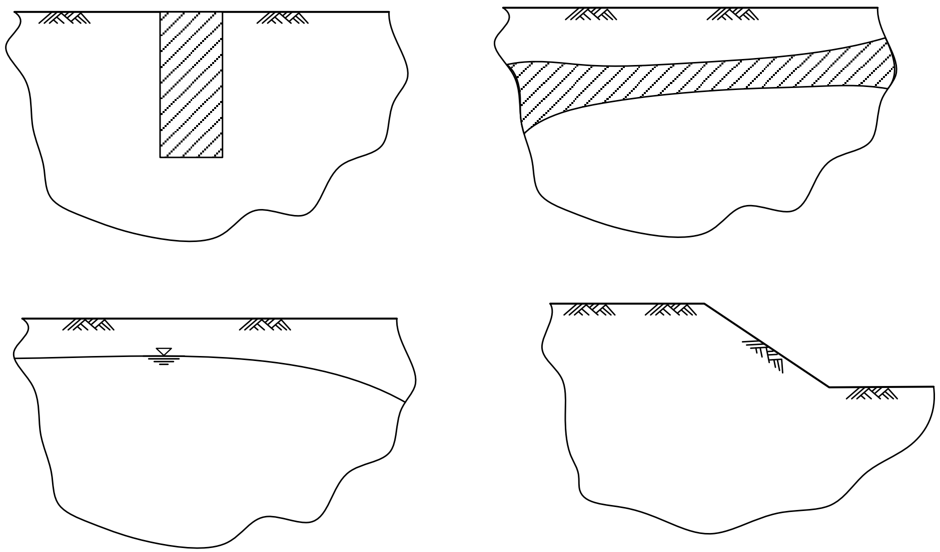

FIGURE 8.40 Initial stresses

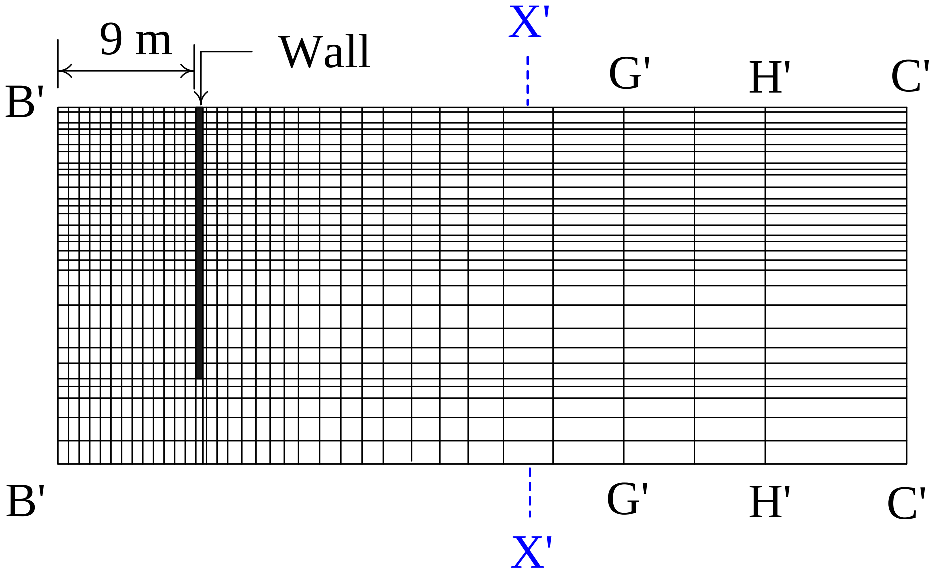

FIGURE 8.42 Plane strain analysis of an excavation

8.7 Structural material models and related parameters

Summarize the contents from Section 7.7

Soldier piles and sheet piles: The nominal Young's modulus is usually reduced by 20%, considering repeated use of the piles.

Diaphragm walls and column piles: The stiffness (*EI*) is usually reduced by 20 to 40%, considering the possibility of bending moment-induced cracking in concrete.

8.8 Mesh generation

8.8.1 Shape of the element

- Avoid irregular shapes
- The closer to 1.0 is the aspect ratio, the better is the shape
- The square or an equilateral triangle is the best choice
- $1.0 \leq L/B \leq 2.0 \sim 2.5$

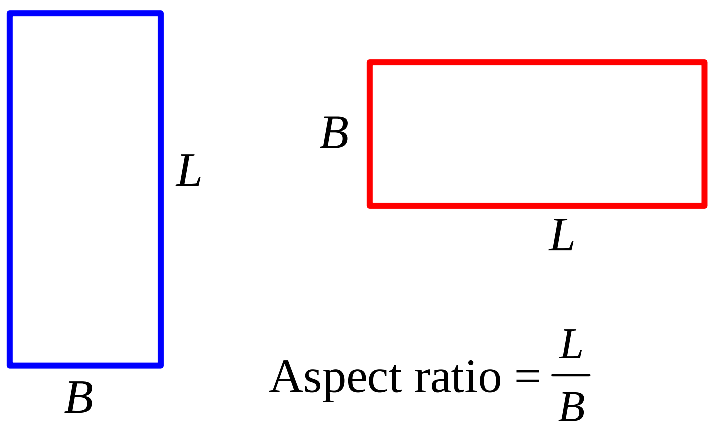

$$\text{Aspect ratio} = \frac{L}{B}$$

FIGURE 8.41 Definition of the aspect ratio

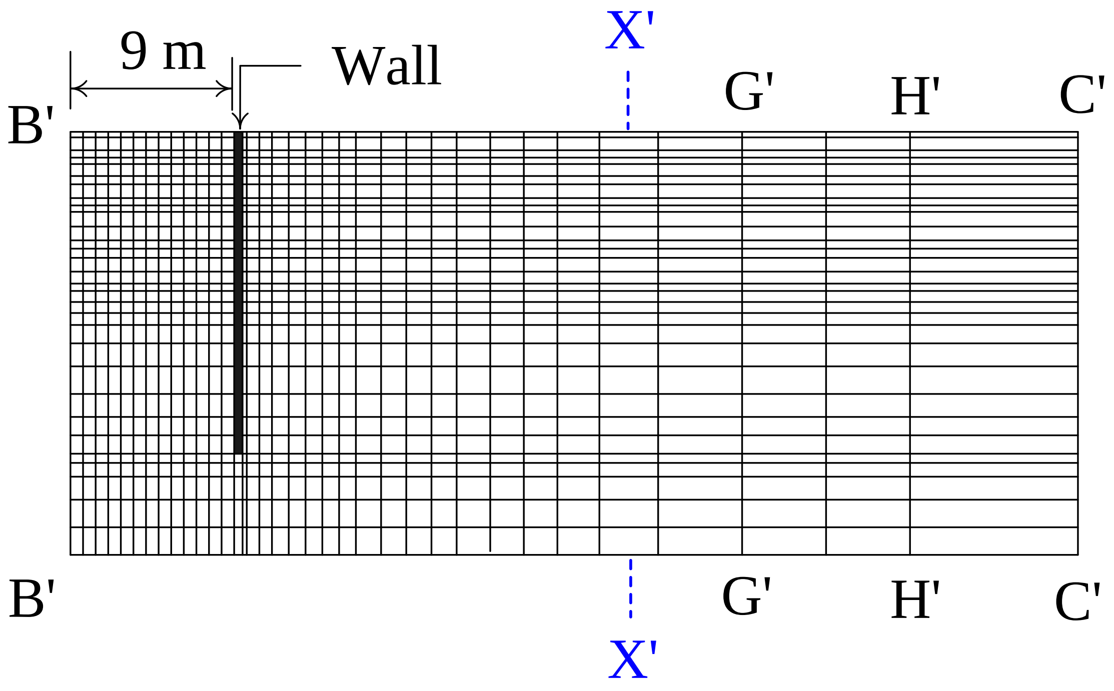

FIGURE 8.42 Plane strain analysis of an excavation

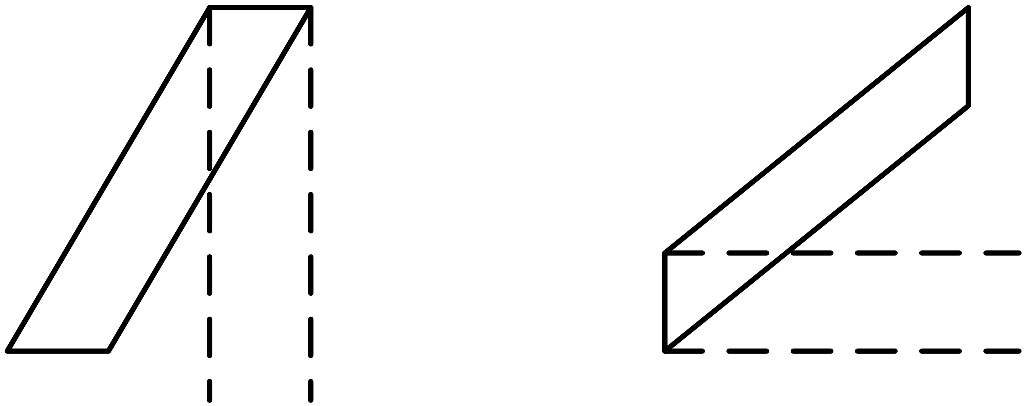

Bad elements

Good elements

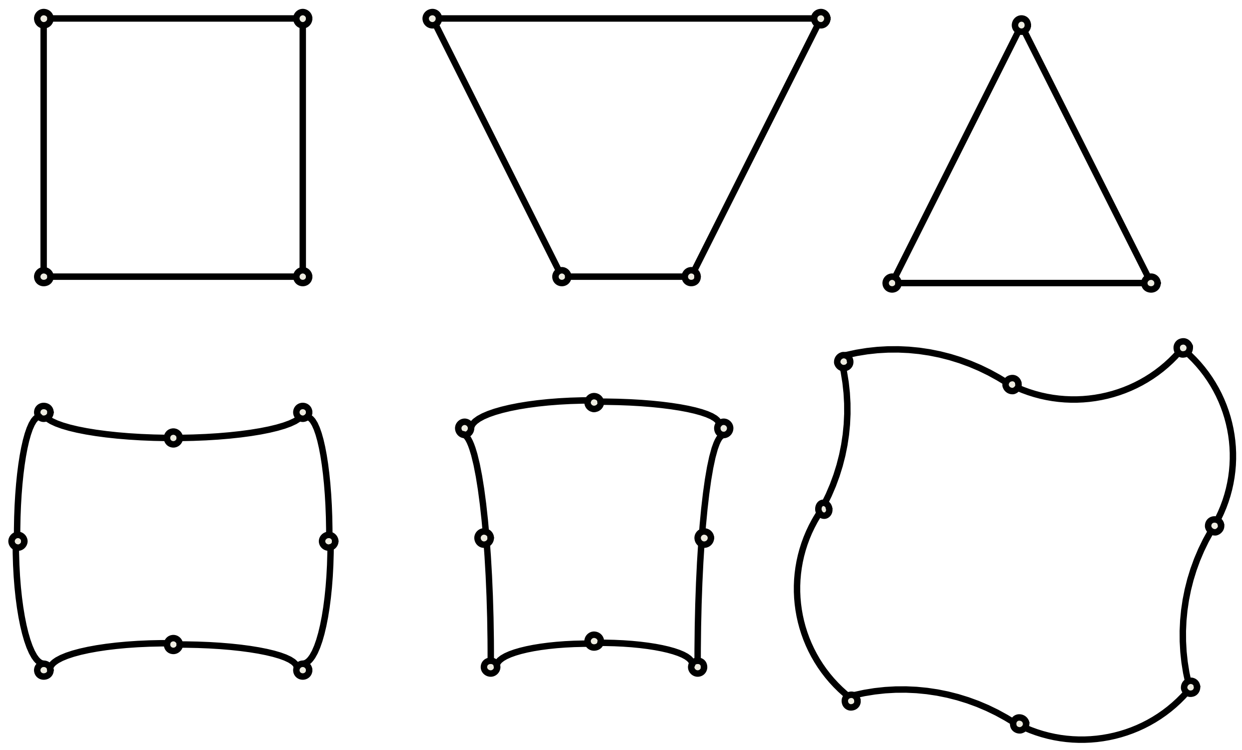

Good elements

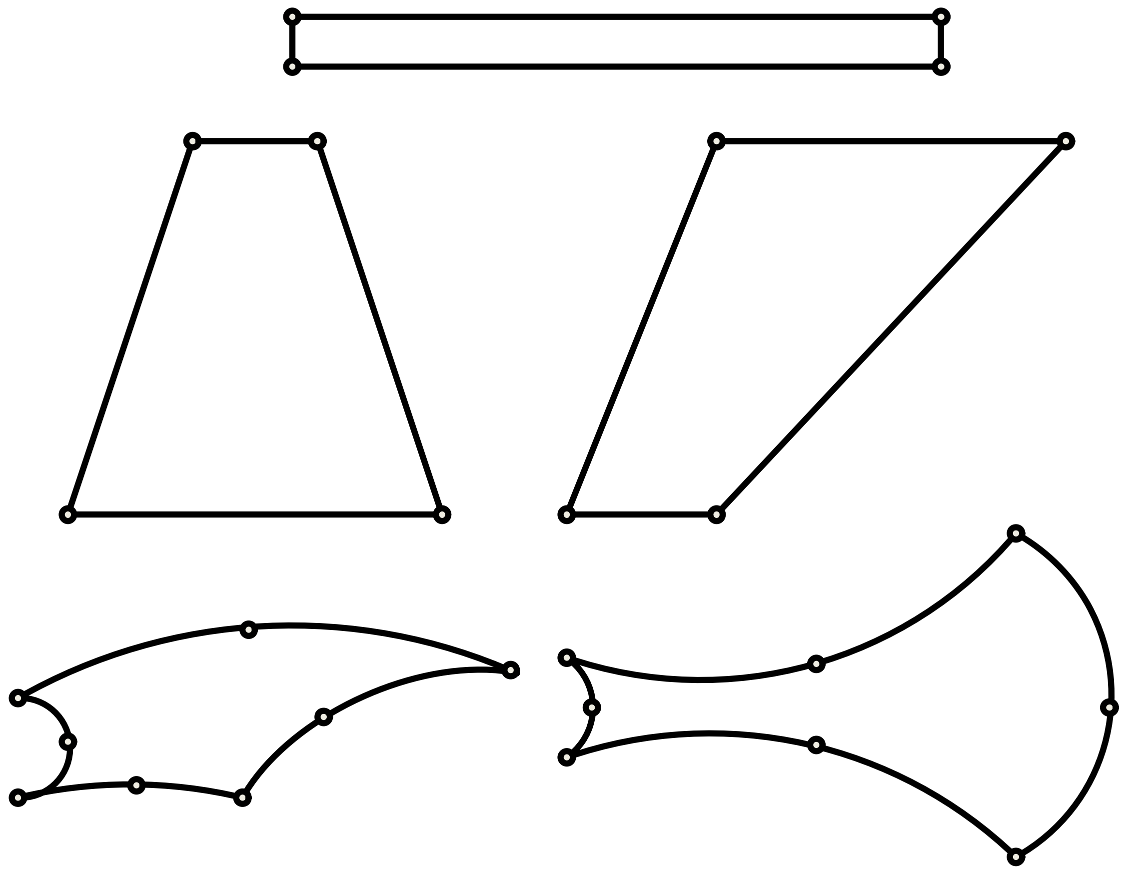

Bad elements

Interested area :

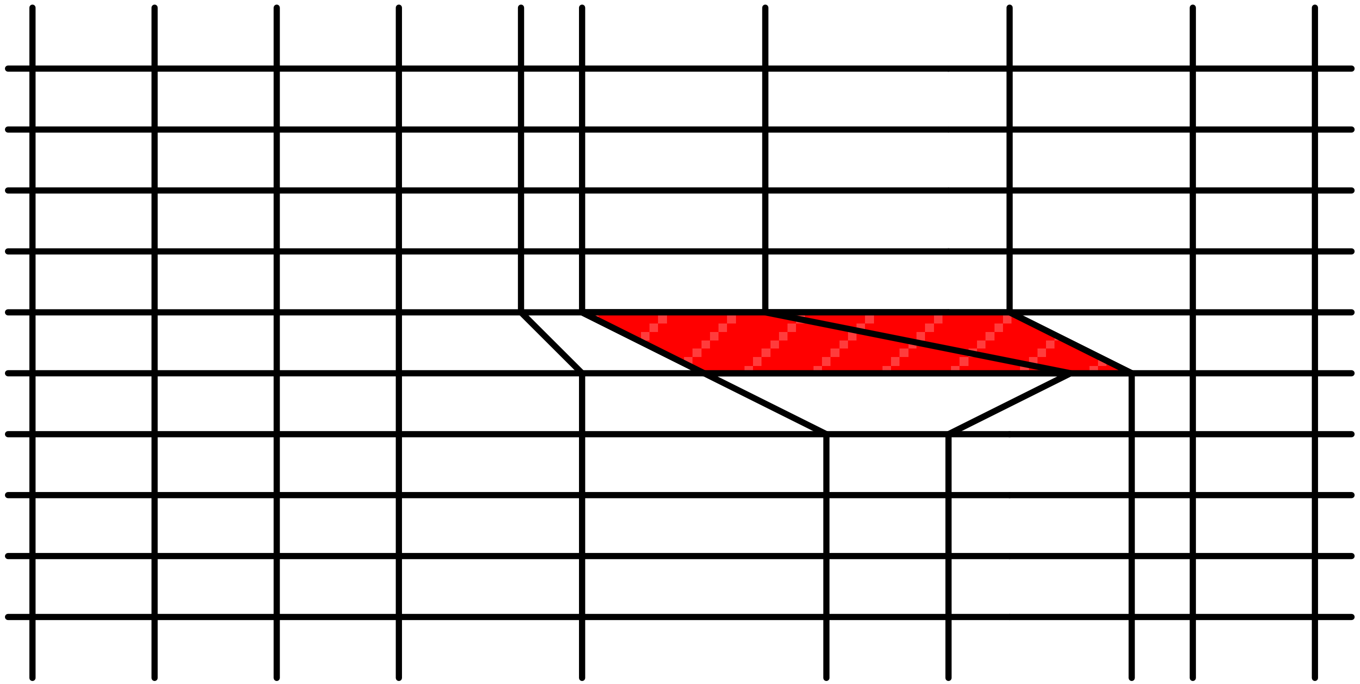

Bad elements confined by good elements

Interested area :

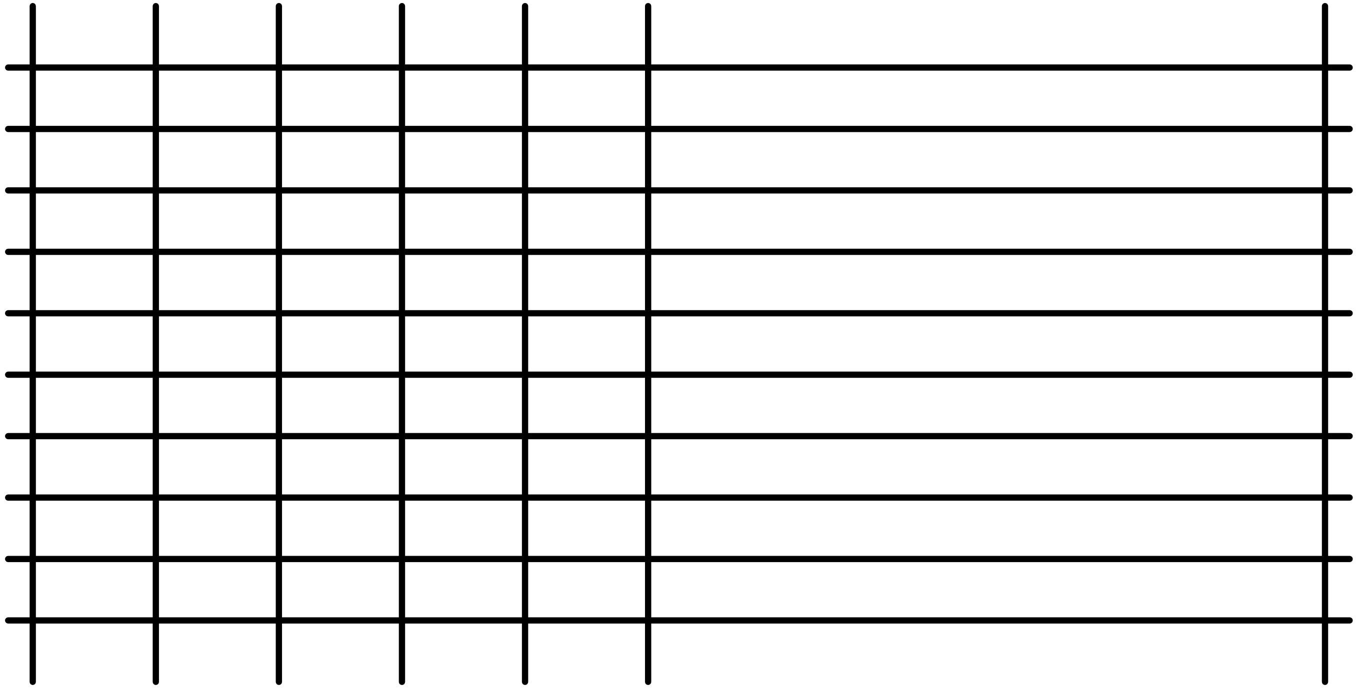

Bad elements allocated near the boundary

8.8.2 Density of mesh

(1) In principle, mesh should be finer in the area of stress concentration or rapid change of stress or strain

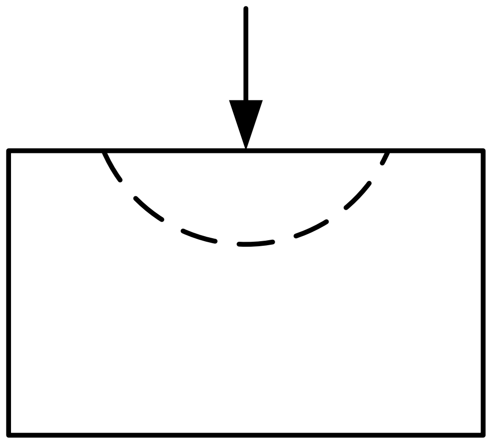

$$\{q\} = [K]^{-1}\{F\}$$

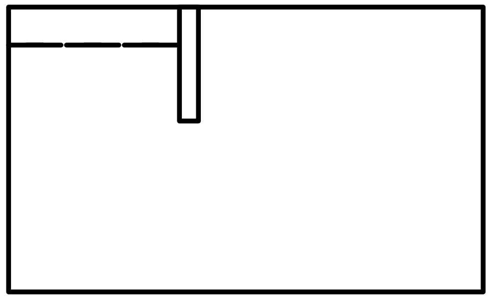

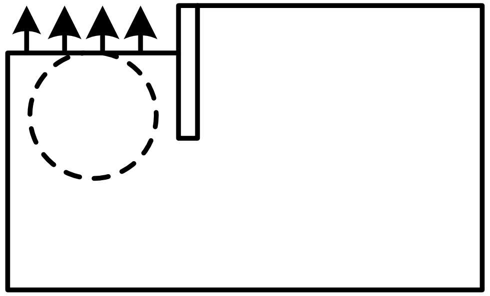

(2) Avoid the large difference in stiffness for the adjacent elements

For example, beam elements

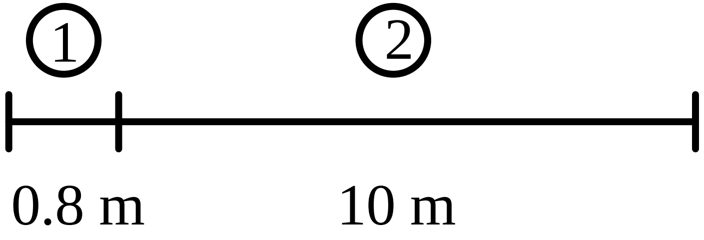

$$K_1 = \frac{12EI}{L^3} = \frac{12EI}{(0.8)^3} = 1{,}953(12EI)$$

$$K_2 = \frac{12EI}{L^3} = \frac{12EI}{(10)^3} = \frac{12EI}{1{,}000}$$

$$\frac{K_1}{K_2} = 1{,}953{,}000$$

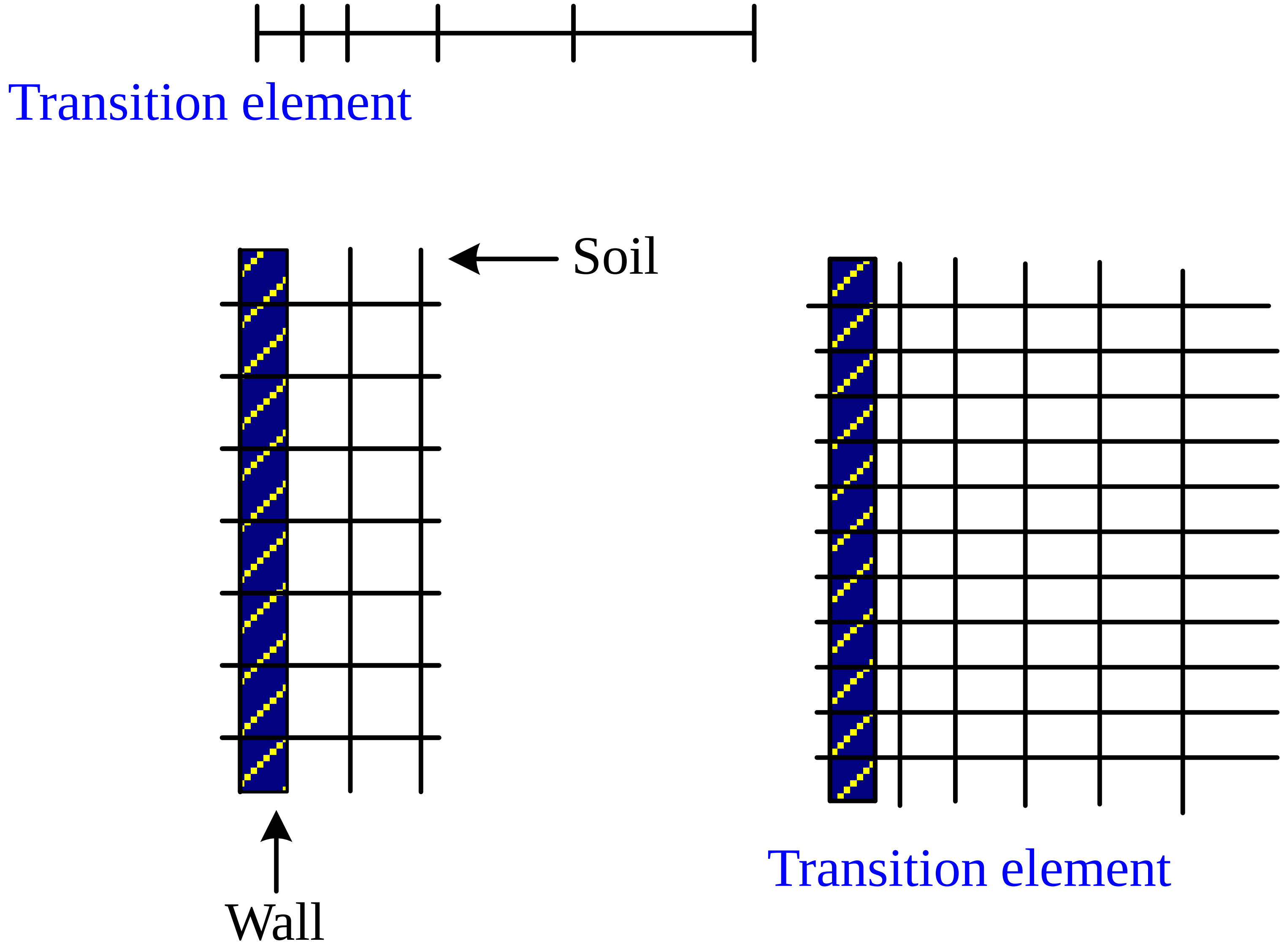
Transition element
Soil
Wall
Transition element

Transition elements

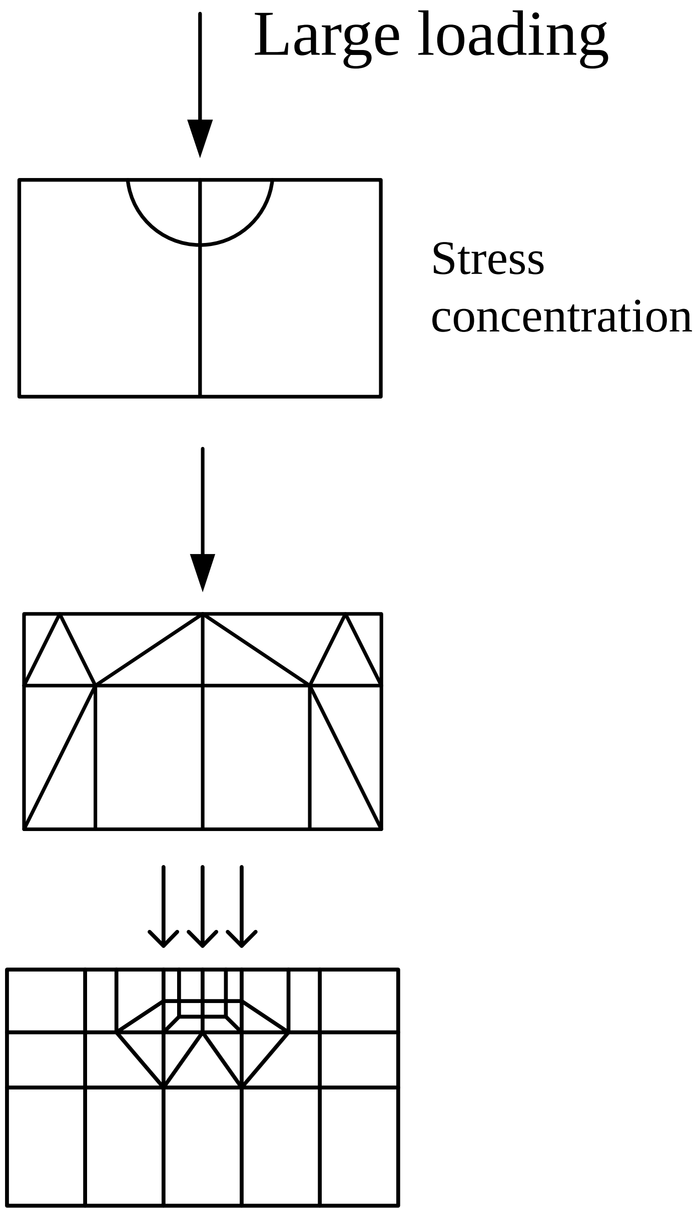

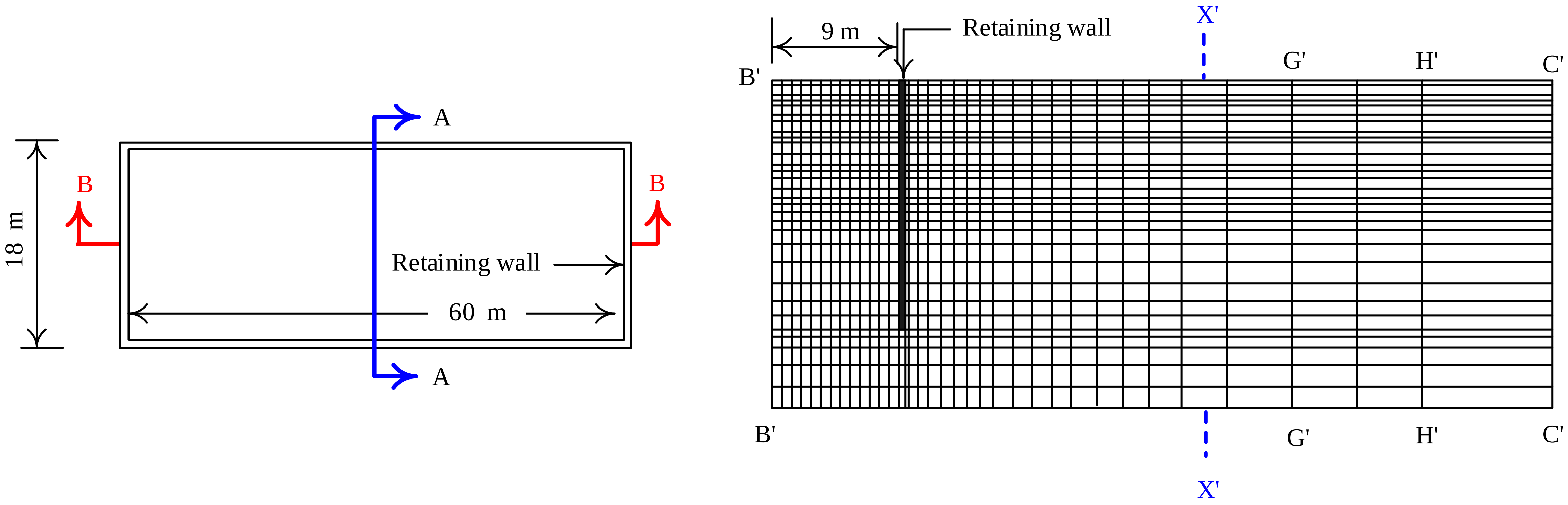

FIGURE 8.42 Plane strain analysis of an excavation

8.8.3 Boundary condition

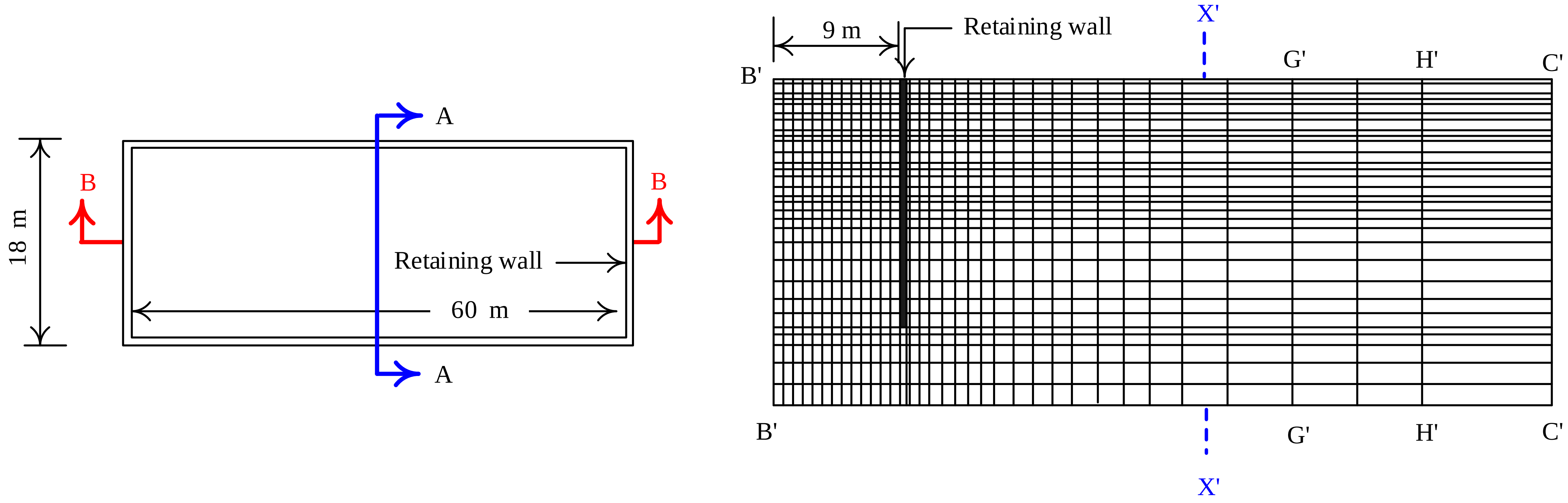

FIGURE 8.42 Plane strain analysis of an excavation

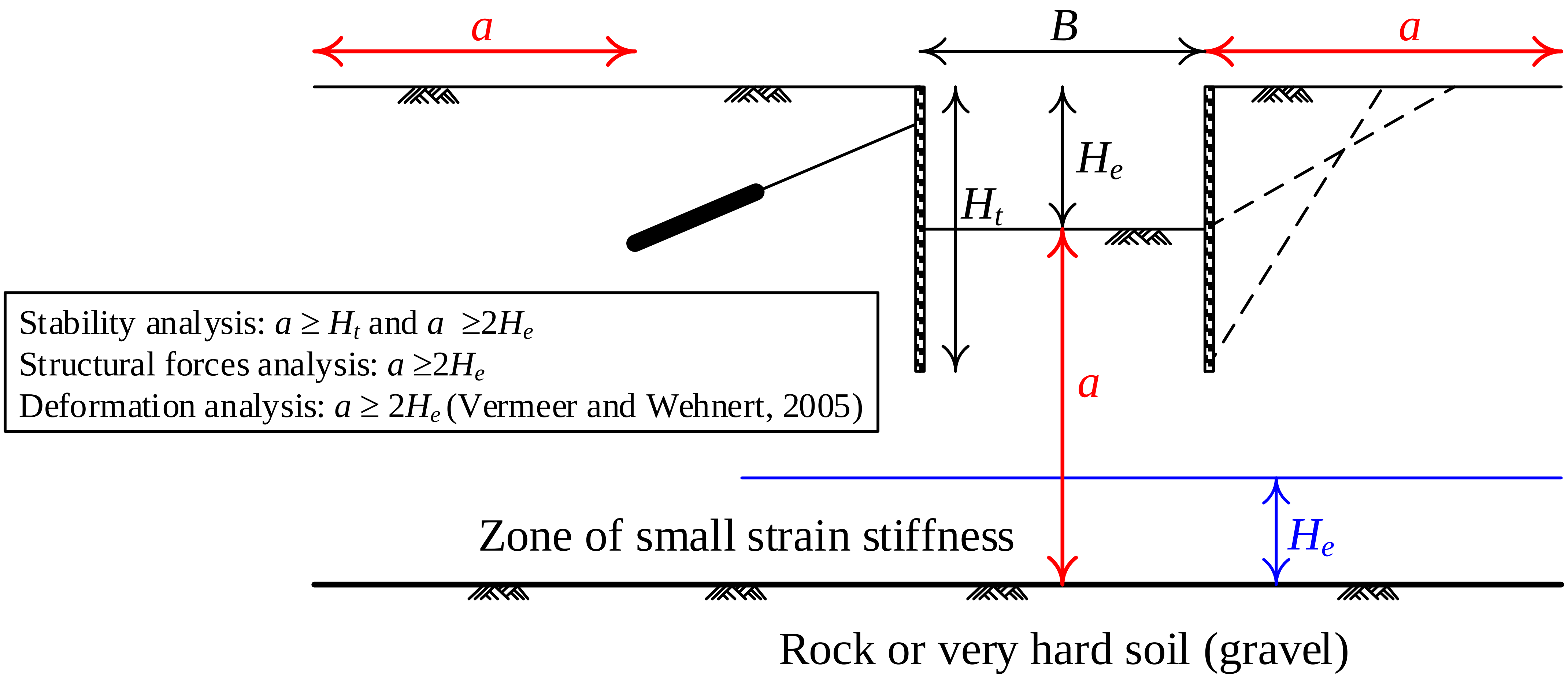

FIGURE 8.43 Distance of finite element mesh boundary (Waterman, 2009)

8.9 Plane strain analysis and three-dimensional analysis

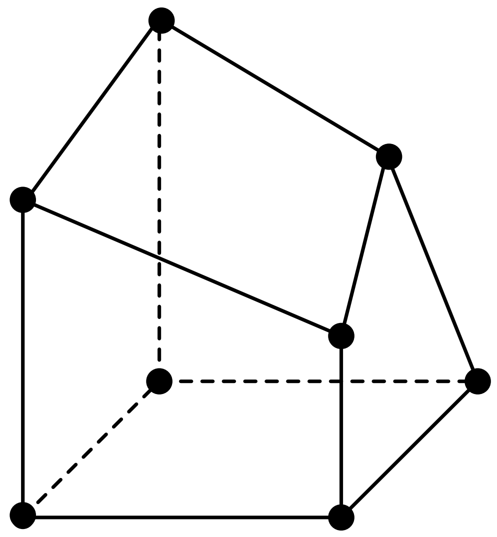

(a)

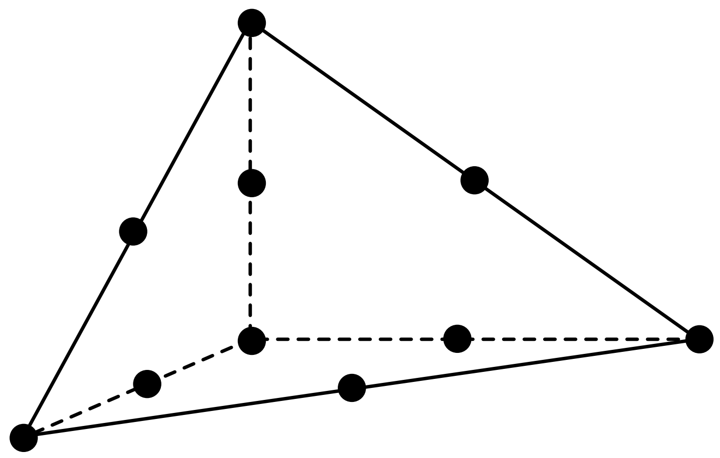

(b)

FIGURE 8.44 3D elements

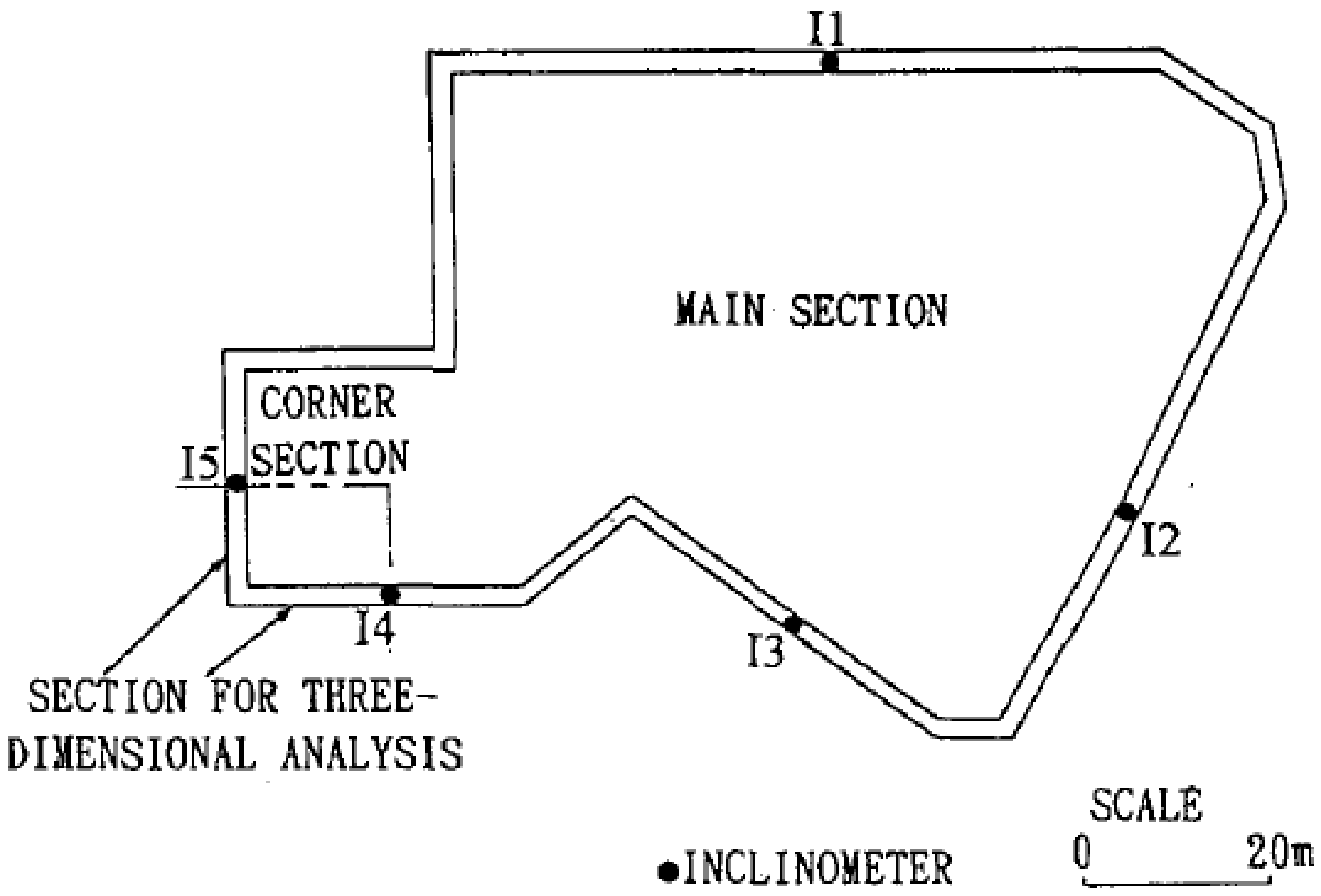

***H_e*=20.3 m,**
***t* =1.1 m**

Ou, et al. . (1996), Three-dimensional finite element analysis of deep excavation, Journal of Geotechnical Engineering, ASCE, No. 5, pp. 337-345.

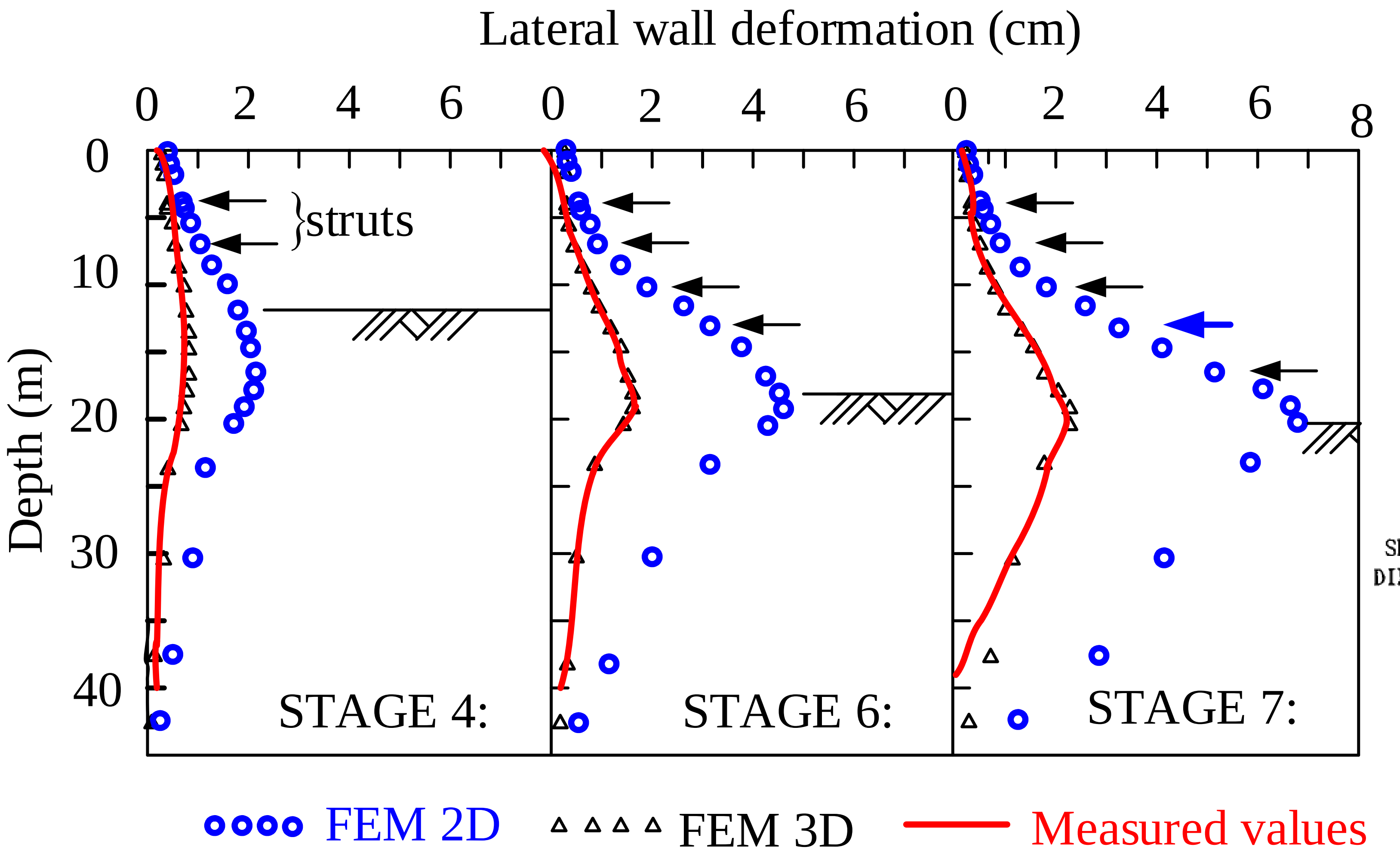

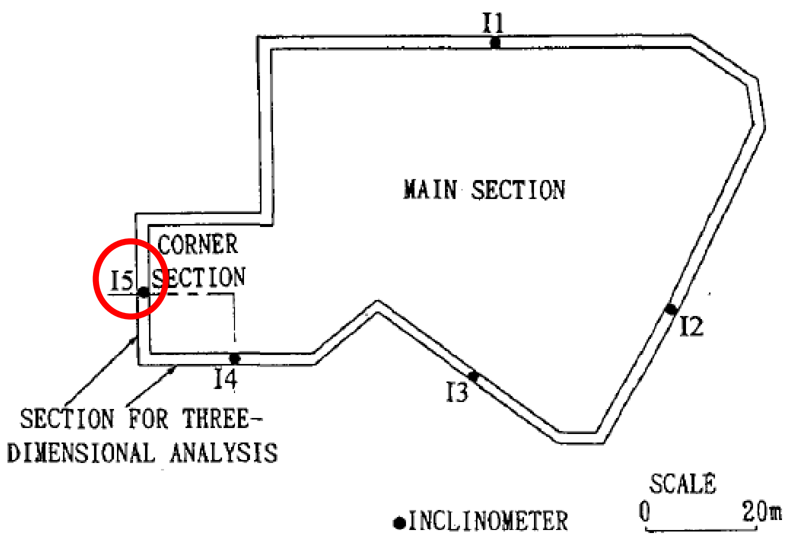

FIGURE 8.45 Comparison of the results from 2D analysis, 3D analysis, and field measurement for the Haihaw excavation

Finite element mesh for the earth retaining wall system of TPKE project

H_e=13.2 m.

Use of DW, CW and BW to form a strut-free excavation support system

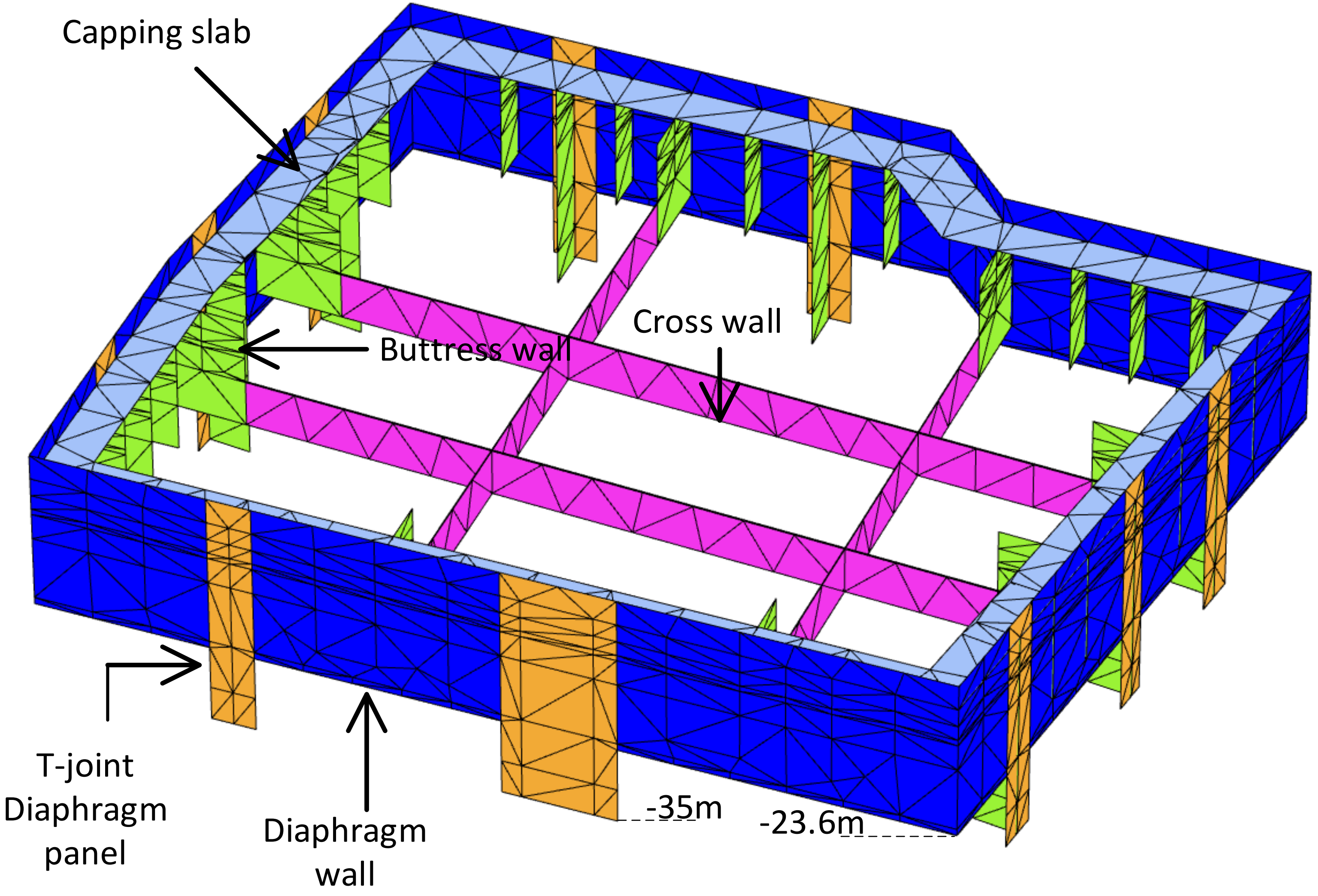

Finite element mesh for the TPKE excavation

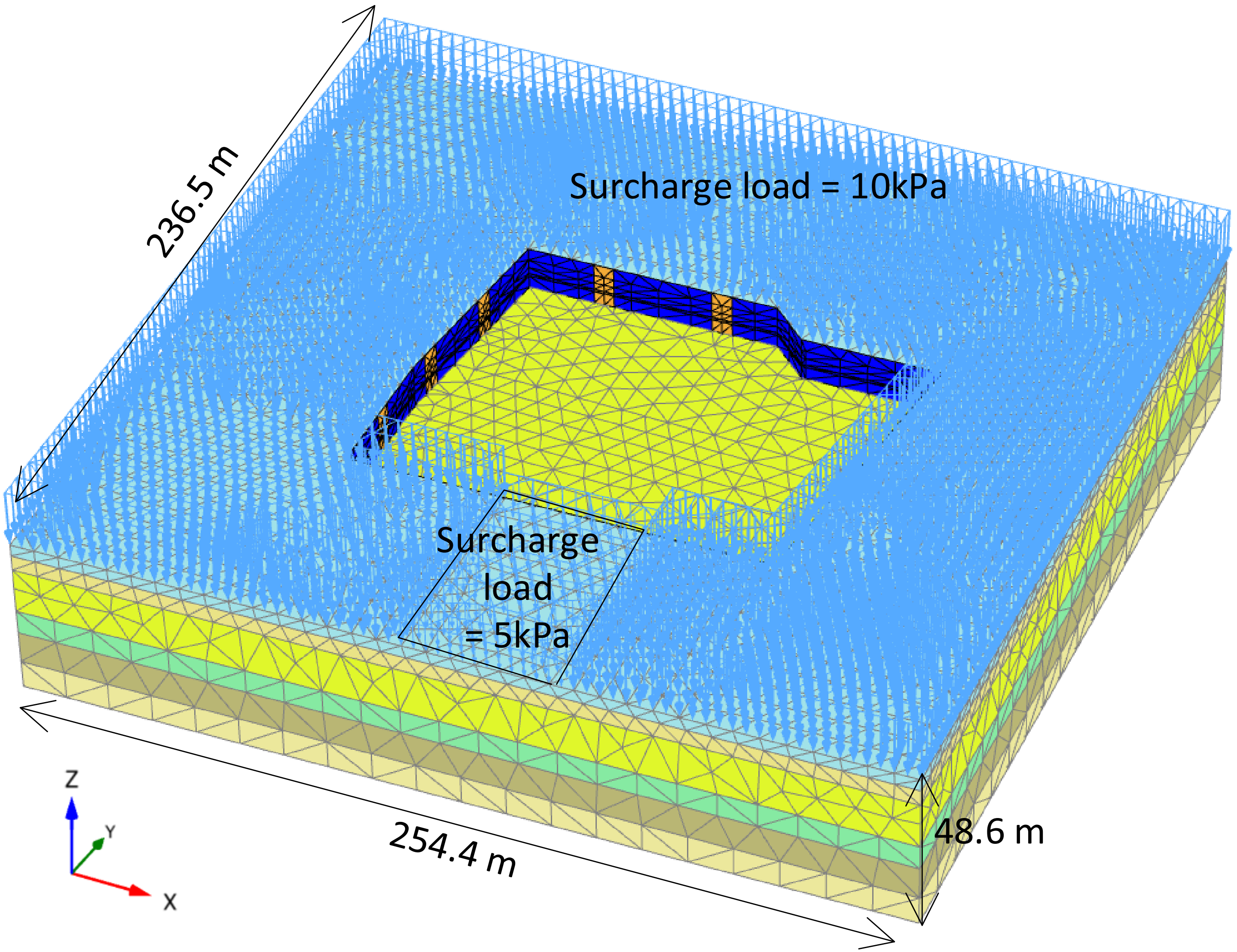

FEM with c, ϕ reduction

$$c_{input} = \frac{c_{original}}{SR}$$

$$\phi_{input} = \frac{\phi_{original}}{SR}$$

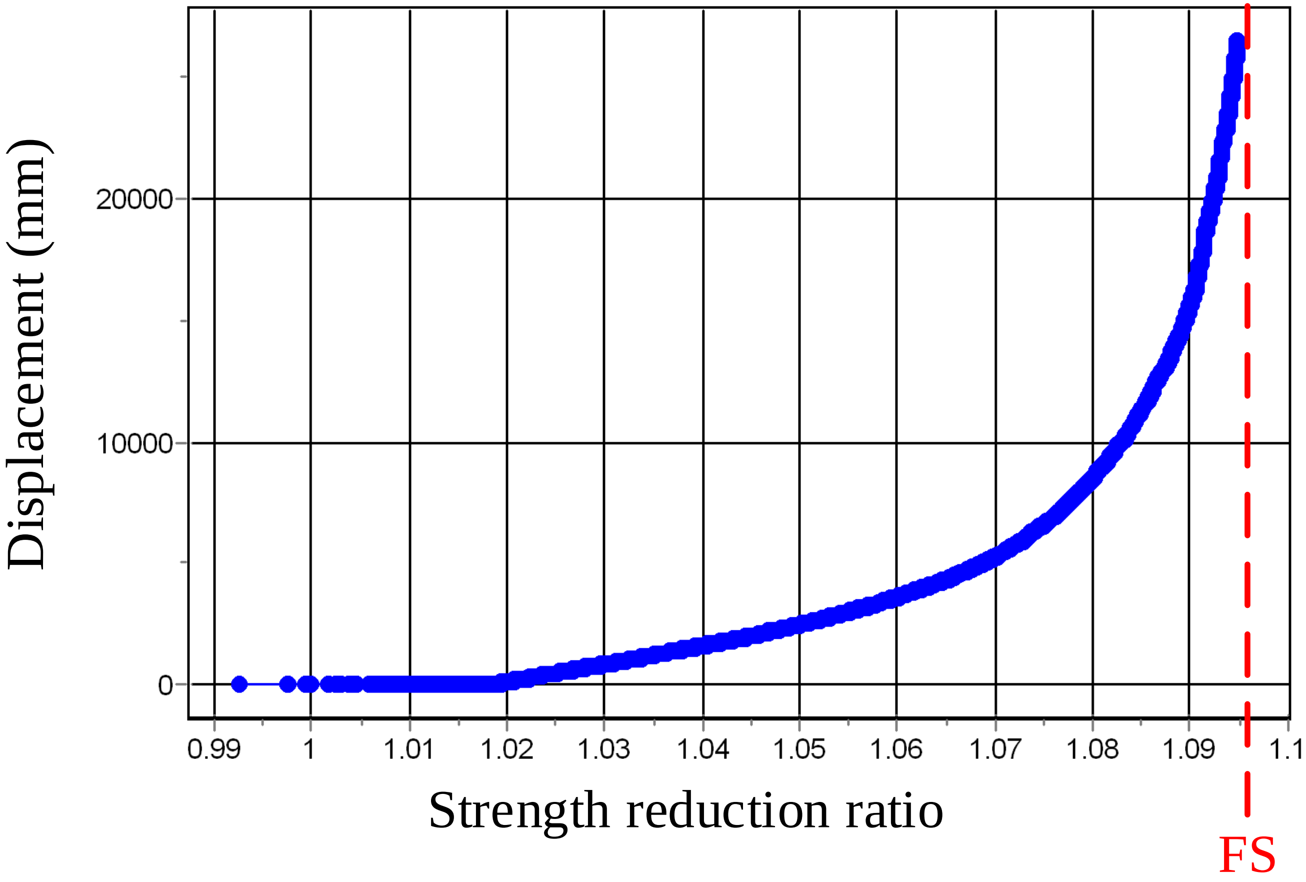

FIGURE 8.46 Variation of wall deflections with reduced strength

For a certain *SR* value,

$\{\Delta q\}$, $\{\Delta\varepsilon\}$, and $\{\Delta\sigma\}$

$$\underbrace{\int_{vol} [B]^T [\sigma]\, d(vol)}_{F_{int}} = \underbrace{\int_{vol} [N]^T \{G\}\, d(vol) + \int_{area} [N]^T [T]\, d(area)}_{F_{ext}}$$

(8.5)

$$\frac{|F_{ext} - F_{int}|}{|F_{ext}|} < \text{tolerated error}$$

(8.18)

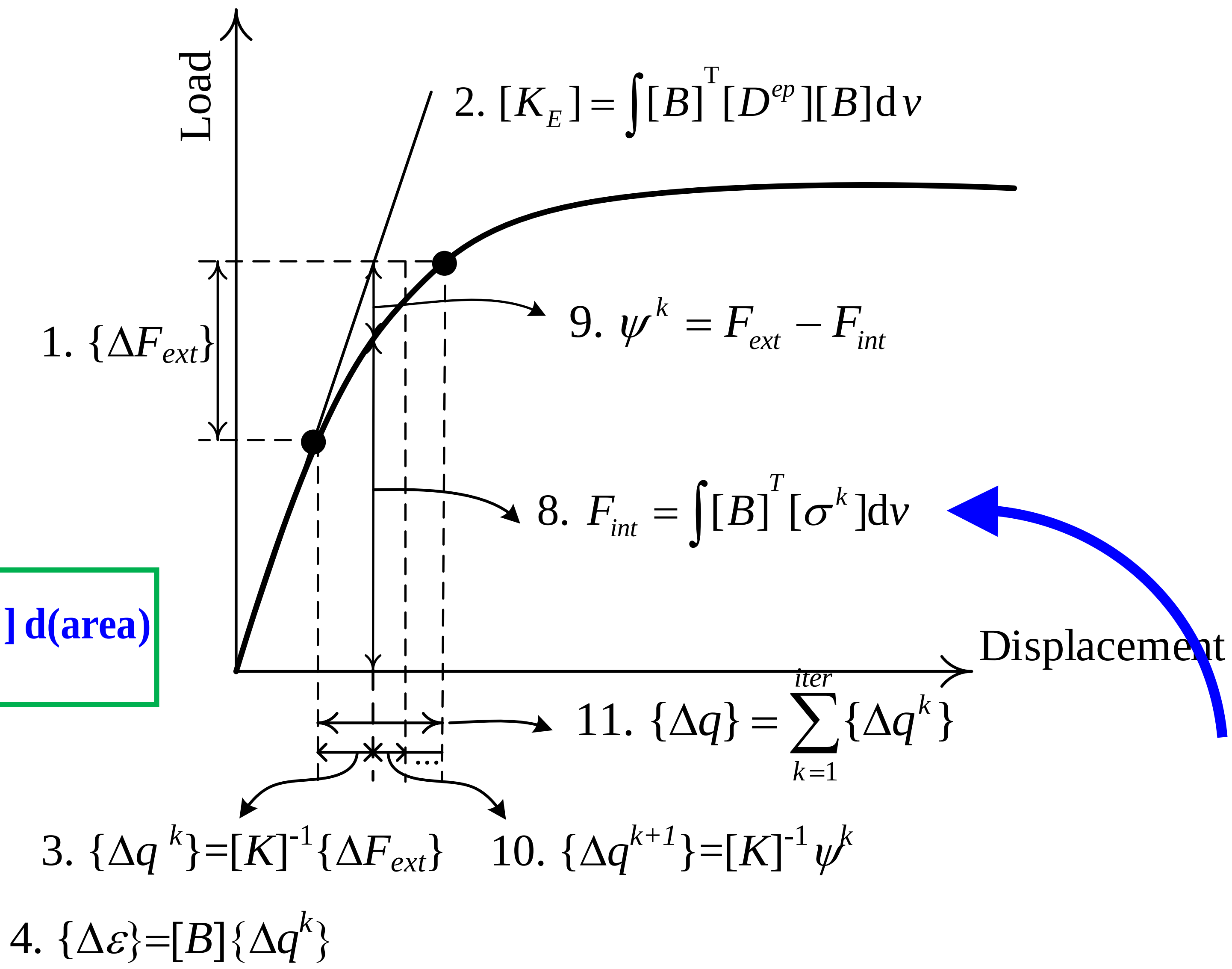

FIGURE 8.4 Procedure for nonlinear finite element computation

Stress integration scheme(e.g. Forward Euler method with subincrements)

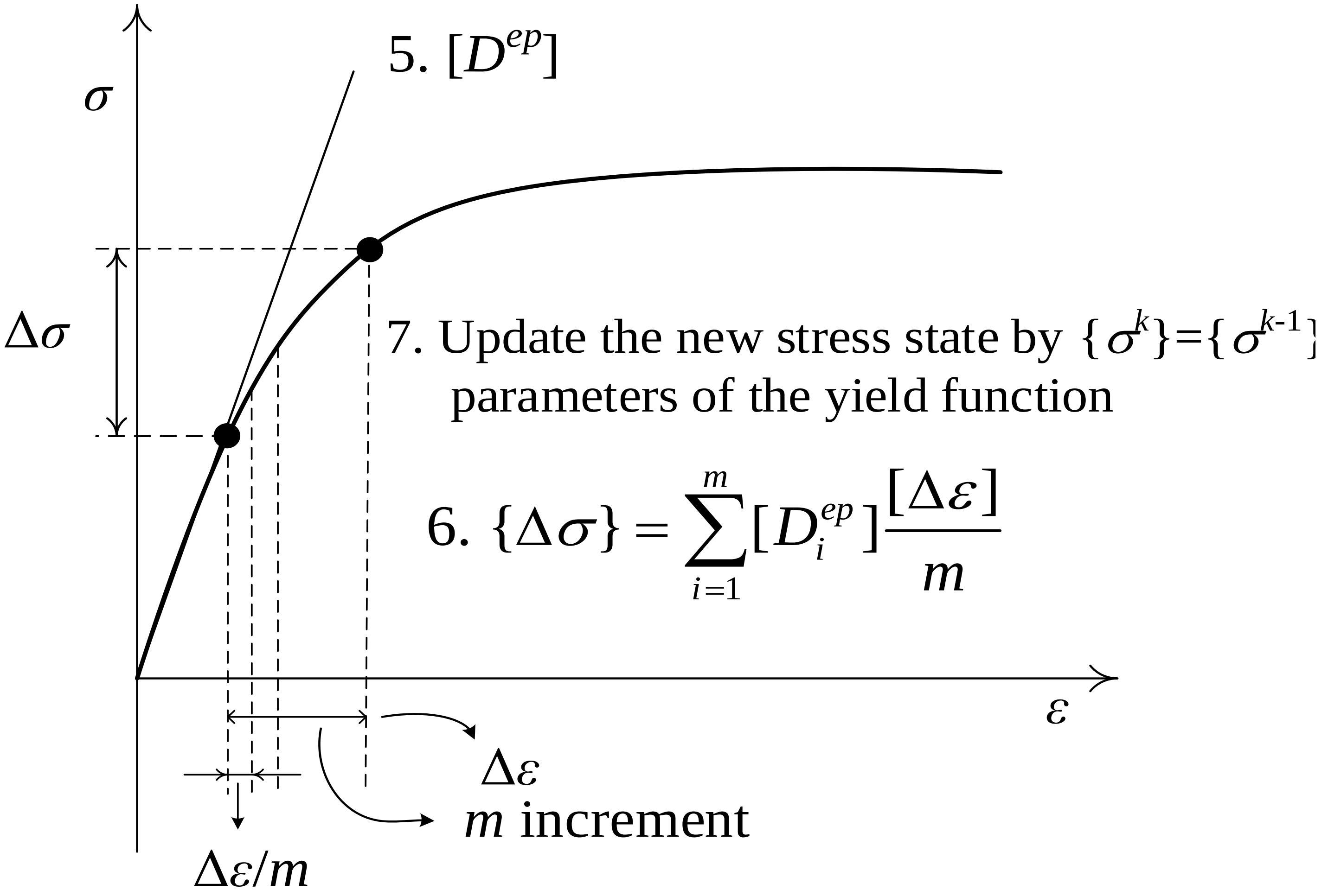

Case study: Taipei Rebar Broadway Case

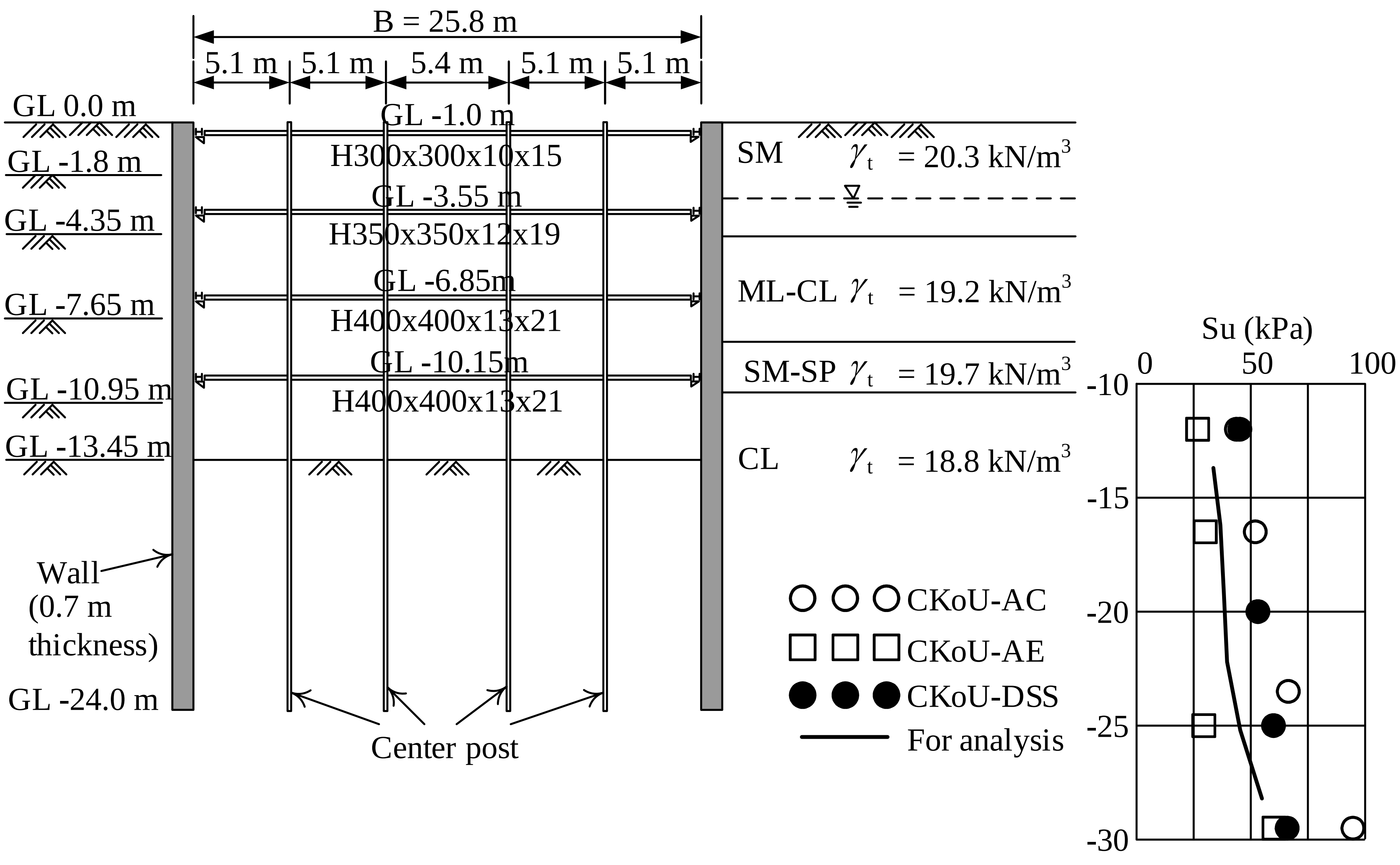

M_p-N_p Boundary

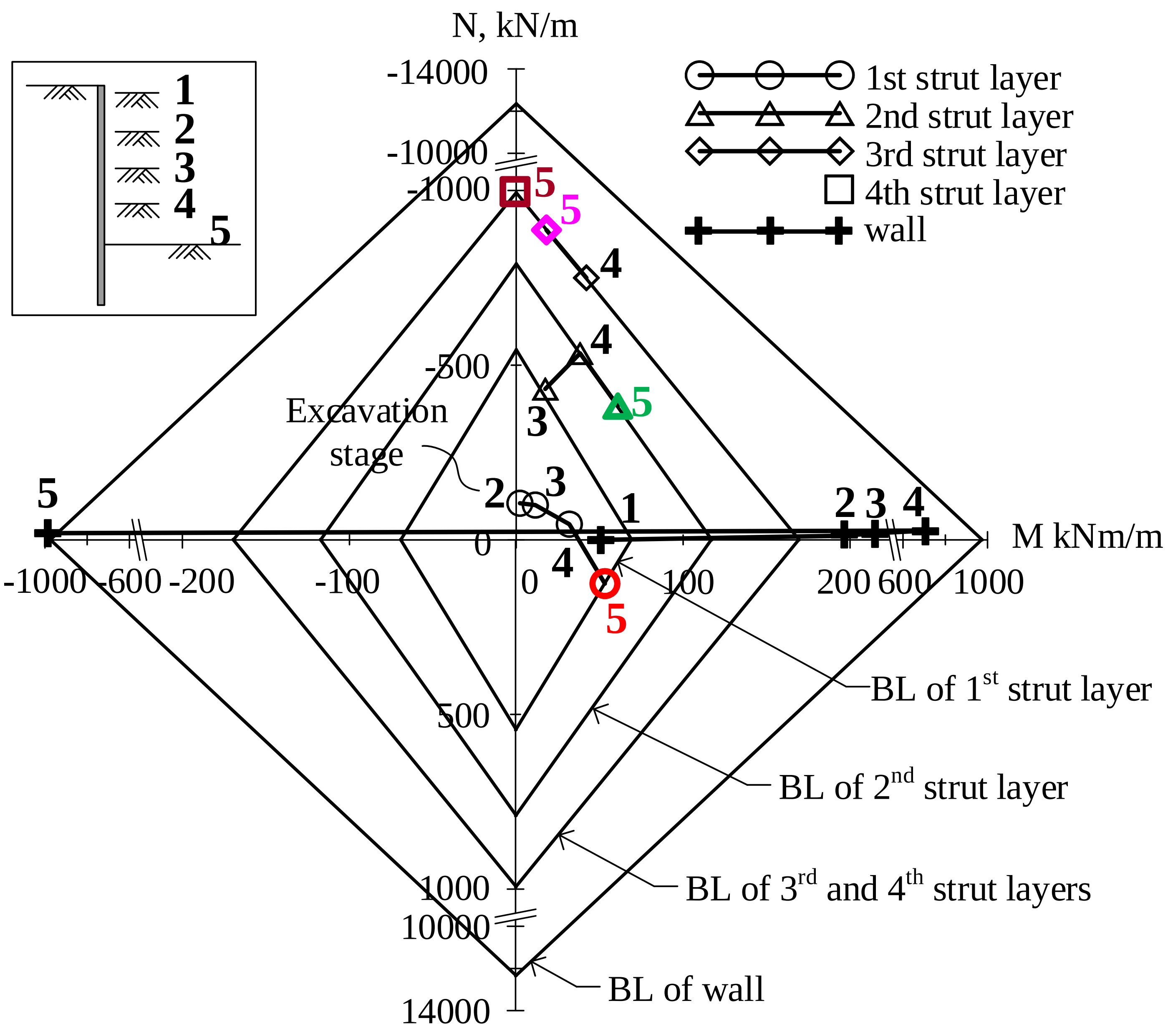

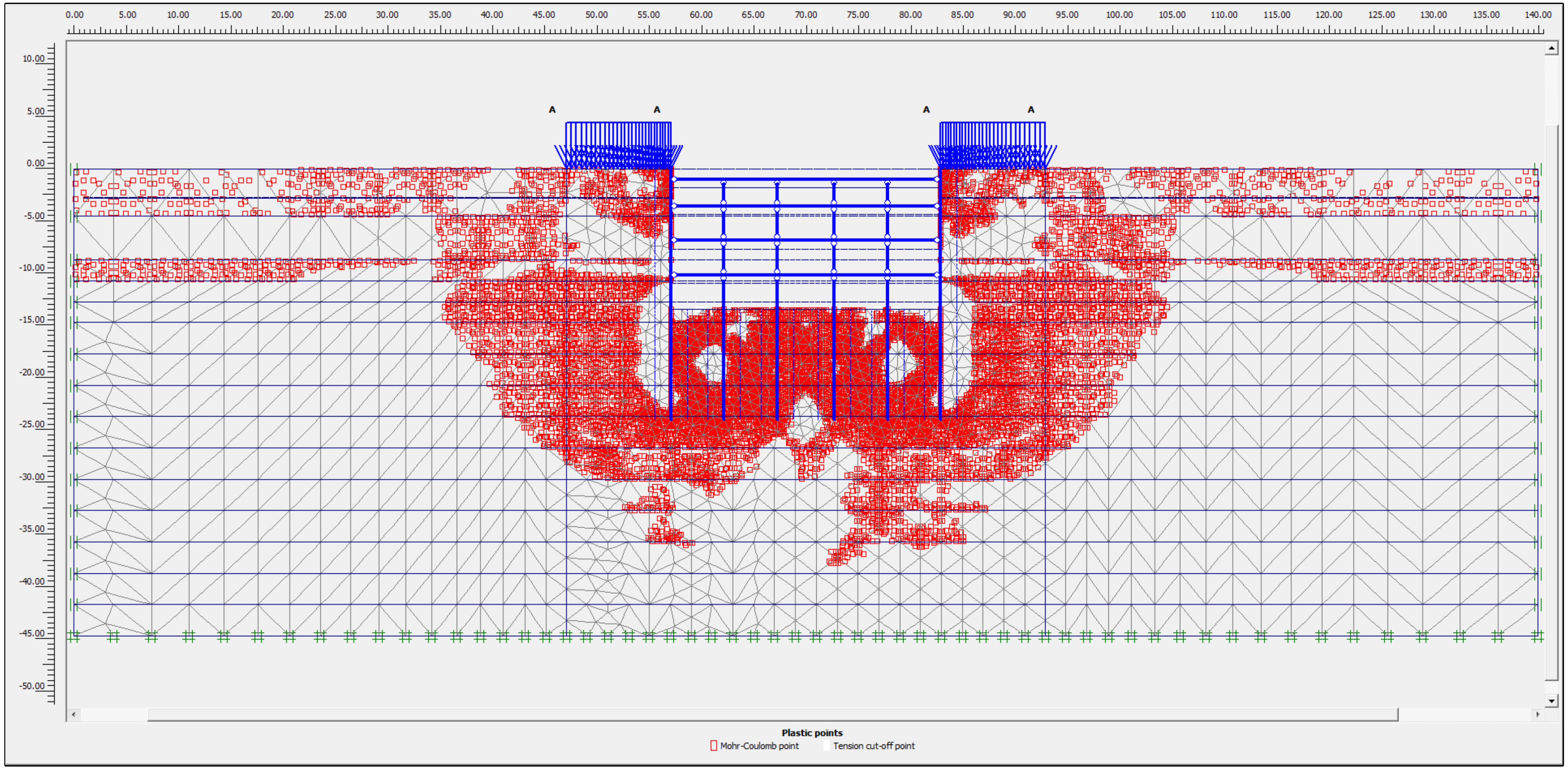

Plastic point plot at SR_{max} as using EP support system

8.11 Finite element analysis procedure

1. Define the problem dimension
2. Set the target geometry and boundaries

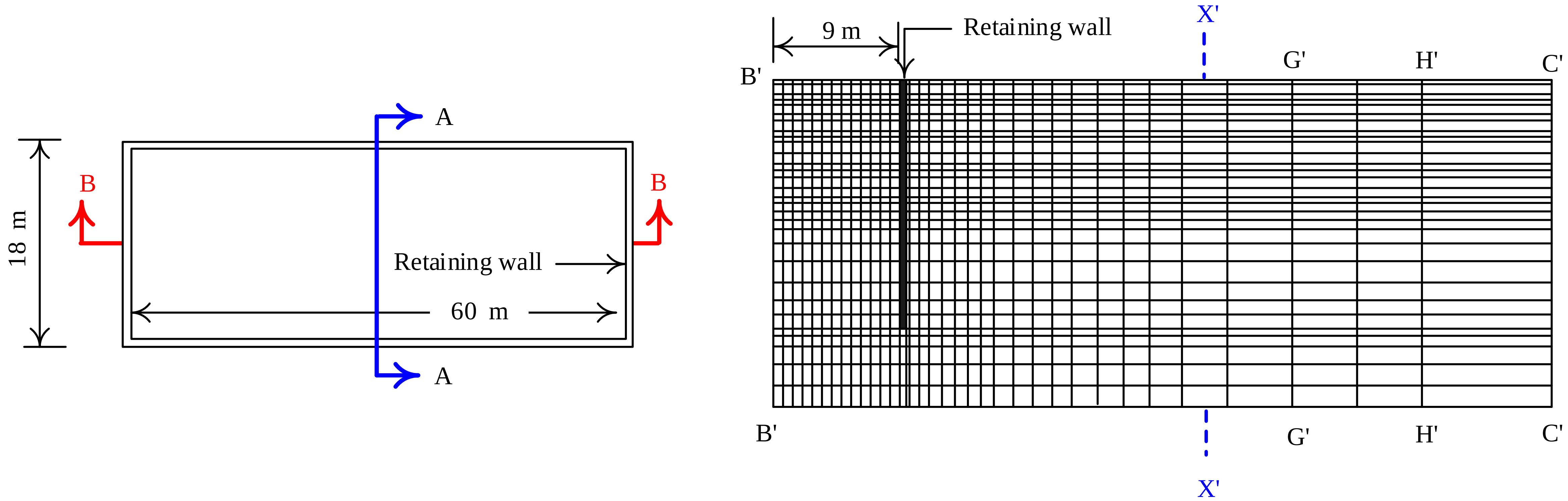

FIGURE 8.42 Plane strain analysis of an excavation

3. Select the material model and evaluate their input parameters

For the target with various stress paths, a high level constitutive model such as the HS or HSS model would be a good choice.

For simple problems, monotonic loading or /unloading for example, the MC model with the parameters obtained from the designated stress path can be selected.

4. Generate the mesh

Inspect the elements to ensure their aspect ratio, and ensure good elements or a finer mesh to be allocated in important or interested regions.

5. Set the ground water level and water pressure

6. Establish initial stresses

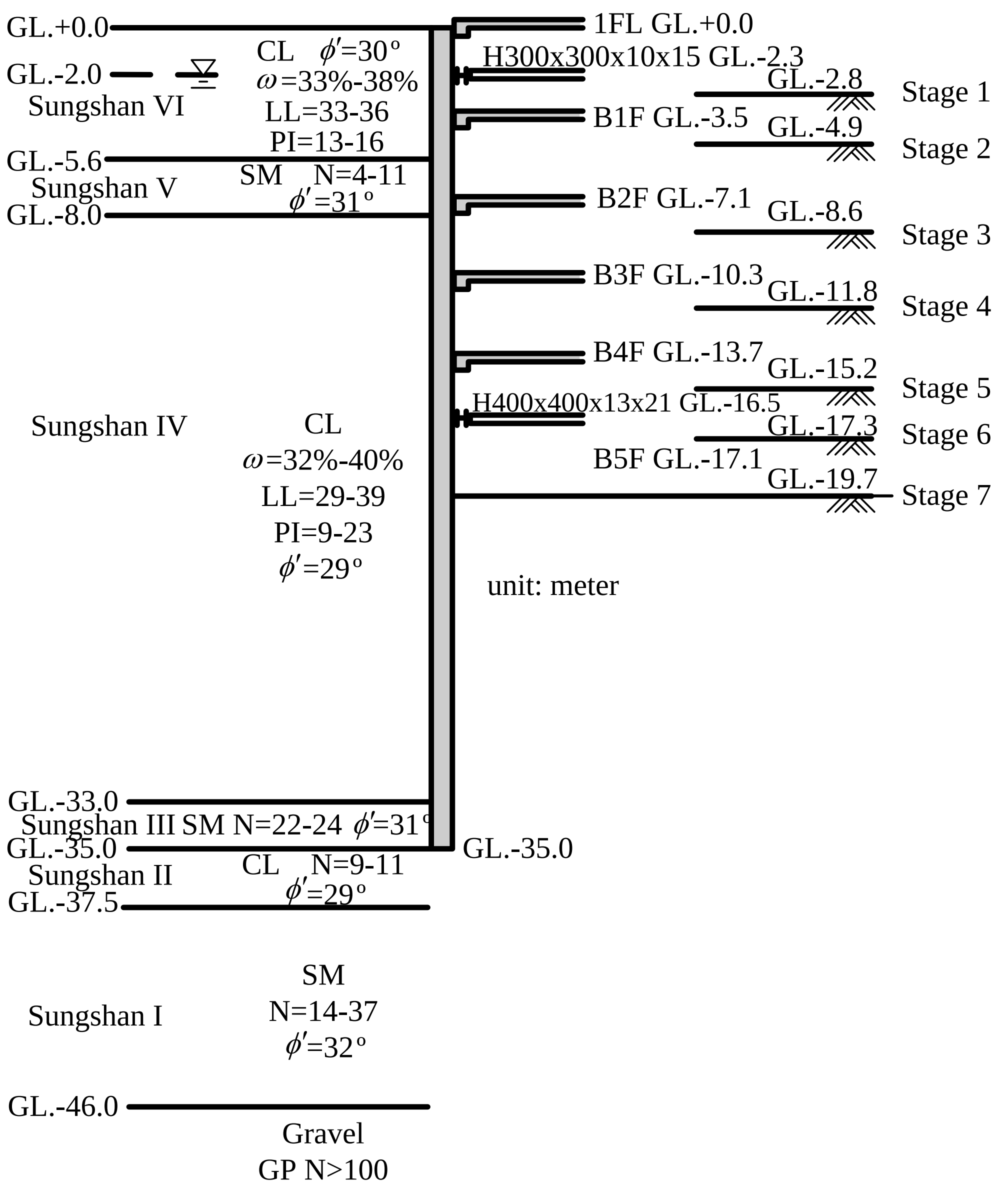

7. Simulate construction procedure including dewatering

In construction practice:

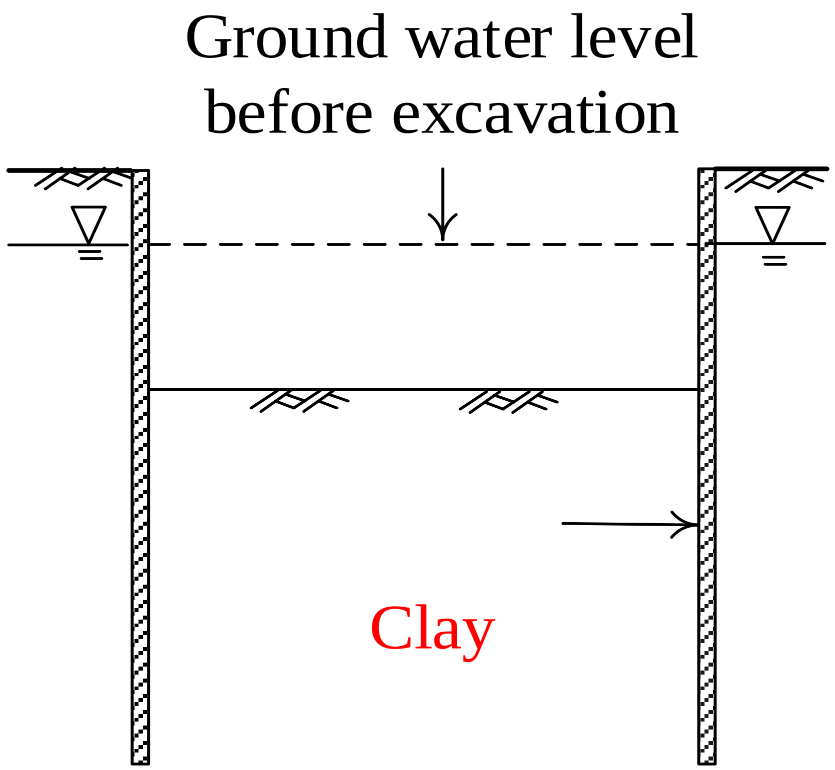

(a)

In FE analysis:

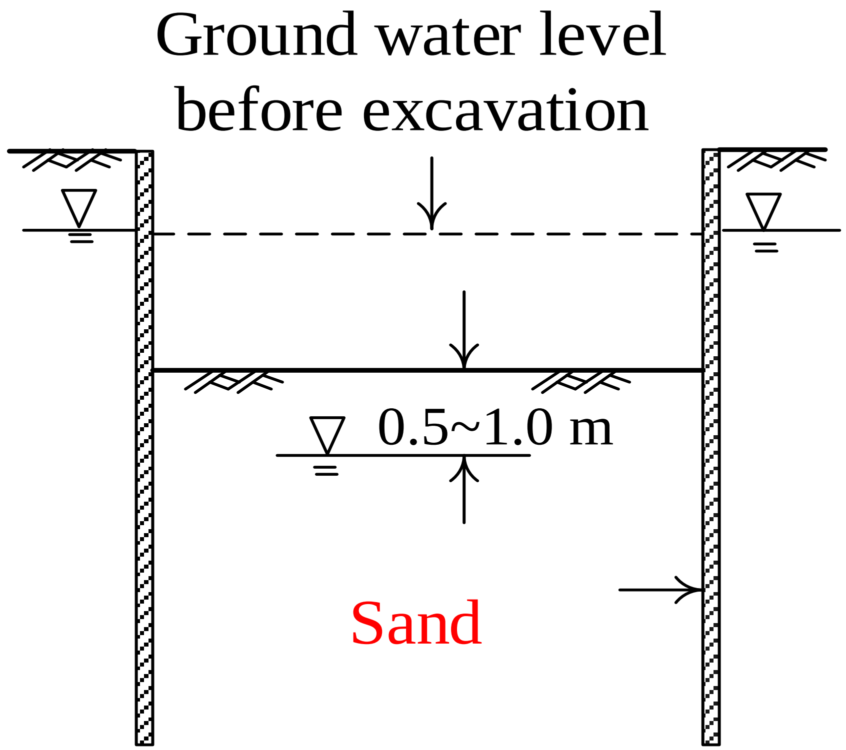

(b)

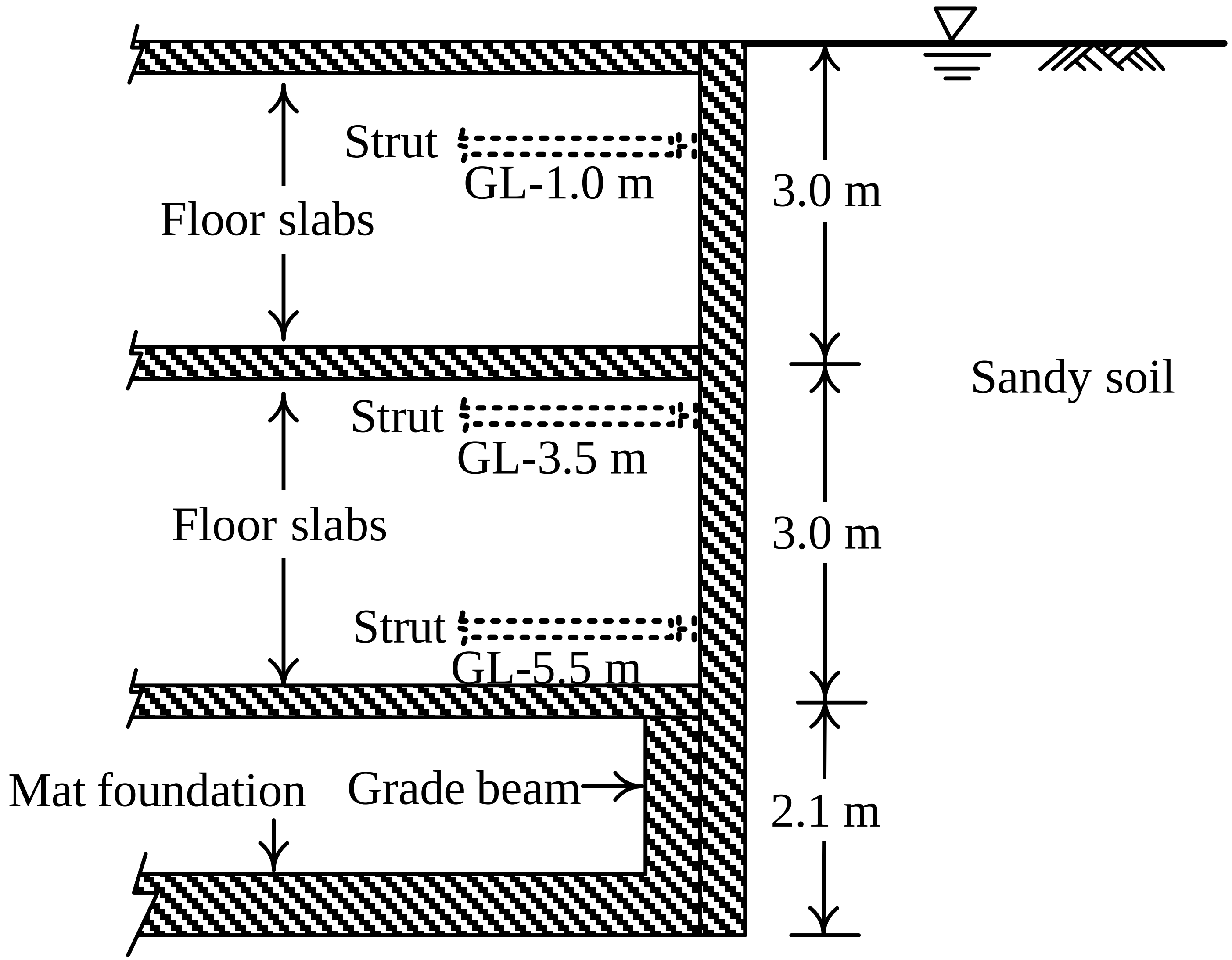

FIGURE 7.5 Profile of a two-story basement with mat foundation

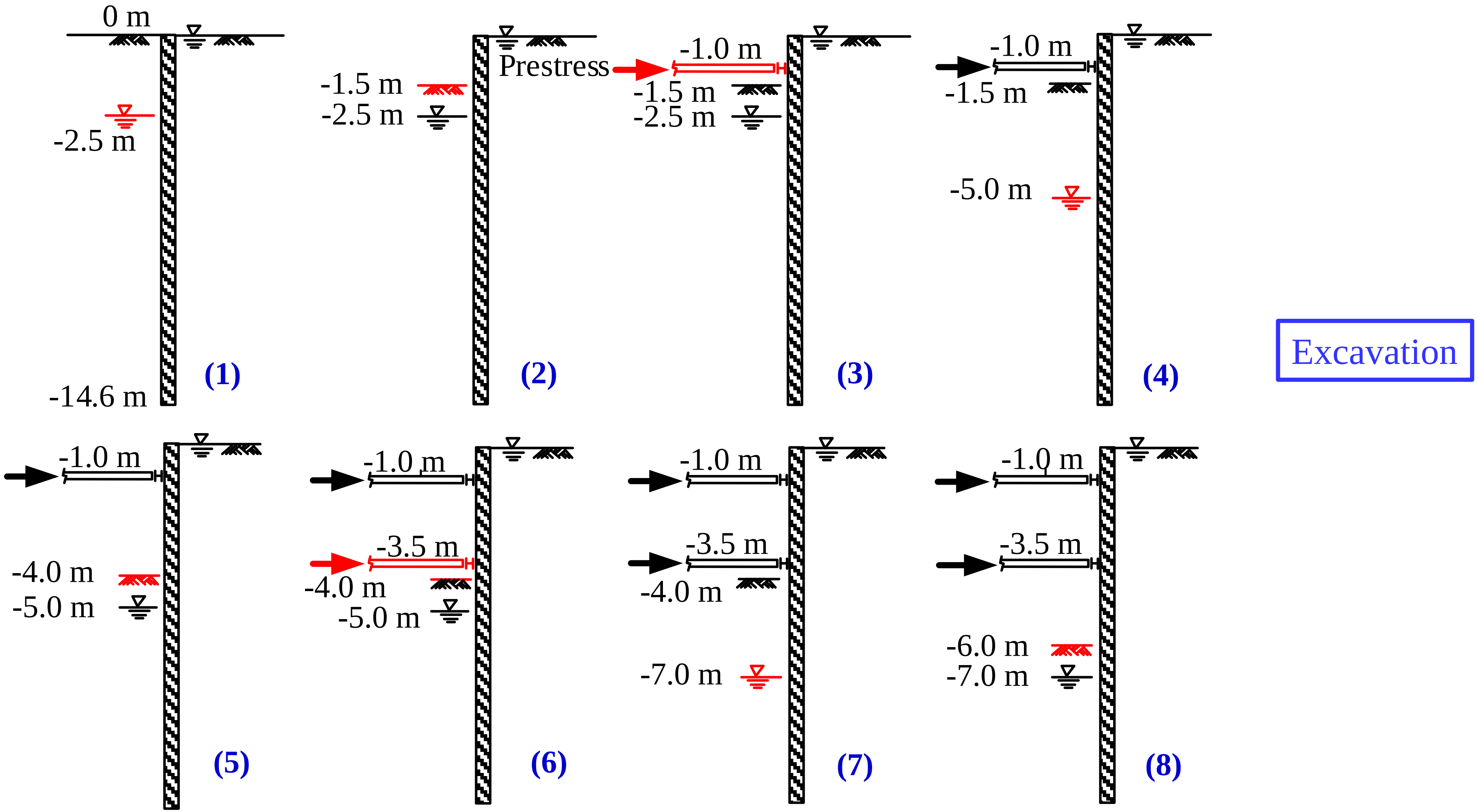

FIGURE 7.6 Procedure of a basement construction

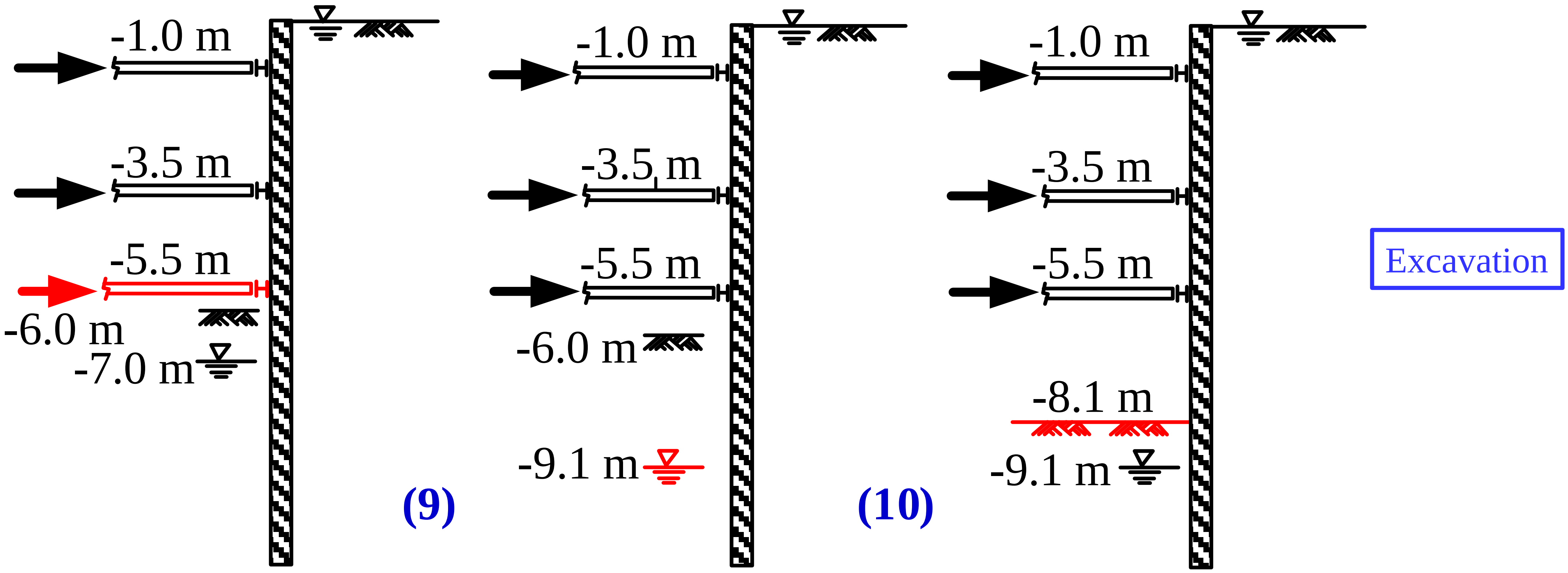

FIGURE 7.6 Procedure of a basement construction

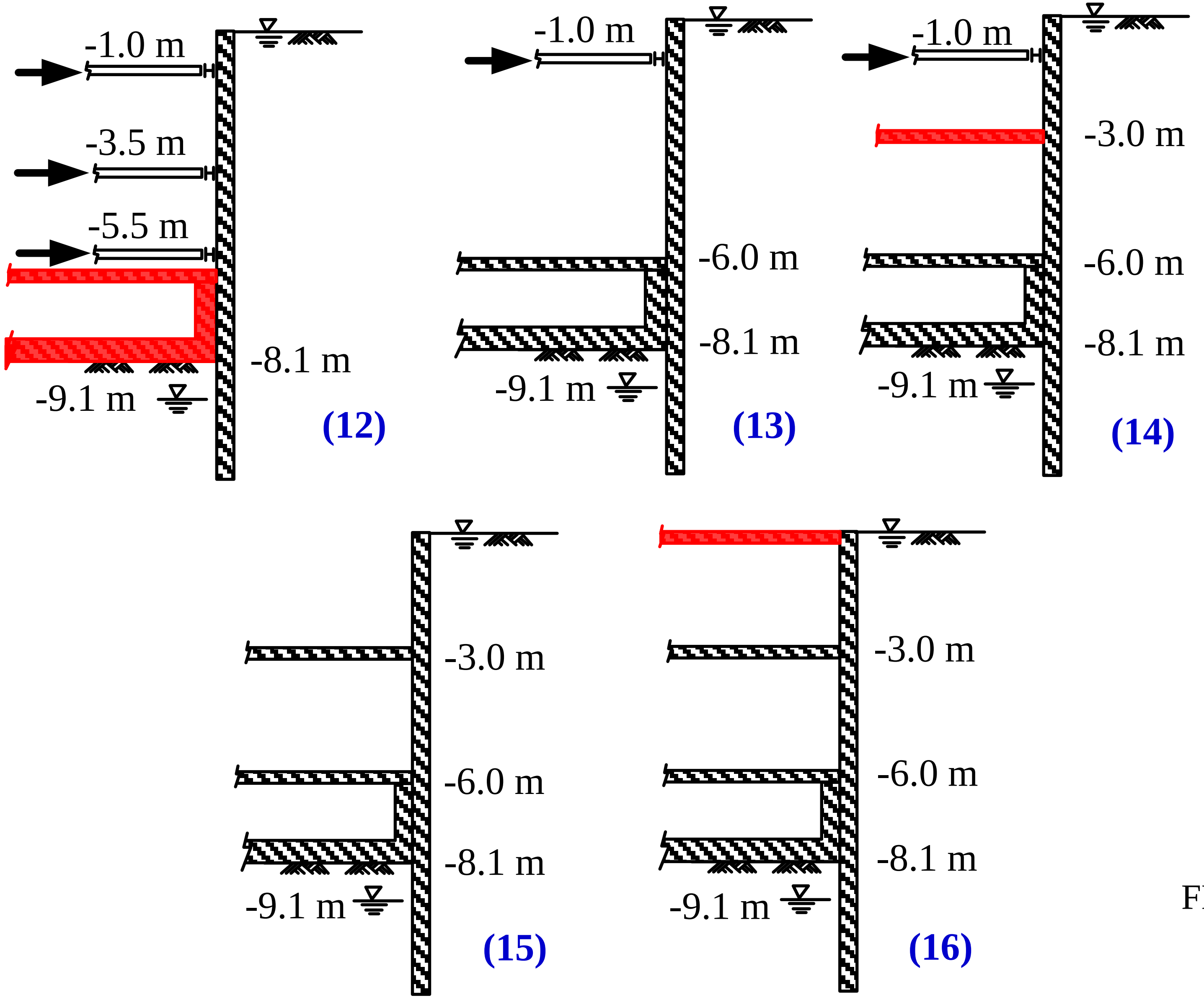

Strut demolish and floor slab construction

FIGURE 7.6 Procedure of a basement construction

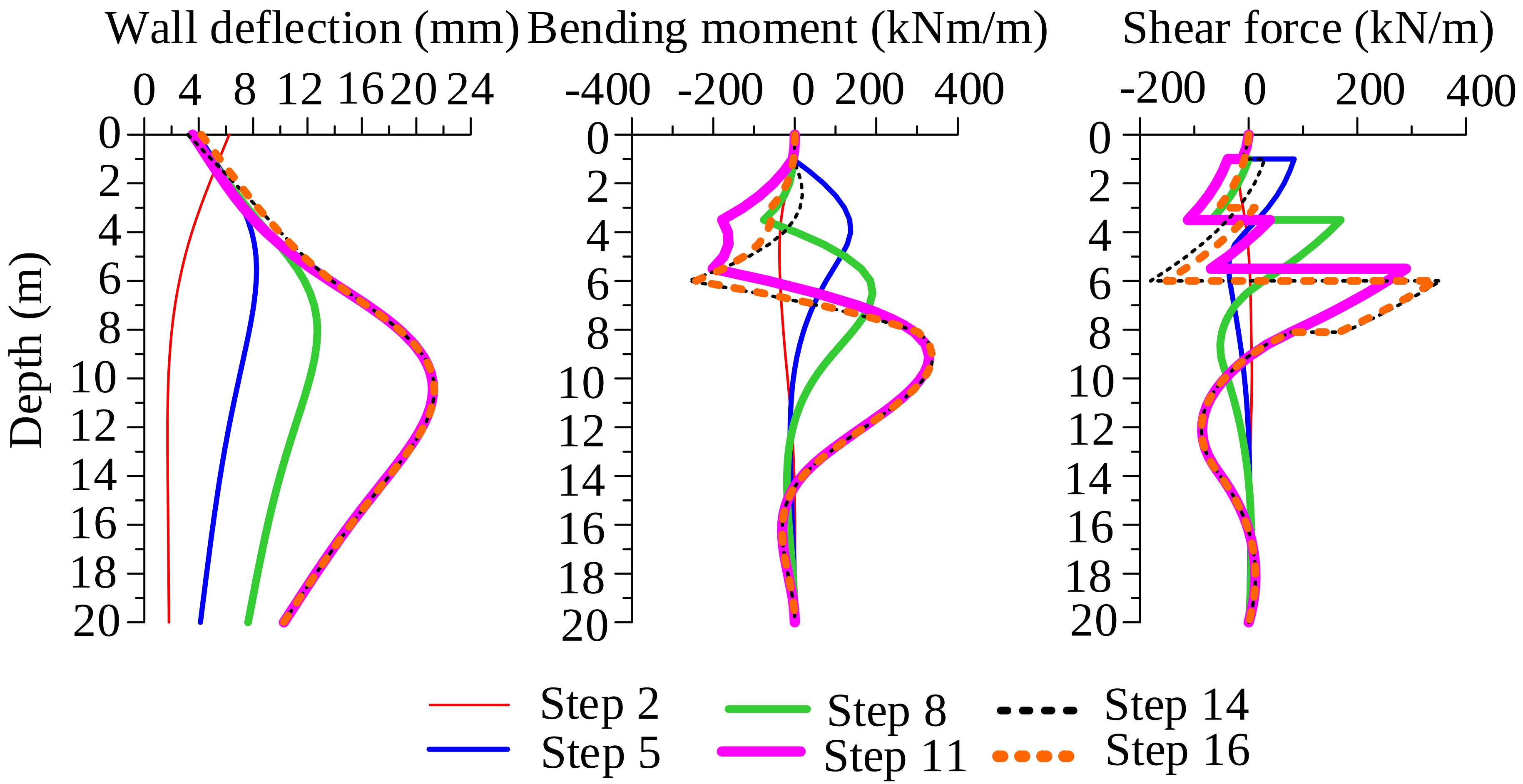

FIGURE 7.7 Deformation, bending moment, and shear force diagrams of the wall computed at main stages

One construction event, one analysis phase

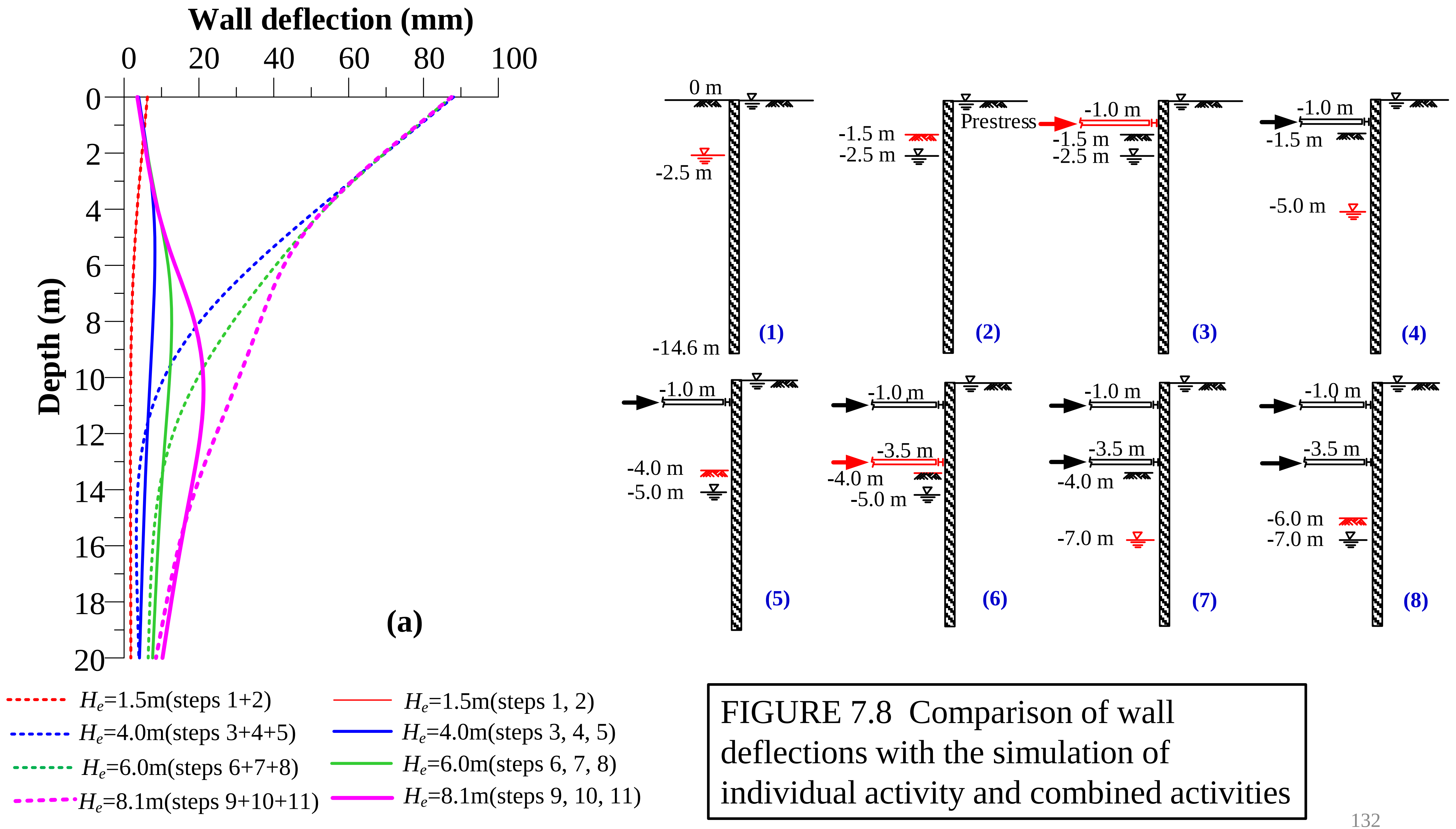

FIGURE 7.8 Comparison of wall deflections with the simulation of individual activity and combined activities

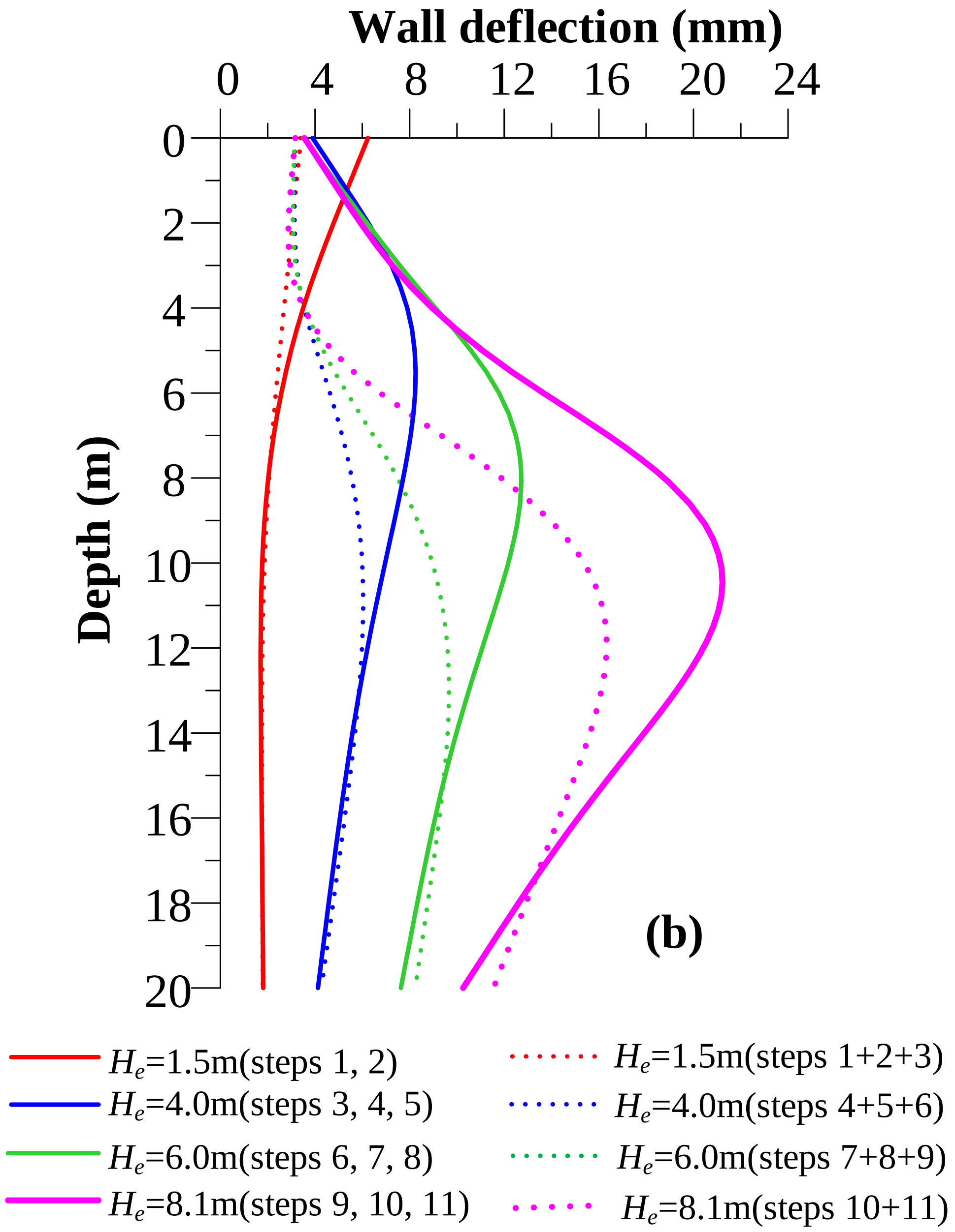

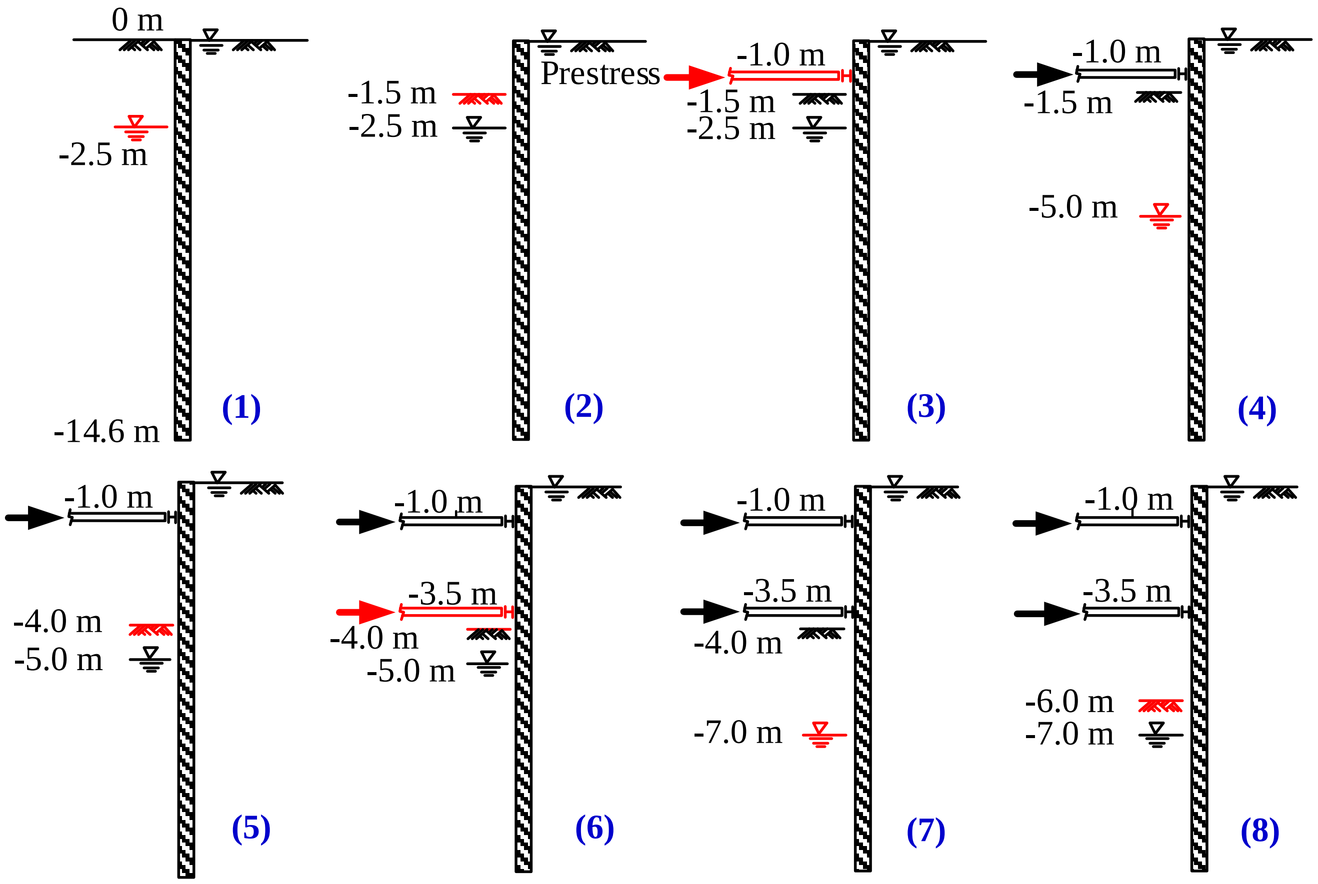

FIGURE 7.8 Comparison of wall deflections with the simulation of individual activity and combined activities

8. Check convergence

$$\frac{\left|F_{ext} - F_{\text{int}}\right|}{\left|F_{ext}\right|} < \textbf{tolerated error}$$

9. Validate the analysis results

(1) Case History

(2) Field Observations

(3) Analytical or Empirical Solutions
(Equations or design charts)

(4) Laboratory Tests

End of Chapter 8

Thank you for your attention!

TPKE project